

Rapports scientifiques et techniques de l'IFREMER



N° 11 1988

DEEP SOFAR FLOAT EXPERIMENT IN THE NORTH-EAST ATLANTIC

Michel OLLITRAUT, Pierre TILLIER, Isabelle BODEVIN
Institut français de recherche pour l'exploitation de la mer
Holger KLEIN
Deutsches Hydrographisches Institut



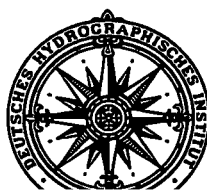
Rapports scientifiques et techniques de l'IFREMER

N° 11 1988

DEEP SOFAR FLOAT EXPERIMENT IN THE NORTH-EAST ATLANTIC

EXPÉRIENCE DE FLOTTEURS SOFAR PROFONDS
DANS L'ATLANTIQUE NORD-EST

Michel OLLITRAUT, Pierre TILLIER, Isabelle BODEVIN
Institut français de recherche pour l'exploitation de la mer
Holger KLEIN
Deutsches Hydrographisches Institut



DEEP SOFAR FLOAT EXPERIMENT IN THE NORTH EAST ATLANTIC

a joint study initiated by

L'INSTITUT FRANÇAIS de RECHERCHE pour L'EXPLOITATION de la MER (IFREMER)
Centre de BREST

DAS DEUTSCHE HYDROGRAPHISCHE INSTITUT (DHI) HAMBURG
and

LE COMMISSARIAT A L'ÉNERGIE ATOMIQUE (CEA) FONTENAY-AUX-ROSES

as part of the

NORDOSTATLANTISCHES MONITORING PROGRAMM (NOAMP)

**Service de la Documentation
et des Publications (S.D.P.)**
IFREMER - Centre de Brest
BP 70 - 29263 PLOUZANÉ
Tél. 98 22 40 13 - Télex 940 627F

ISSN - 0761-3970

© Institut français de recherche pour l'exploitation de la mer, 1988

Contents

1 INTRODUCTION	5
2 THE FIELD EXPERIMENT	7
3 DATA PROCESSING	17
3.1 Errors on float position	19
3.2 Final positions, filtered and interpolated	22
4 BASIC RESULTS AND STATISTICS	31
5 STATISTICS AND PLOTS OF INDIVIDUAL FLOATS	55
6 APPENDICES	117
6.1 Appendix A : Float and Listening Station Technical Characteristics	117
6.2 Appendix B : Calendars	119
6.3 Appendix C : List of tables and figures	120
7 REFERENCES	121
8 ACKNOWLEDGMENTS	122

Abstract

Lagrangian measurements of mesoscale motions near the bottom of the North East Atlantic were made by tracking SOFAR floats. 14 deep floats ballasted for 3500 dbars were launched near 47°N, 20°W and followed during one year by 4 autonomous listening stations moored around the launching zone at a hundred kilometres distance. After one year the floats have dispersed in a zone of 300 km x 300 km indicating a very weak mean current but strong topographic influences.

Résumé

Des mesures lagrangiennes des échelles moyennes dans les couches profondes de l'Atlantique Nord-Est ont été réalisées à l'aide de flotteurs SOFAR. Quatorze flotteurs ballastés pour 3500 dbars ont été lâchés vers 47°N, 20°W et suivis pendant près d'un an grâce à 4 stations d'écoute autonomes mouillées à quelques 100 km autour de la zone de lâcher. Après un an les flotteurs se sont dispersés dans une zone d'environ 300 km x 300 km, et révèlent une circulation générale très faible mais une forte influence de la topographie sous-marine.

1 INTRODUCTION

In order to investigate local transport and the fate of matter released at the seabed, the Nord-Ost-Atlantisches Monitoring Programm (NOAMP) was carried out by the Deutsches Hydrographisches Institut (DHI) in Hamburg, with funds from the Bundesministerium für Forschung und Technologie (BMFT) of West Germany. Between September 1983 and May 1986 six oceanographic campaigns took place in a zone situated roughly between 46 and 49° N and between 17 and 23° W. Hydrographic and geochemical data were collected at different times of the year and current meter moorings deployed in the centre of the zone. A detailed description of the experiment is given by Mittelstaedt et al., 1986.

To complement Eulerian data and add knowledge about spatial scales and dispersion near the sea bottom, it was decided to conduct a deep drifting float experiment. Responsibility for this experiment was shared between DHI and IFREMER and funds came from BMFT, IFREMER and CEA (Commissariat à l'Energie Atomique). CEA was involved because the NOAMP region is close to the OECD (Organization for Economic Cooperation and Development) Nuclear Energy Agency dump site, and was interested in water particle motion near the bottom.

In May 1985, 14 deep drifting floats were launched in a cluster in the NOAMP area near 47°N, 17°W, at depths varying from 3700 to 4000 m. A fifteenth deep float was launched later in August, in the same area, at 3800 m depth. A sixteenth float was launched further north in the main thermocline at 900 m depth with the purpose of tracking a ring seen on XBT profiles (Mittelstaedt, 1987).

The deep floats consist of hollow glass spheres, which are slightly less compressible than seawater, so that their density increases less rapidly with depth than does that of the surrounding water. If correctly ballasted, they can attain a stable mid-depth equilibrium level at which they will remain for long periods of time (one to several years in practice). At these levels, the floats drift freely with the currents, acting like quasi-Lagrangian tracers. They would follow particle paths if particles moved on isobaric surfaces, but particles move on constant density surfaces in the ocean, at least for mesoscale time periods (particles are isopycnic and our floats were isobaric). However, generally isopycnic and isobaric surfaces are not very different in the deep ocean.

Every four hours, each float emits a low frequency (780 Hz) acoustical signal that is later heard and recorded by autonomous listening stations situated on moorings some 100 to 200 km from the launching zone.

From the times of arrival of the signals received at two or more listening stations, whose positions are precisely known, estimates of positions of the floats can be obtained using least squares minimisation and knowledge of the sound speed in the region (Ollivault, 1987).

This direct current-measurement instrument has been named the SOFAR float, for Sound Fixing and Ranging (Rossby, Voorhis and Webb, 1975).

Floats and listening stations used in this study were developed at IFREMER by P. Tillier. These floats also measured temperature and pressure and telemetered the data to listening stations using successive pairs of acoustical signals whose times of emission are separated by an interval proportional to the temperature or pressure value. The floats would gradually sink, because glass creeps under the high pressure found in the deep ocean, but this was compensated for through a sacrificial anode controlled by a feedback circuit attached to the pressure sensor.

The listening stations were recovered in June 1986. Although the data tapes were full at that time, roughly 360 days of data were accessible.

2 THE FIELD EXPERIMENT

Five listening stations were moored in early May of 1985 from the German research vessel METEOR, and were recovered in early June of 1986. Unfortunately, one station did not function and another stopped after ~ 200 days. Nevertheless, the data from the four stations permitted adequate tracking of the floats. Table 1 below gives the station characteristics.

Listening station	Position	"Launch" date	Clock advance at launch	"Recovery" date	Clock advance at recovery	Days of data usable
N13	46°56.3'N 21°24.9'W	1985 May 9 7h40 UT	+ 20 ms	1986 June 16 8h30 UT	+ 694 ms	358
N15	48°24.7'N 20°44.3'W	1985 May 9 9h50 UT	+ 5 ms	1986 June 16 9h10 UT	+ 10230 ms	371
N17	46°04.8'N 19°38.7'W	1985 May 10 11h50 UT	+ 5 ms	1986 June 16 9h10 UT	+127385 ms	347
N19	46°57.6'N 17°46.0'W	1985 May 11 6h20 UT	+ 13 ms	1986 June 16 9h30 UT	+ 89 ms	195

Table 1: Characteristics of NOAMP listening stations.

On each station the acoustic receiver was situated at 1500 m depth. In this table launch or recovery dates actually refer to the time when clock advances were checked with CUT. IAT-CUT (International Atomic Time - Coordinated Universal Time) increased by + 1 s on the 1st of July 1985, which has been taken into account in the corrected advance given in the table (i.e. the measured advance minus 1 s). Figure 1 shows the mooring configuration used while Figure 2 shows the location of the four listening stations.

Also shown in Figure 2 are the launch positions of the floats (see also an enlarged view in Figure 2 bis).

The floats were deployed in trios : three floats were mounted in a housing on board the ship, the housing lowered to the nominal depth and then opened to release the floats (Figure 3). Four trios separated by roughly 30 km (order of first baroclinic Rossby radius) were launched in this way. We also launched a duo (floats # 77 and 78) but float # 77 was never heard.

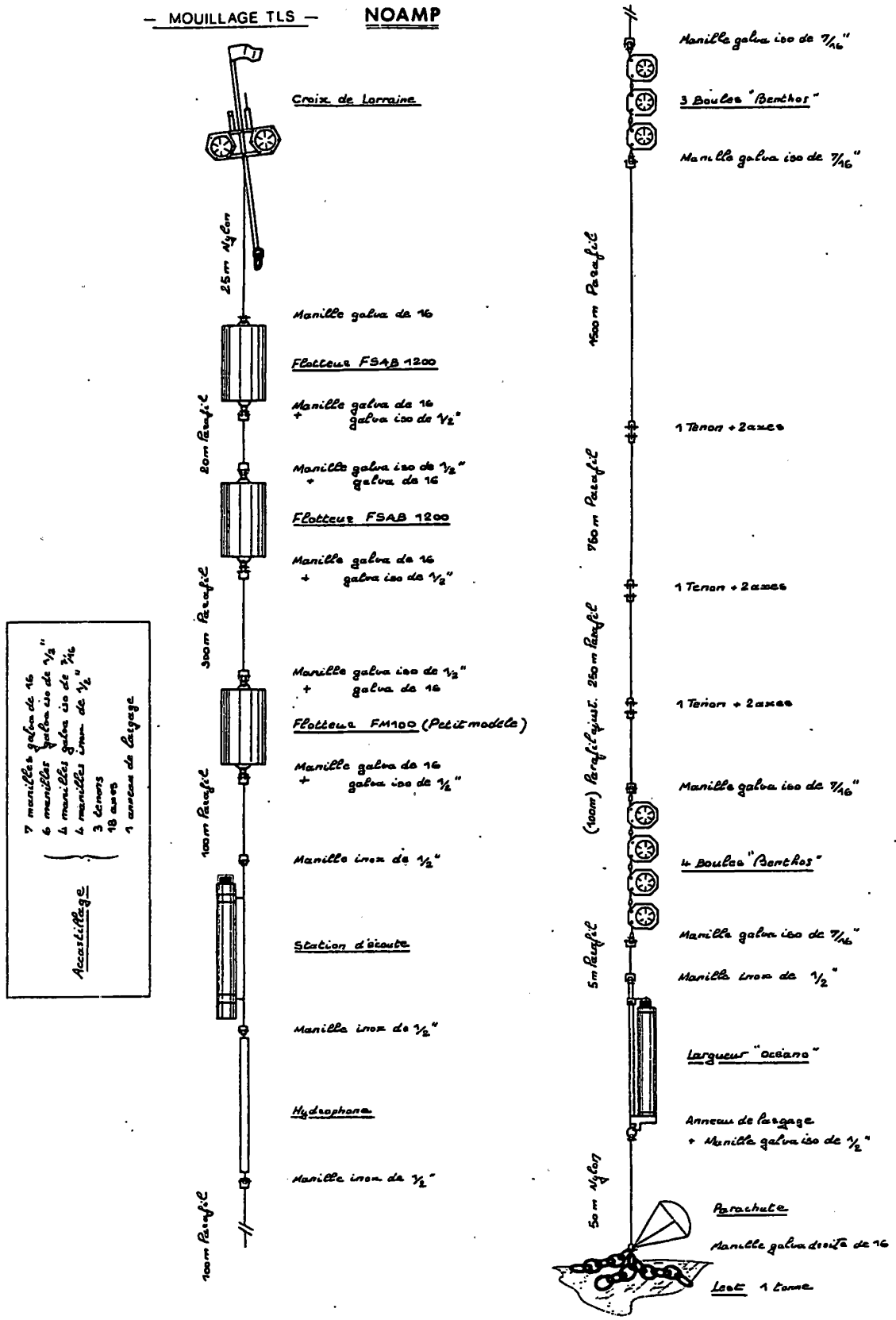


Figure 1: Mooring configuration for the autonomous listening stations used during NOAMP.

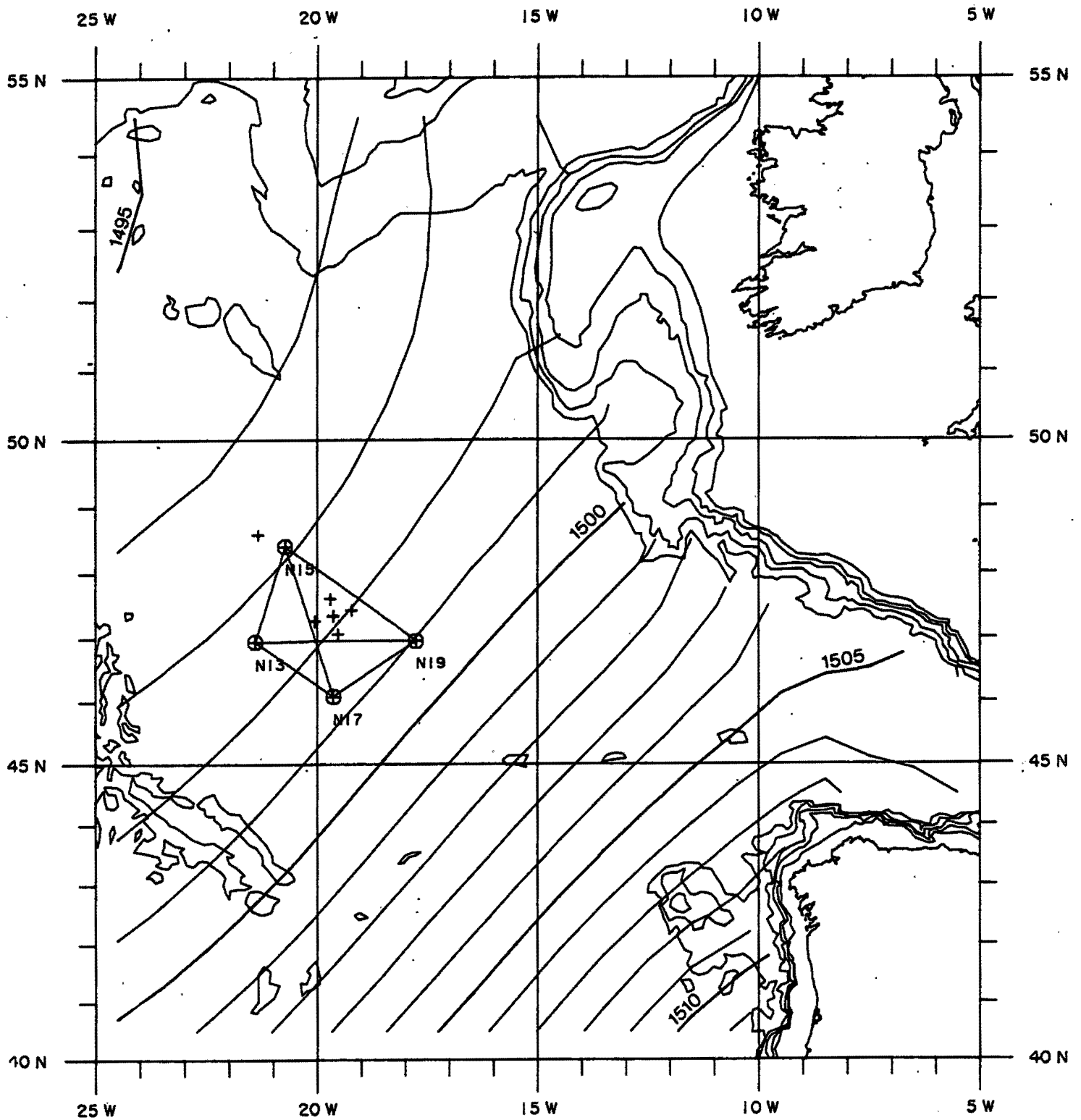


Figure 2 : Location of the NOAMP listening stations (represented by ⊕) together with the launch positions of the floats (represented by +). Depth contours at 200, 500, 1000, 2000 and 3000 m. Contours of sound speed at 1500 m were calculated from the Levitus Atlas (Levitus, 1982).

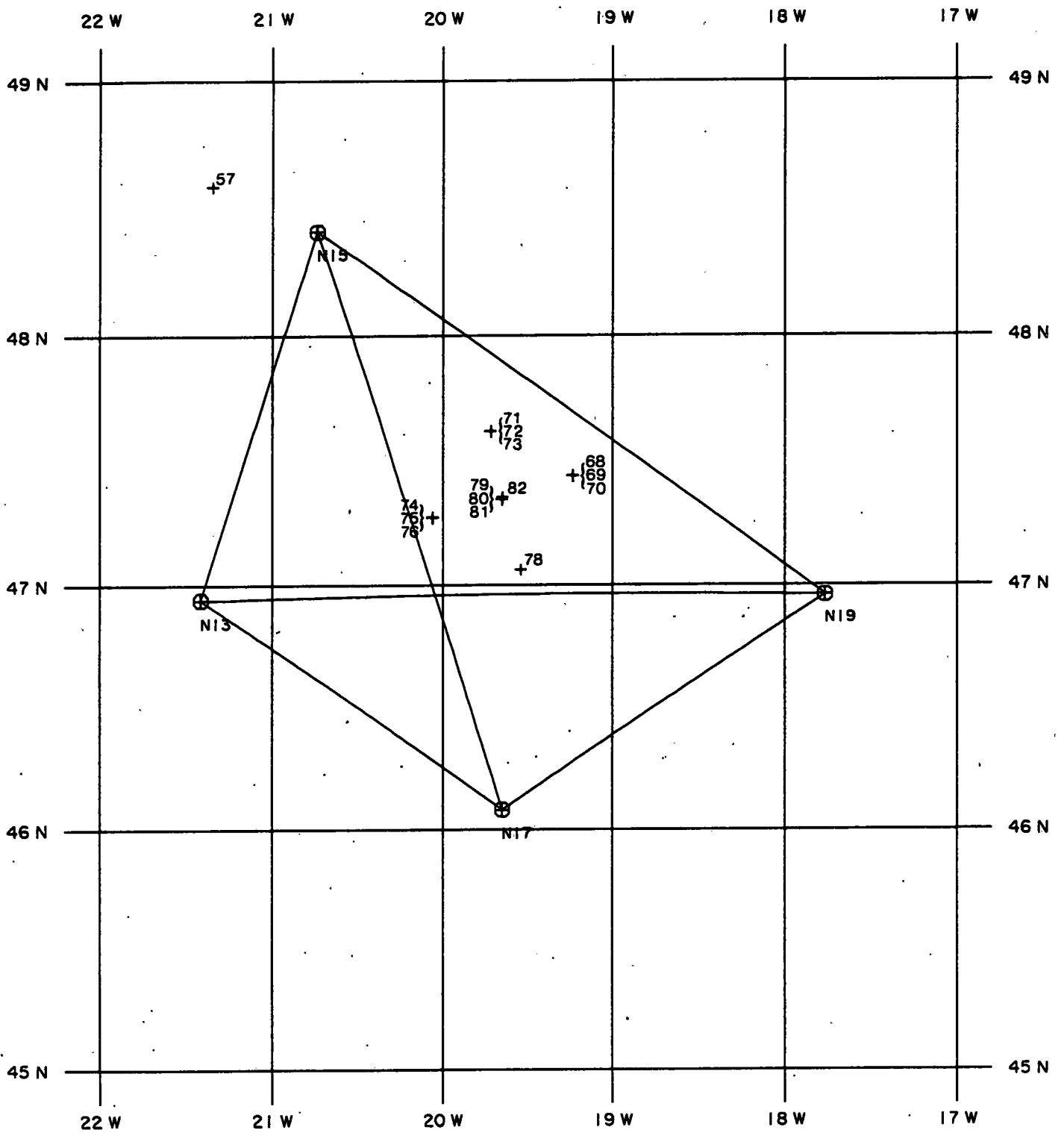


Figure 2 bis : Location of NOAMP listening stations and launch positions of the floats.

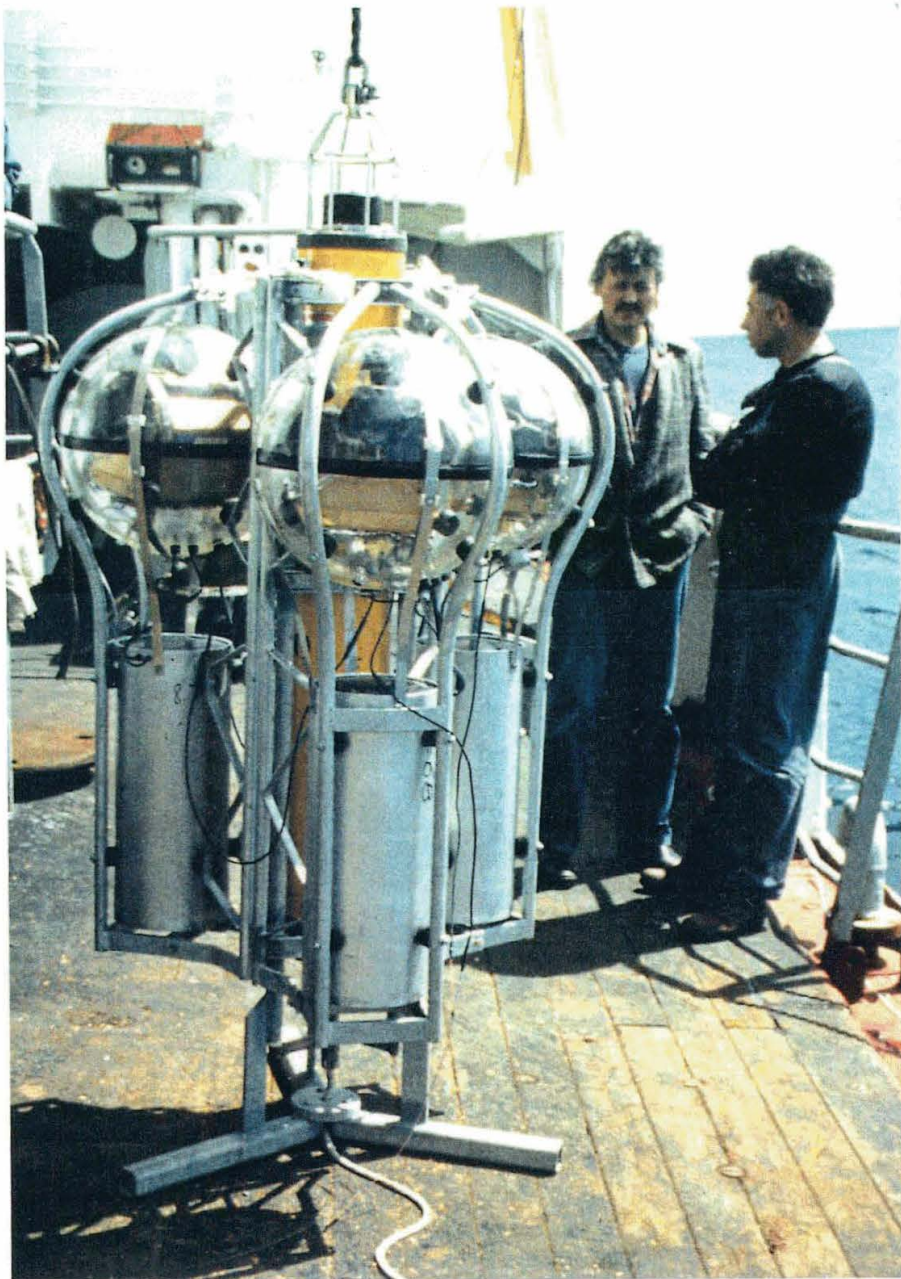


Figure 3 : A trio of floats. The housing opens at a prescribed depth releasing the three floats at the same depth.

This launching scheme was intended to permit estimation of one particle and two particle diffusivities (Batchelor, 1952) ; with each trio giving two independant pairs of particles. Furthermore it was hoped to assess small-scale dispersion since at the beginning the three floats of a trio would be released almost at the same point, if ballasted to attain the same equilibrium pressure.

Float #	Main pong time	First press. (dbar)	Last press. (dbar)	First temp. (°C)	Last temp. (°C)	Launch point	Last point approx.	Launch date	Life time (days)
68	0h10mn	3800	2850	2.7	2.9	47°26.4'N 19°13.8'W	~47°26'N ~16°24'W	13.05.85 18h UT	346
69	0h20mn	3960	3500	2.7	2.7	idem	~47°32'N ~22°49'W	idem	285
70	0h30mn	4100	3750	2.7	2.7	idem	~48°34'N ~22°25'W	idem	261
71	0h50mn	4100	4000	2.7	2.7	47°37.1'N 19°42.9'N	~46°N ~19°38'W	13.05.85 24h UT	203
72	1h00mn	4100	2700	2.7	3.2	idem	~47°N ~21°46'W	idem	356
73	1h10mn	3900	3500	2.7	2.8	idem	~45°50'N ~19°32'W	idem	346
74	1h30mn	4040	3500	2.8	2.8	47°16.3'N 20°3.5'W	~47°26'N ~19°W	14.05.85 15h UT	354
75	1h40mn	3840	3500	2.8	2.8	idem	~45°30'N ~20°21'W	idem	246
76	1h50mn	3750	3500	2.8	2.7	idem	~46°56'N ~21°43'W	idem	136
77									
78	2h20mn	4100	3500	2.7	2.7	47°3.7'N 19°32.0'W	~48°23'N ~20°47'W	14.05.85 22h UT	297
79	2h40mn	3970	3500	2.7	2.8	47°20.7'N 19°38.8'W	~45°45'N ~20°W	15.05.85 5h UT	344
80	2h50mn	4070	3500	2.7	2.8	idem	~46°30'N ~20°W	idem	238
81	3h00mn	3750	3500	2.7	2.7	idem	~45°19'N ~19°51'W	idem	344
82	3h40mn	3770	3050	2.7	3.1	47°21.2'N 19°38.6'W	~47°14'N ~18°35'W	21.08.85 21h UT	165
57	3h30mn	930	800	≈5.2	≈7.5	48°35.4'N 21°20.7'W	~50°19'N ~21°53'W	19.05.85 5h UT	279

Table 2 : Life histories of all the floats.

Table 2 and Figure 4 summarize the life histories of all 16 floats : of the 16 floats only one could not be heard. A few had a rather short life for various possible reasons. Ray tracing between the deep floats and the listening stations shows that sound is attenuated by reflections on the sediment bottom and the surface before reaching the stations (Figure 5). Due to the proximity to the bottom, floats can be hidden by the topography. As a consequence, NOAMP deep floats were heard only within a distance of O(200 km). In comparison float # 57 at thermocline depth was heard by the southern station N17 at O(500 km) distance because of sound trapping in the SOFAR channel (minimum of the sound speed profile).

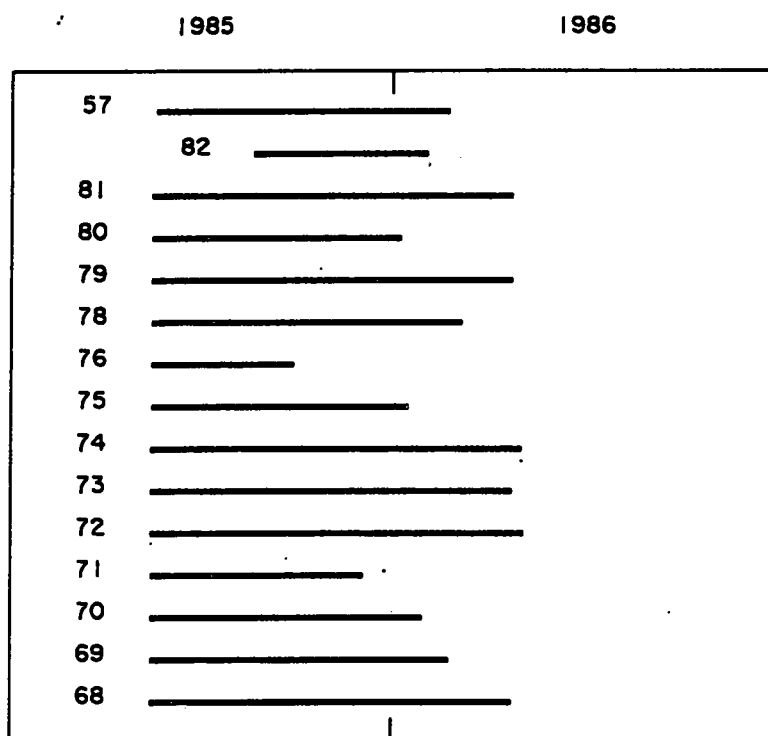


Figure 4 : Bar graph showing the time that each float was tracked.

It was intended to release the deep floats at 3500 dbars. As can be seen in Table 2 and in Figure 6, this was only partly successful. This may be due to the relative homogeneity of the deep waters which requires very precise float ballasting, or to the glass spheres not having identical elastic behaviour. The depth-correcting circuits attempted afterwards to correct the initial differences in equilibrium level. On all but three cases, they succeeded, or were progressing toward succeeding (Figure 6). We have no firm explanation for the three floats which overshot the equilibrium depth.

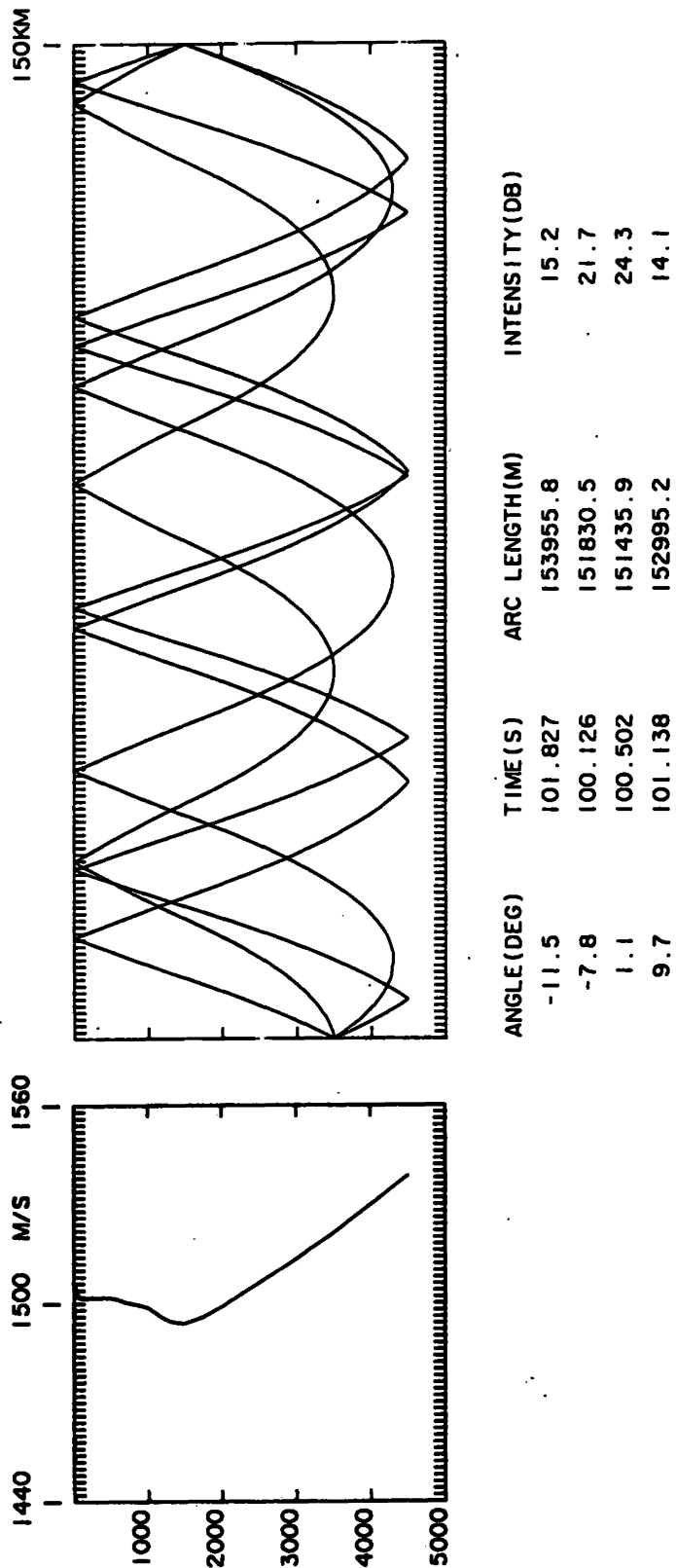


Figure 5 : Sound rays for the sound speed profile calculated from Levitus *T* and *S* profiles centered at 46.5N, 19.5W (Levitus, 1982). They are typical of the rays that are recorded at the NOAMP listening stations.

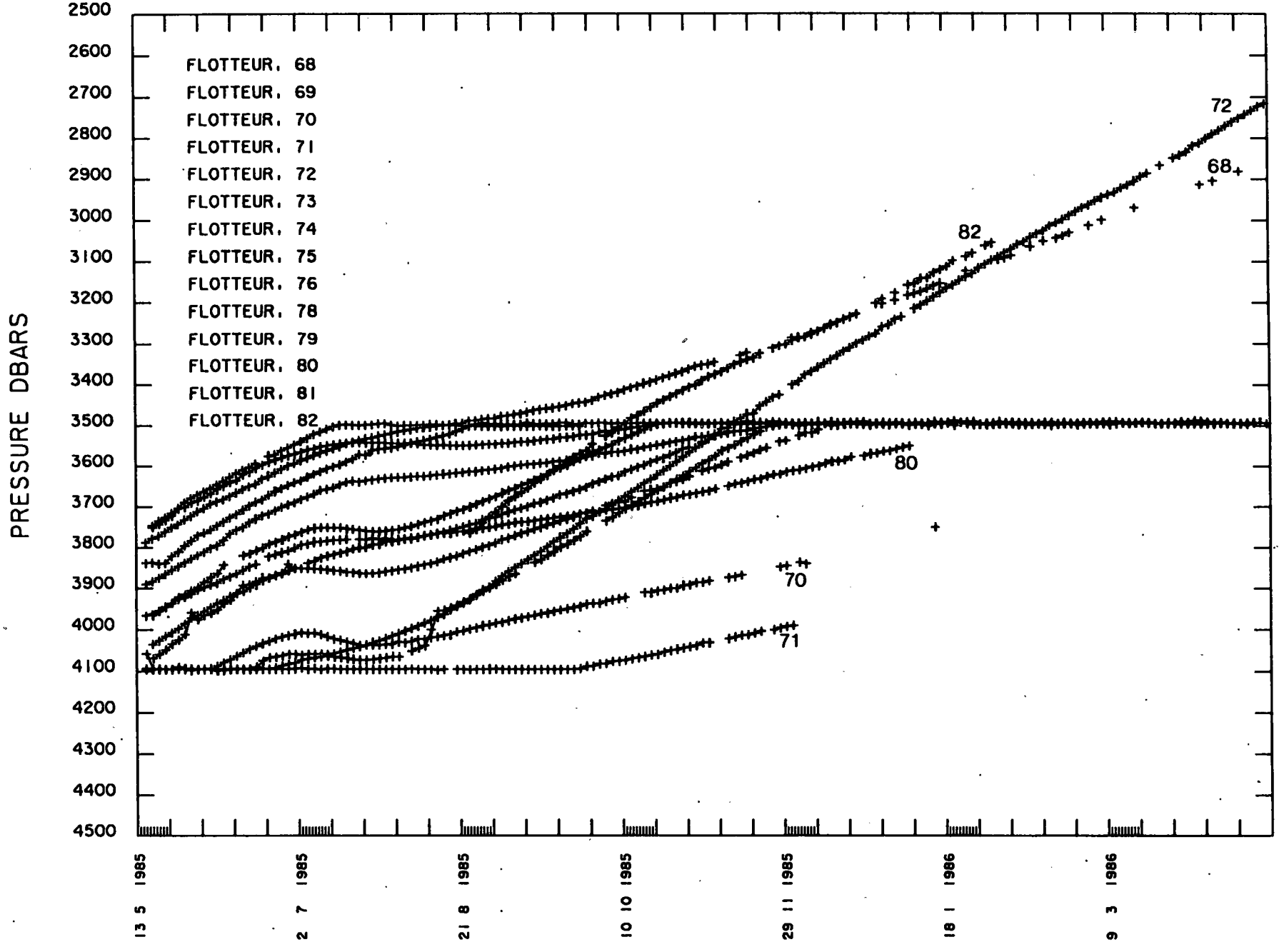


Figure 6 : Pressure history for the 14 deep floats.

3 DATA PROCESSING

The following is an overview of the processing done to obtain the final trajectories. First, the cassette tapes recovered from the listening stations at the end of the experiment are read with a SEADATA reader and the raw data dumped on an HP1000 computer disk. To each station corresponds one data file containing the signals sent by all the floats (if the signals have been strong enough to be heard), as well as noise. Such a data file consists of consecutive records, each of which contains the reception time and correlation value for the four best correlated signals (float or noise) received in a 10 mn period at a particular station. Figure 7 shows an example of the acoustic signals received at a listening station. The signal received at a station is correlated with a reference signal and the better the correlation the darker the dot on the plot. In Figure 7, the horizontal scale is graduated in seconds and there is a horizontal dotted line every 10 days. The times of arrival are those of float # 68, 69 and 70 (the three black curves) and to the right of these principal arrivals can be seen the telemetries for pressure and temperature every two days. Floats emitted their signals at different times so that it is possible to differentiate them on such a plot : for example, float # 68 emitted at 0h10mn, 4h10mn, 8h10mn,..., whereas float # 69 emitted at 0h20mn, 4h20mn, 8h20mn, and so on... (every four hours NOAMP floats emitted a 40s long FM chirp around 780 Hz ; see technical characteristics in Appendix A).

The next step is to select times of arrival of the signal sent by each float from every listening station capable of hearing that float. The same is done for the temperature and pressure telemetry and, after merging results in one file for each couple (float, station) containing only these 3 values together with the date.

At this stage temperature and pressure are calculated in physical units, the station clock advances are taken into account and, if necessary, doppler correction on the radial velocity done (in fact it was not necessary to make the doppler correction for the deep floats because of their low velocity). For NOAMP deep floats (# 68 to 82 inclusive) differences between secondary and principal arrivals were related to temperature and pressure by :

$$\begin{aligned}\Delta t \text{ (s)} &= 120 + \text{modulo} (50 \times T^{\circ}\text{C}, 480) \\ \Delta t \text{ (s)} &= 120 + \text{modulo} (.5 \times P \text{ dbar}, 480)\end{aligned}$$

while for float # 57 we had :

$$\begin{aligned}\Delta t \text{ (s)} &= 120 + \text{modulo} (50 \times (T-4)^{\circ}\text{C}, 480) \\ \Delta t \text{ (s)} &= 120 + \text{modulo} (.5 \times (P-500)\text{dbar}, 480)\end{aligned}$$

The temperature or pressure values so obtained are 48h average values.

DONNEES FLOTTEURS DERIVANTS

STATION AUTONOME D'ECOUTE NO: N13
 EXPERIENCE NO: 1
 CANAL NO: 1

COR MIN : 4#
 COR MAX : 5#

JOURS PAIRS ET IMPAIRS

12 5 1985
 MIN: 1#

12916

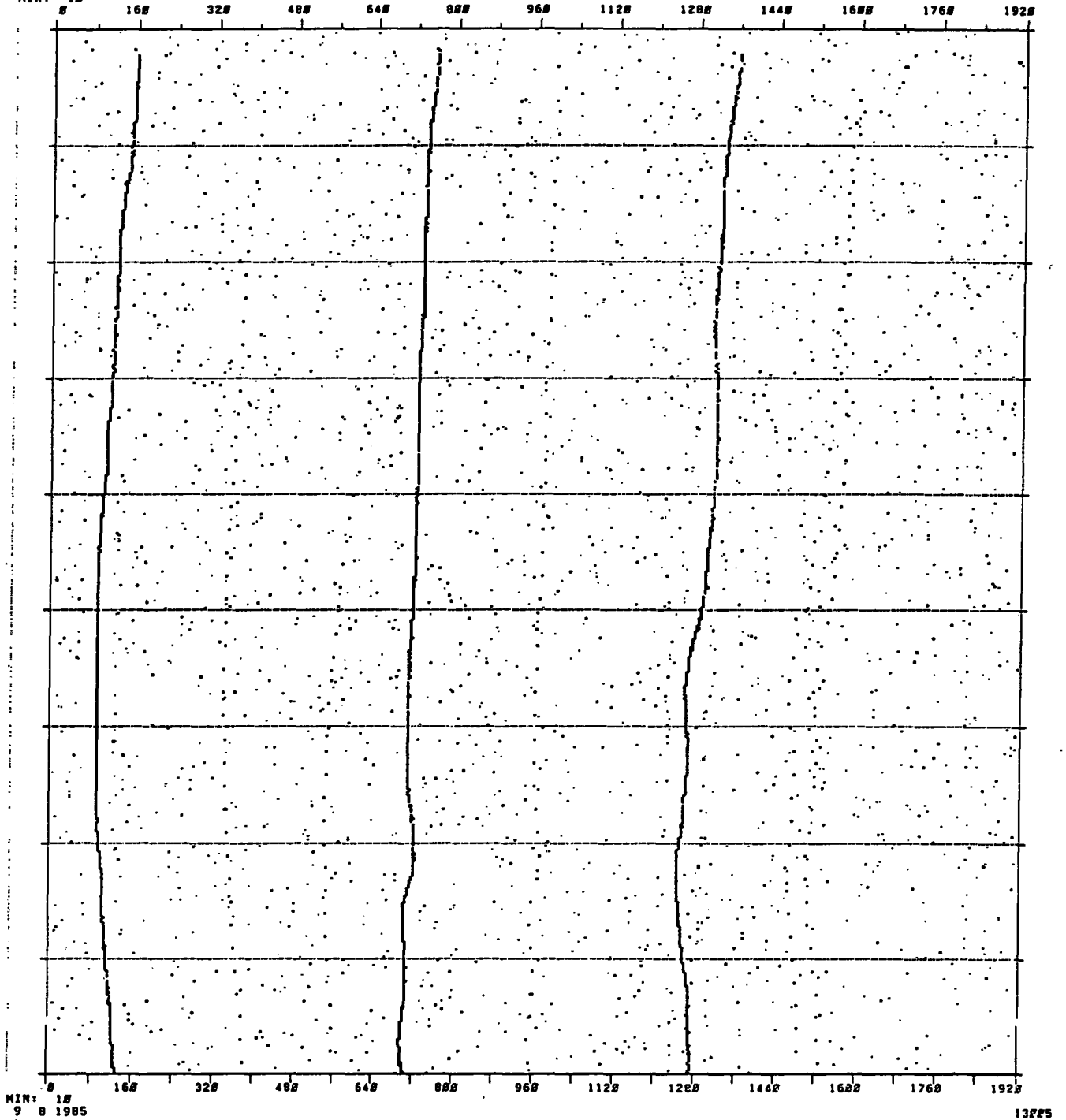


Figure 7 : Times of arrival received at listening station N13. The figure shows the first 32 minutes of each four hour period. The horizontal scale is graduated in seconds and there is a horizontal dotted line every 10 days. The times of arrival are those of floats 68, 69 and 70. One can also see to the right of the principal arrivals (the three black curves), the telemetries for pressure and temperature every two days.

It is then possible to calculate float positions. Because the time of emission of a given float is accurately known, one can calculate its distances to the various listening stations using an assumed mean speed of sound between the float and a given station. In the vicinity of the float position the constant distance curves from the different stations cross each other as shown in Figure 8. If there were no errors and no drift in the float clock these curves should cross at the same point, the float position.

Given three or more stations, we can determine the best position (and the float clock drift) in the least squares sense. Or in mathematical terms, if T_i is the actual time of sound propagation between the float and the i^{th} station, \tilde{T}_i the time of propagation, given the assumed mean sound speed, between the unknown position (x, y) of the float and the i^{th} station, and if d is the float clock drift ; we have to find x, y (and d) which minimize $\sum = (T_1 - \tilde{T}_1 + d)^2 + \dots + (T_i - \tilde{T}_i + d)^2 + \dots + (T_n - \tilde{T}_n + d)^2$.

The more the stations, the better the determination. The final result is one file per float containing raw positions.

All this processing is fully explained in the IFREMER Scientific and Technical Report n° 7 (Ollitrault, 1987).

This method is quite good if there are no systematic errors in the data. Unfortunately there exist many sources of systematic errors (and random errors). A detailed study of these errors is included as an appendix in the above IFREMER report. Here we shall mention only a few of them.

3.1 Errors on float position

The clocks in the floats and listening stations can have drifts amounting to several seconds per year, and even more.

With three or more stations it is possible to estimate float clock drifts but the estimates for the NOAMP floats were noisy and biased, probably because of other errors not having been corrected. However it was found that the float clock drifts should not be large, $\sim O(1 \text{ s})$ after one year, except for float # 82 whose advance was roughly $+ 2 \text{ s}$. So it was decided to put all float clock drifts equal to 0 s , except float # 82 clock drift which was put constant at $+ 2 \text{ s}$.

For the station clock drifts we can do little more than check the clock at the beginning and the end of the experiment and apply a linear correction. That has been done for the four NOAMP listening stations whose drifts (see Table 1) were :

- $+ 0.7 \text{ s}$ after 402 days for N13.
- $+ 10.1 \text{ s}$ after 403 days for N15.
- $+ 0.1 \text{ s}$ after 401 days for N19.
- But $+ 127.4 \text{ s}$ after 402 days for N17.

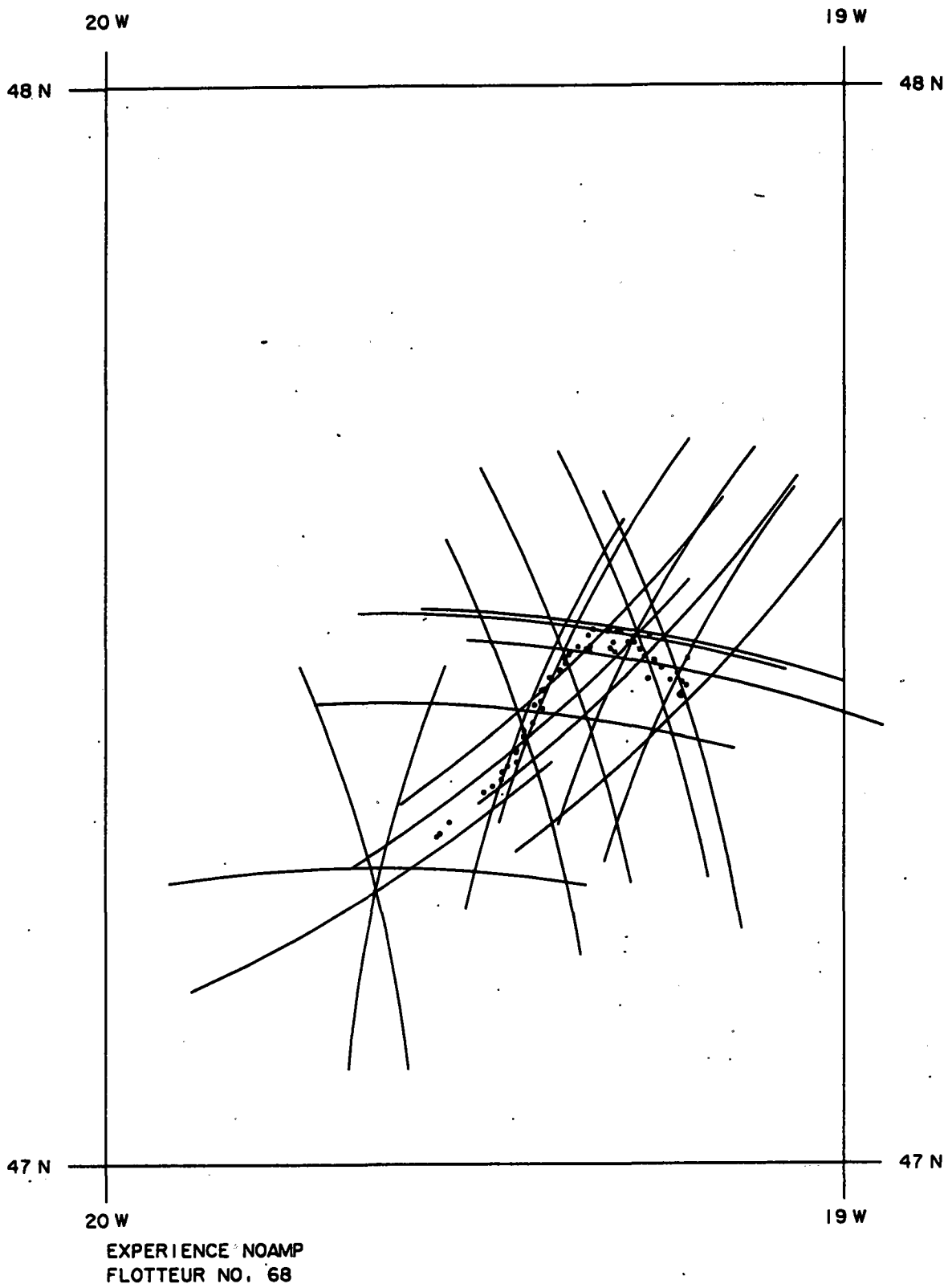


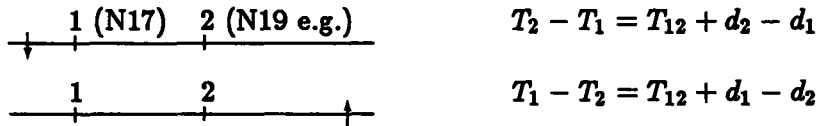
Figure 8 : Arcs whose distances to listening stations are given by the recorded time of propagation multiplied by the assumed speed of sound.

The station N17 drift is very large and should exhibit a non linear evolution.

In fact, after having corrected the times of arrival of this station for the linear trend, there were residuals of order 10 s for the times of propagation to this station, given the positions obtained by least squares fit to the three other times (Figure 9).

The non-linear drift of listening station N17 was estimated in the following manner :

Consider the line joining the station N17 with any other, for example N19, (in fact we should say the orthodromy) and a float which is crossing this line but outside the segment [N17, N19]. Then the difference of the times of propagation to the two stations gives the time of sound propagation between the two stations T_{12} plus the difference of the station drifts (d_1 and d_2).



with T_{12} = sound speed \times dist (1,2).

This is a good determination since there are only two unknowns : the mean speed of sound and $|d_1 - d_2|$. Using all possible differences, a kind of skewed parabolic curve for the non-linear evolution of N17 clock drift was determined and then used to correct the times of arrival (Figure 10).

The mean speed of sound between a given position and a listening station may vary in a range between 1470 and 1510 m.s^{-1} , due to geographical variations in the sound speed profiles (Figure 2 and Figure 11) and ray geometry (Figure 5). For the tracking we have used a constant sound speed equal to 1495 m.s^{-1} but as can be noted in Figure 12 where we have plotted the times of propagation versus the date, for a few days after launching, there seems to be some 20 m.s^{-1} anomaly for the mean sound speed used at N15 e.g. But these anomalies which can be inferred from instantaneous sound speed profiles such as those shown in Figure 11, are not stationary in time and are space dependant.

These errors seem large (order 5 km over 100 km) and a better tracking will be done later using all sound speed profiles of the region. It is hoped that this procedure will diminish the errors.

Other errors are due to the correlation in the listening station, (order .5 to 1 s), to the unknown current between the float and the listening station (order .2 s), or to the imprecise position of the listening station (order .3 s).

Of these, the correlation is certainly the most important : The correlator does not give the exact time of arrival of the signal which may be off by order (.1 s), and it is difficult (if not impossible) to distinguish between successive arrivals corresponding to different eigenrays which are separated by only a few tenths of a second.

However we think that the global error due to the correlation should not exceed 1 s since only the signal which has the highest correlation in a 2 s interval is conserved. Simulations are presently underway to assess this problem.

One further source of error which must be considered is the geometric error due to the relative positions of the float and the listening stations. Figure 13 shows the sizes of error ellipses calculated for a least squares estimate with the four NOAMP stations and the assumption of a Gaussian random error with 1 s standard deviation on the times of propagation. Formulae to calculate these ellipses are given in Ollitrault (1987). As can be presumed, position estimates are more reliable when inside the polygon whose apexes are the stations.

Globally, over the whole NOAMP region, calculated float positions are estimated as accurate to within $O (\pm 5 \text{ km})$ with better accuracy near the center of the zone and lesser accuracy on the surroundings.

3.2 Final positions, filtered and interpolated

First, the position estimates were checked for bad points by first differencing latitude and longitude time series and by visual examination, and the bad points removed.

Missing positions were completed by linear interpolation on latitude and longitude series when gaps were smaller than 10 days and the series so obtained was filtered with a running symmetrical Gaussian filter whose standard deviation was 12h (i.e. three sampling intervals, since floats emitted every 4h) to remove inertial and tidal motions. Note that a position was conserved after filtering only if it existed before interpolation.

Finally, we fitted an interpolating natural cubic spline (Burden and Faires, 1985) to interpolate position gaps smaller than 10 days and estimate velocity components every 4h sampling interval.

Figure 14 shows what kind of fit has been obtained with this procedure.

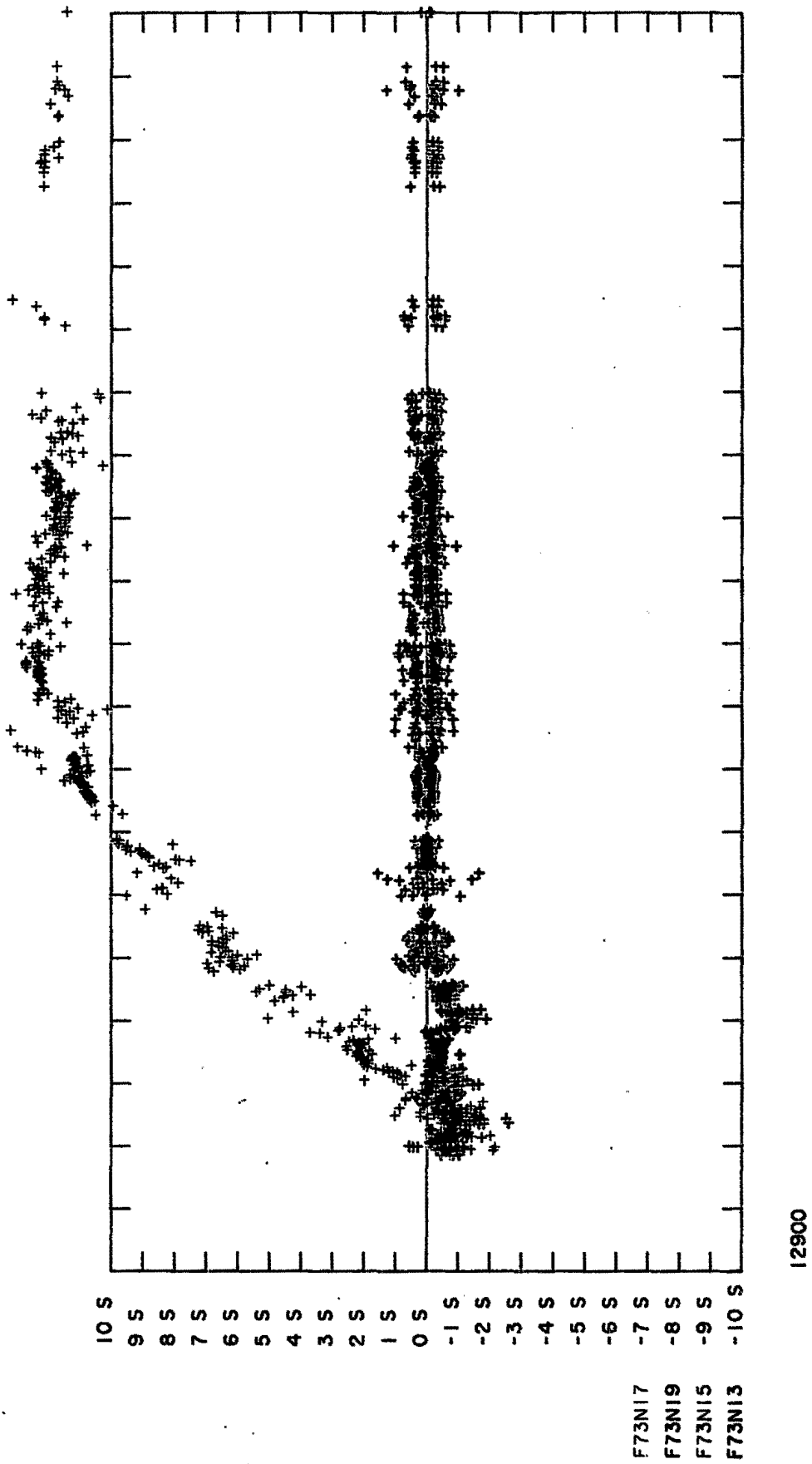


Figure 9 : Residual drift of N17 listening station as obtained by using float position determined by the three other stations.

sound speed 1500 m/s

- △ N15,N17
- N13,N17
- + N19,N17
- ☆ float 82 without drift
- ★ " " with drift +1s

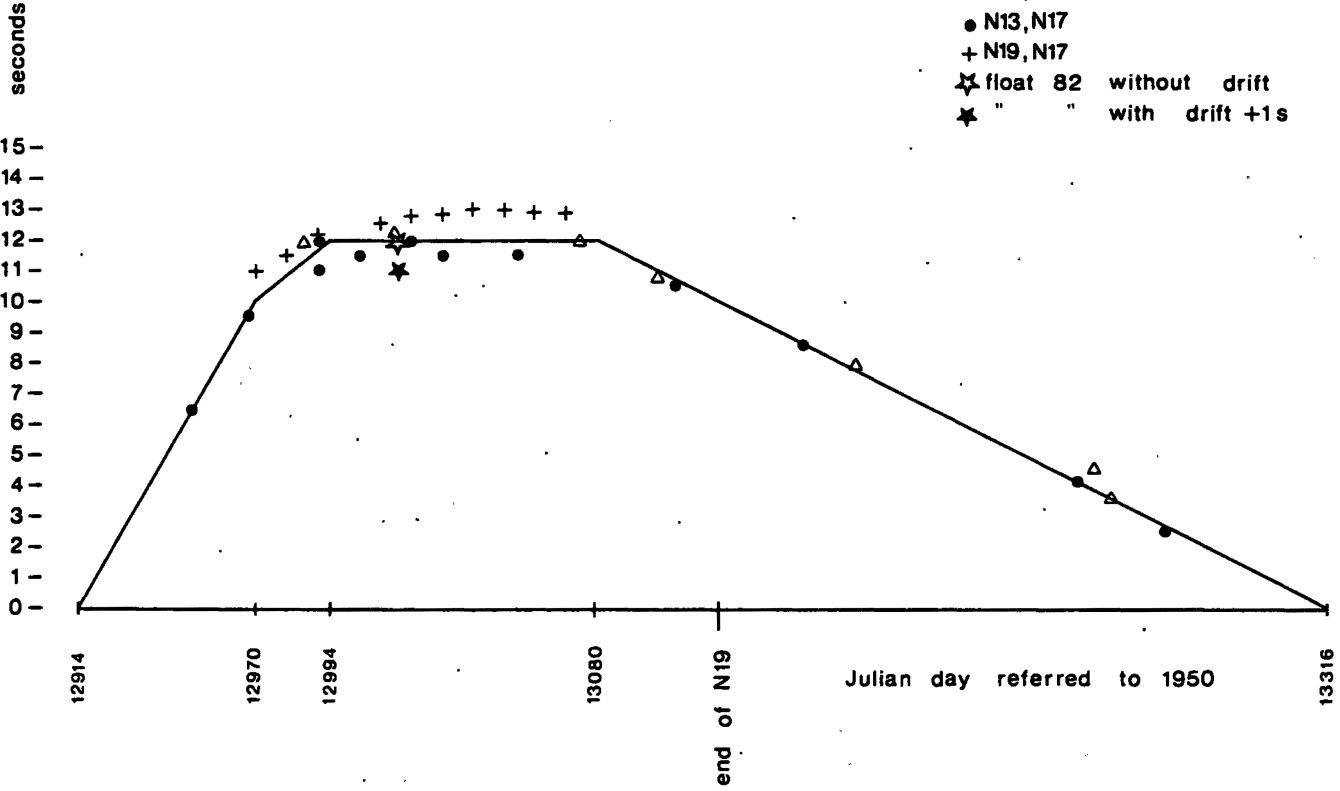


Figure 10 : N17 listening station non-linear drift assumed in the processing, and determined as explained in the text.

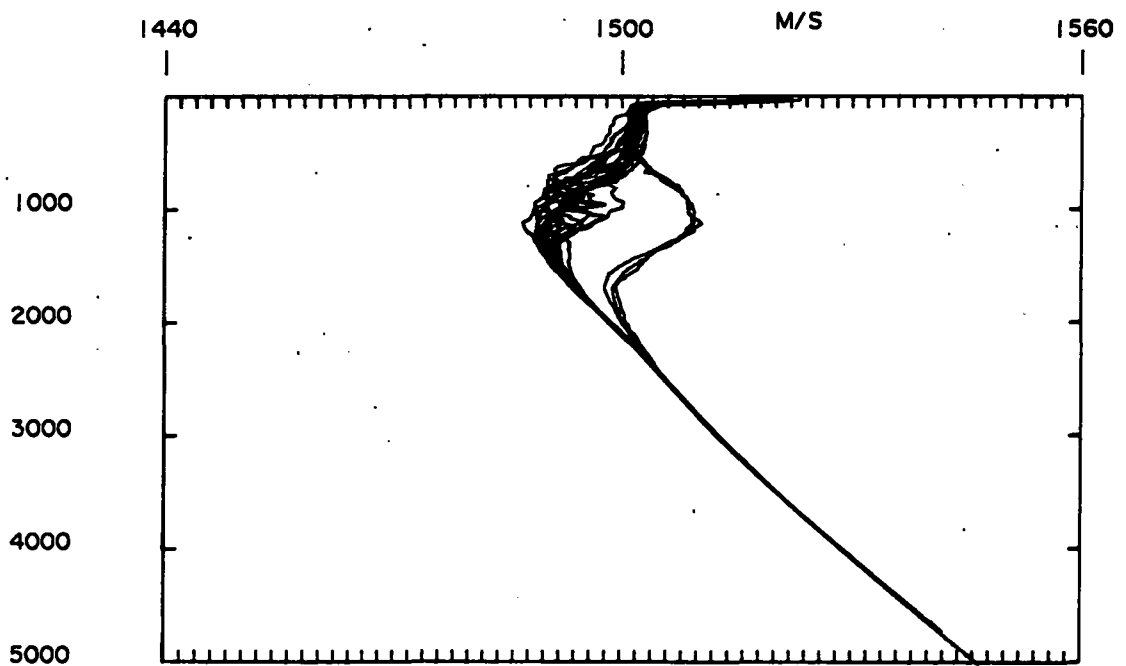
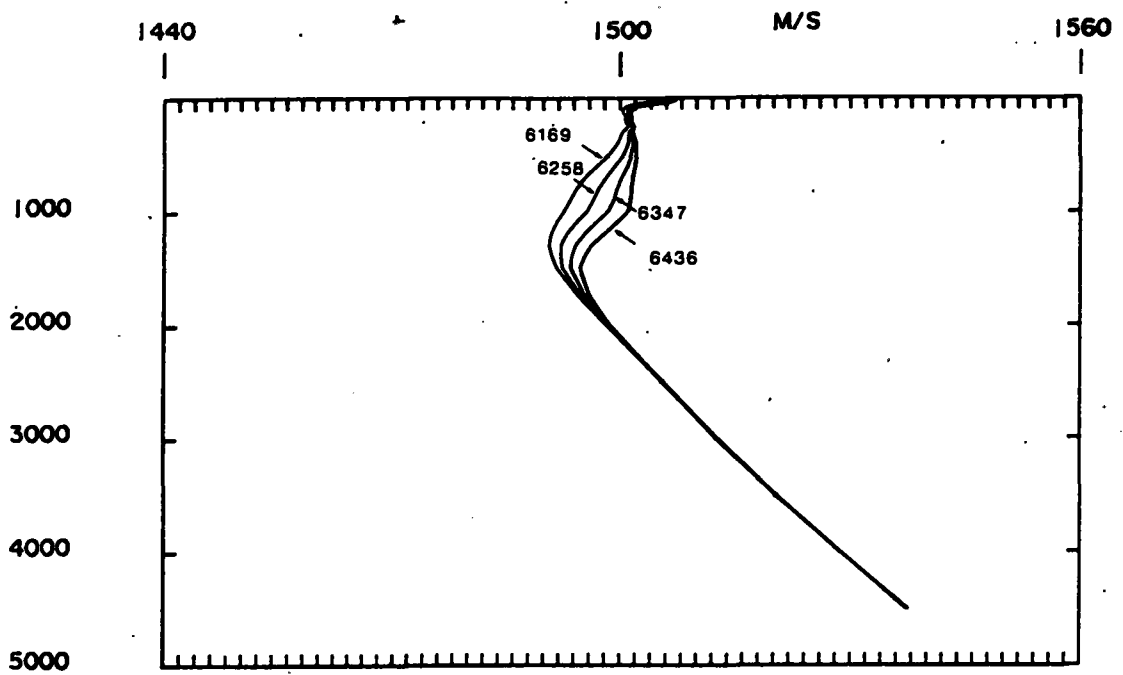


Figure 11 : Sound speed profiles in the top figure are calculated from Levitus *T* and *S* profiles centered at 48°5N-21°5W (n° 6169), 47°5-20°5W (n° 6258), 46°5N-19°5W (n° 6347), 45°5N-18°5W (n° 6436) showing the variation of the mean profiles across the NOAMP region. Profiles in the bottom figure are from CTD measurements obtained in 1983.

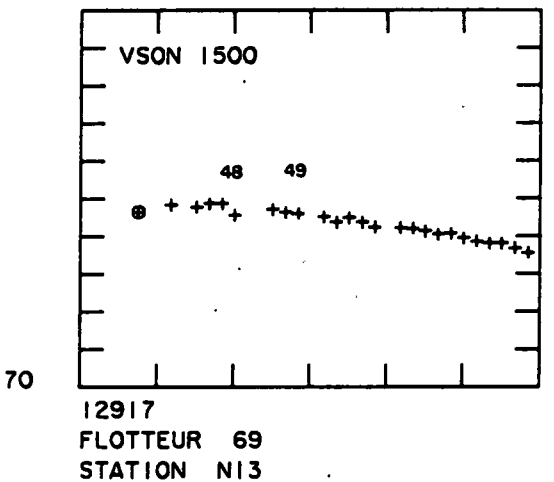
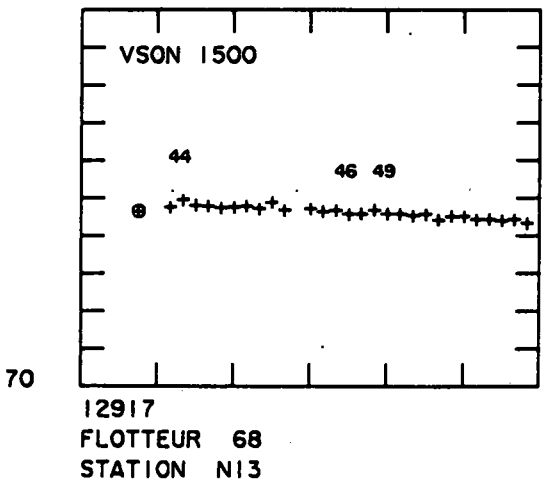
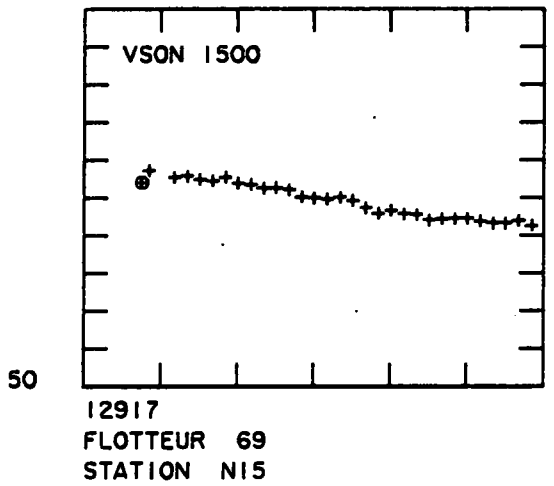
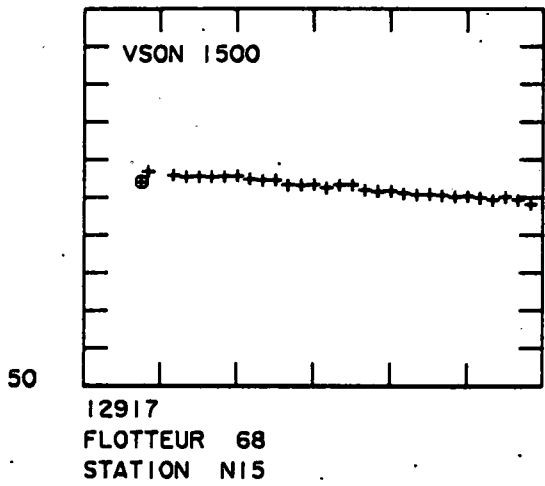
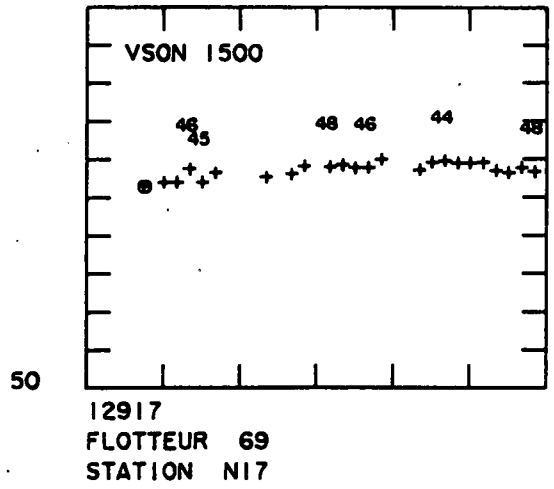
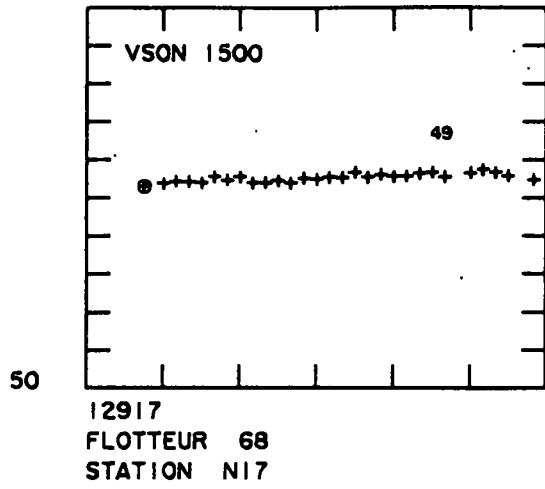


Figure 12 : Times of propagation (ordinates) versus date (abscissae) for six days after launching. The time of propagation at launching, given the mean speed of sound assumed is indicated by \odot . The vertical scale spans 100 s. The assumed sound speed is 1500 m s^{-1} . The correlation values are shown above points computed from correlations whose values are less than 50.

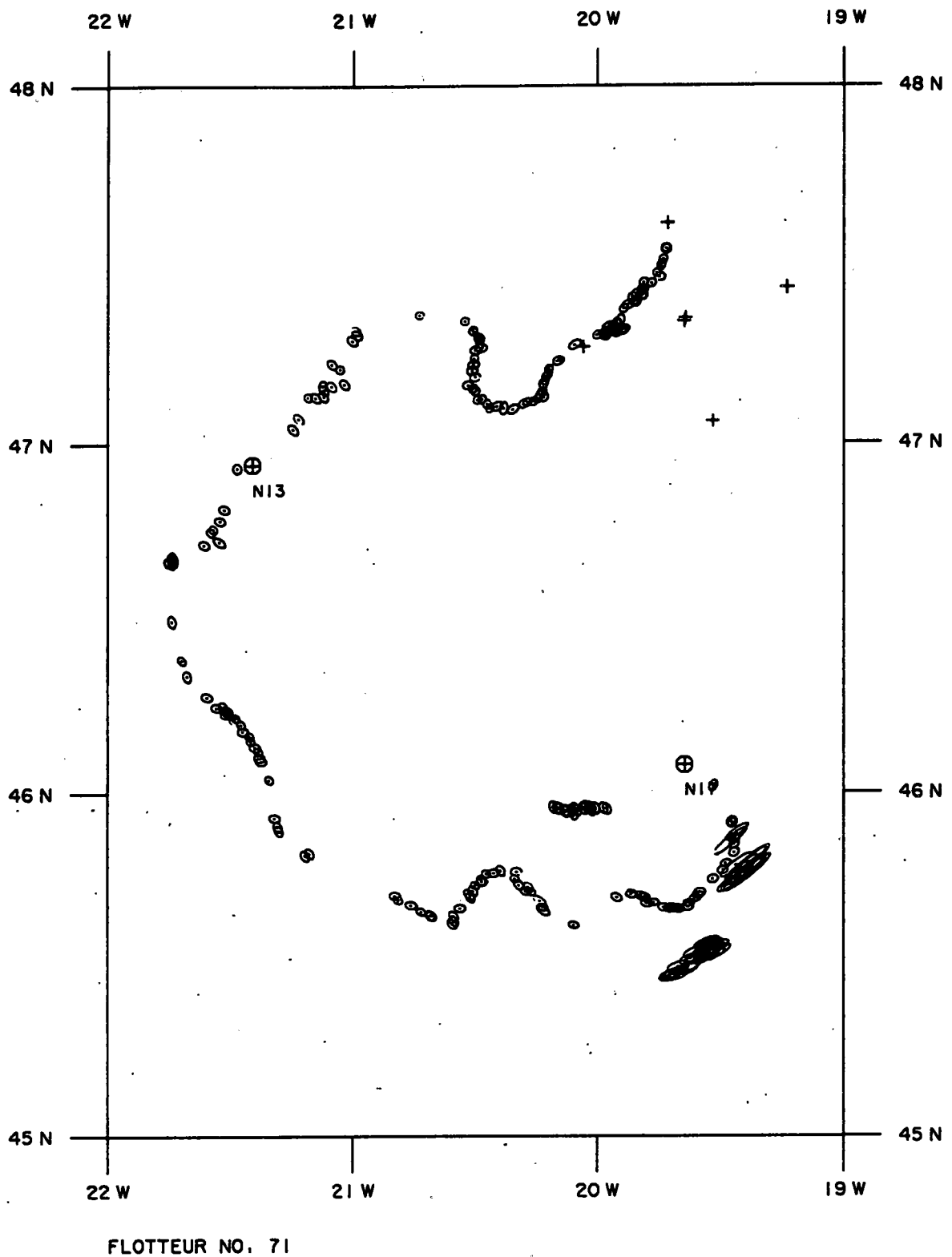


Figure 13 : Error ellipses on position due to geometry of float and station positions. Here probability is ~ 0.5 to find the true position inside the ellipse given a 1 s standard deviation on each time of propagation to the listening stations.

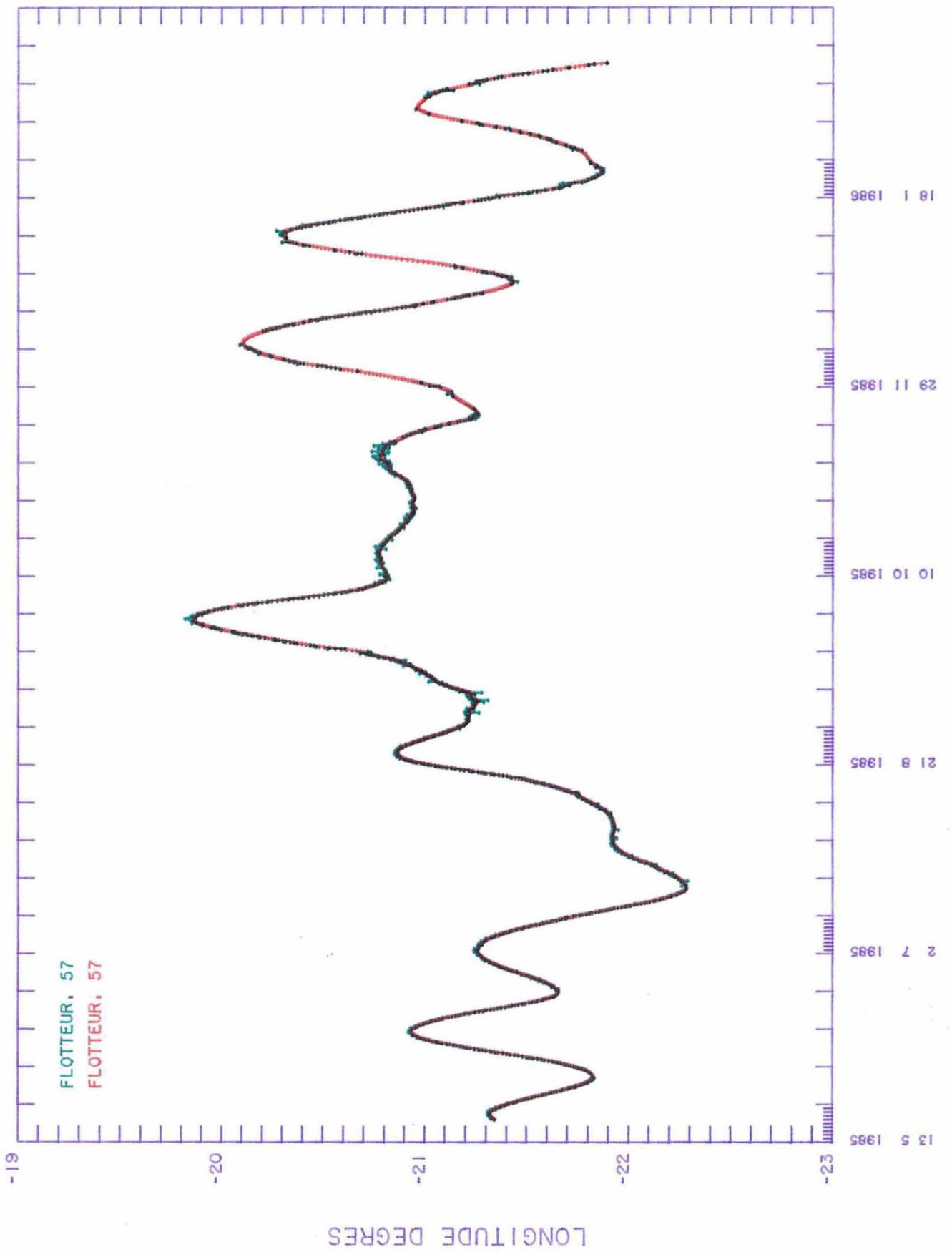


Figure 14 : The curve in green gives the raw longitudes (obvious bad points have already been rejected) and the curve in red is the final fit.

4 BASIC RESULTS AND STATISTICS

Figure 15 shows a composite plot of all float trajectories. The uppermost trajectory is that of float # 57 near 800-900 meters depth, and there is an arrow every 50 days. Deep floats seem to be strongly influenced by topography and have dispersed roughly in a zone $O(200-300 \text{ km})$ in diameter with a weak mean current $O(0.3 \text{ cm.s}^{-1})$ to the southwest after one year. Float # 68 went to the east but it was no longer in the deep layers and so is not relevant. A simpler view may be given by Figure 16 showing overall displacement for each float over its lifetime (given in month near the last position).

For each float, basic statistics (mean velocity, variances and covariance of velocity components, mean and eddy kinetic energy) will be found in section 5 of this report together with individual plots for pressure, temperature and velocity. Table 3 gives an overview of these "Lagrangian" statistics.

Float #	Life time days	\bar{x} km	\bar{y} km	\bar{u} cm.s^{-1}	\bar{v} cm.s^{-1}	$\text{var}(u)$ $\text{cm}^2.\text{s}^{-2}$	$\text{var}(v)$ $\text{cm}^2.\text{s}^{-2}$	covar $\text{cm}^2.\text{s}^{-2}$	EKE $\text{cm}^2.\text{s}^{-2}$	MKE $\text{cm}^2.\text{s}^{-2}$
68	346	213	0	0.6	0.0	5.4	12.0	2.3	8.7	.2
69	285	-269	13	-0.9	0.0	8.2	11.7	0.0	9.9	.6
70	261	-237	145	-0.9	0.6	7.3	6.7	0.8	7.0	.7
71	203	6	-203	0.0	-1.0	18.9	18.2	-0.1	18.5	.5
72	356	-155	-76	-0.4	-0.2	4.6	7.4	1.8	6.0	.1
73	346	15	-230	0.0	-0.7	9.6	8.8	-0.1	9.2	.2
74	354	80	22	0.2	0.1	10.6	10.0	-0.7	10.3	.0
75	246	-23	-231	-0.1	-0.9	12.2	14.1	-5.3	13.1	.5
76	136	-125	-44	-0.9	-0.3	11.0	8.1	-1.5	9.6	.6
77										
78	297	-94	172	-0.3	0.6	7.8	10.3	1.8	9.0	.2
79	344	-32	-205	-0.1	-0.6	4.2	5.9	1.7	5.1	.2
80	238	-23	-111	-0.1	-0.5	6.1	9.1	3.6	7.6	.1
81	344	-16	-261	-0.0	-0.8	2.6	4.3	1.1	3.4	.3
82	165	80	-16	0.5	-0.1	3.5	12.5	2.0	8.0	0.2
57	279	-39	222	-0.1	0.8	33.5	76.5	-2.5	55.0	0.3

Table 3 : Elementary Lagrangian statistics for all the floats.

In this table, \bar{x} and \bar{y} are eastward and northward displacement respectively, u and v east and north velocities.

We can also obtain "Eulerian" statistics by using velocities of floats found inside a given box. We have used $1^\circ \times 1^\circ$ square boxes and the trajectories whose pressure was greater than 3450 dbars. Figure 17 gives an overview of the results. Figure 18 gives mean currents and r.m.s. ellipses for boxes where the number of floats \times days is greater than 50 (number of floats \times days for all the boxes can be found in Figure 17). Table 4 gives the statistics corresponding to Figure 18. In this table is given in this order :

- latitude and longitude of the center of the $1^\circ \times 1^\circ$ square box under consideration,
- number of floats \times days (NFD),
- mean east velocity in cm.s^{-1} and its 90% confidence interval calculated with a Student law with N degrees of freedom ($N = \text{INT}(\text{NFD}/10) + \text{number of floats in the box}$; since we have assumed a Lagrangian integral time scale of 10 days, based on Freeland, Rhines and Rossby (1975)),
- mean north velocity in cm.s^{-1} and its 90% confidence interval,
- east and north velocities variance and covariance in $\text{cm}^2.\text{s}^{-2}$,
- principal standard deviations s_1 and s_2 in cm.s^{-1} and their 90% confidence intervals (given here as a percentage i.e. probability $(\sigma < \text{inf} \times s) = 0.05$ and probability $(\sigma < \text{sup} \times s) = 0.95$) calculated with a chi square law since $(N - 1)s^2/\sigma^2 = \chi_{N-1}^2$,
- the direction of the greatest principal deviation,
- an isotropic test for the principal variances with a 90% confidence level. Assuming $\sigma_1 = \sigma_2$, $\frac{s_1^2}{s_2^2}$ should follow a Fisher law with $(N - 1, N - 1)$ degrees of freedom. If the result of the statistical test is negative we can suspect non isotropy.
- eddy kinetic energy in $\text{cm}^2.\text{s}^{-2}$ and ratio of eddy over mean kinetic energy.

The calculation of dispersion coefficients is deferred to a later paper but a first look at trio dispersion can be obtained through Figure 19 which displays floats displacements in a sequence of 50 day periods.

Although the deep floats varied in depth from 2600 to 4100 meters (Figure 20 or Figure 6) eddy statistics should not be very different since the zero crossing of the first baroclinic mode is around 1500 meters (Figure 22). Only three of the floats (# 68, 72 and 82) rose above 3500 dbars, and for depths greater than 3400 meters (3500 dbars corresponds roughly to 3435 m) we can also assume quasi constant second and third mode baroclinic structure.

No trio was successfully deployed in the sense that no three floats arrived at the same depth upon deployment. However the coherent vertical structures over intervals of order 300 meters observed during the first days after launch support our statistical hypothesis about mesoscale motions and lend confidence to further dispersion studies using this data set.

The temperature plot shown on Figure 21 bis (for floats # 78, 79 and 81) suggests a north south gradient of $0.1^\circ/100$ km at 3400 meters depth which is quite strong. On individual trajectories (see section 5), Taylor column- like structures may be seen on occasions. Figure 23 shows a bathymetric map of the NOAMP zone obtained with a "Seabeam" sonar. A transparency of it is included in this data report to superpose on individual trajectories revealing topographic constraints.

Motions with frequencies greater than 1 cycle.day^{-1} have been filtered, but such filtering should not alter the float trajectories significantly since Lagrangian displacements associated with periods smaller than 1 day are small compared to mesoscale Lagrangian displacements (even though velocities are not). It is hoped that we will be able to learn more about these submesoscale motions in the future through better data processing.

As seen in Tables 3 and 4, mean velocities for the deep floats are $O(1 \text{ cm.s}^{-1})$ while r.m.s. velocities are $O(3-5 \text{ cm.s}^{-1})$. Deep jet-like motion (velocities up to 10 cm.s^{-1} for 10 to 20 days) have been occasionally observed. They are not at first sight associated with funneling by deep canyons, but the "Seabeam" survey does not cover the region concerned and we must be careful about conclusions requiring detailed knowledge of the topography.

A dimensional analysis of the dispersion of the float cluster implies mesoscale horizontal eddy diffusivity $K_H \approx O(10^6 \text{ cm}^2.\text{s}^{-1})$ at 3400 meters depth). Comparable thermocline values are $O(10^7 \text{ cm}^2.\text{s}^{-1})$ (Freeland, Rhines and Rossby, 1975).

Eddy Kinetic Energy (EKE) is $O(10 \text{ cm}^2.\text{s}^{-2})$ for the deep floats around 3400 m and $O(50 \text{ cm}^2.\text{s}^{-2})$ for float number 57 at 800 meters depth. These values are fully compatible with those obtained by eulerian measurements in the same region. Eulerian measurements at the same latitude but west of the mid-Atlantic ridge indicate EKE of $O(40 \text{ cm}^2.\text{s}^{-2})$ near 4000 m, showing that EKE at great depths is less in the eastern basin than in the western basin (Colin de Verdière, Mercier and Arhan, 1988).

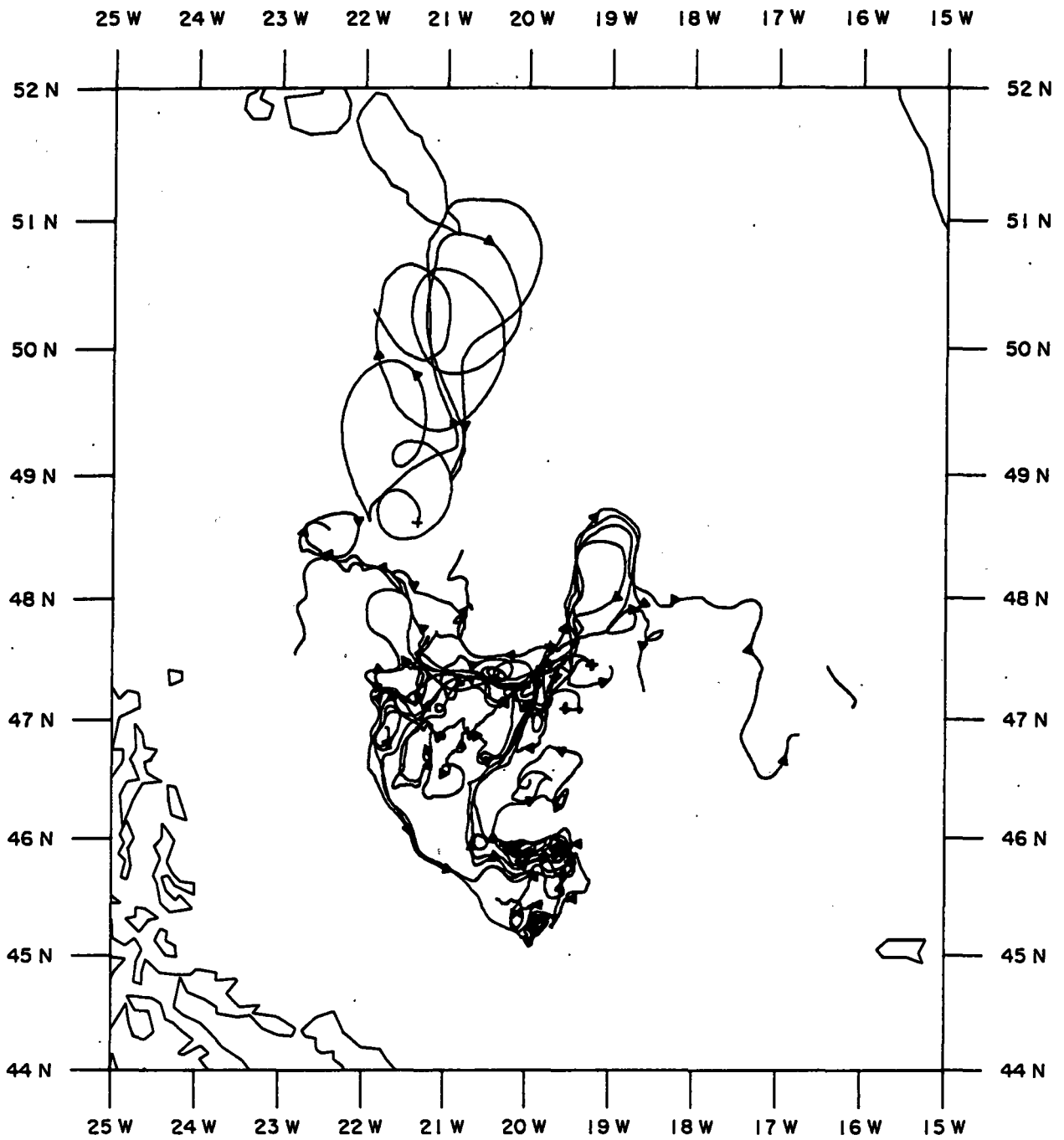


Figure 15 : All the float trajectories. The uppermost trajectory is that of float # 57 (at ~ 800 m depth). There is an arrow every 50 days.

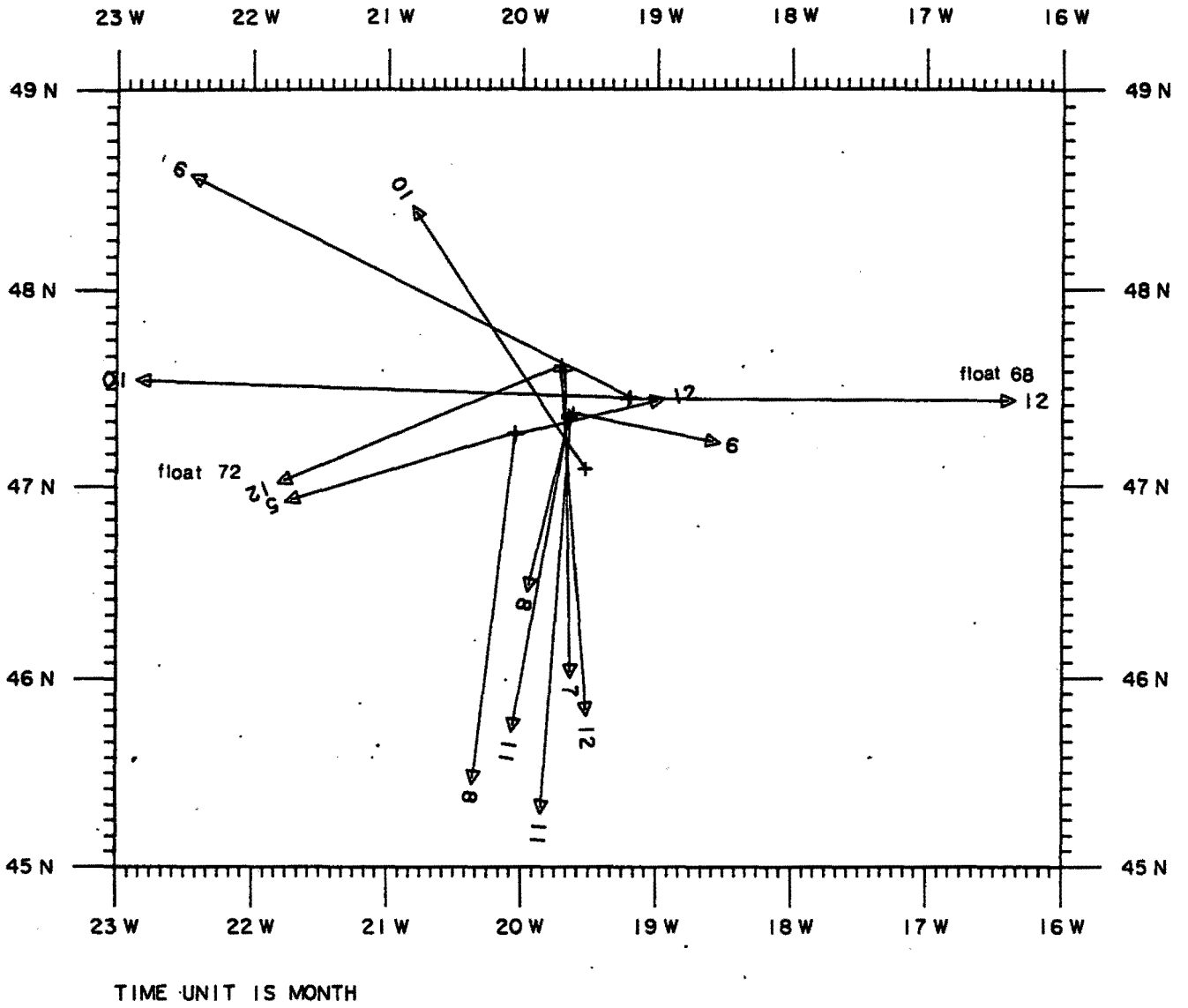


Figure 16 : Composite first and last point plot for the deep floats. The number of months is indicated near the last position of the floats.

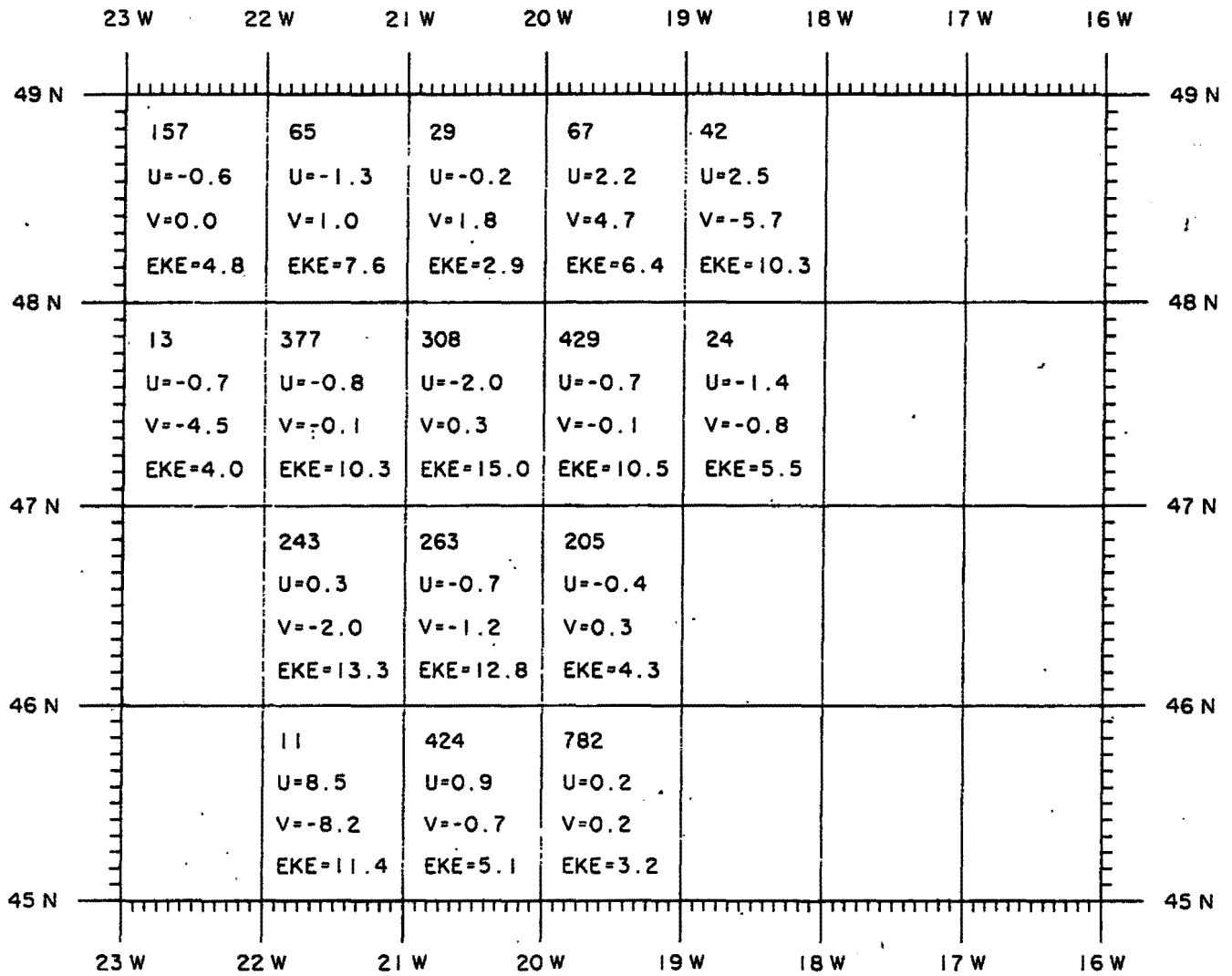


Figure 17 : Elementary "Eulerian" statistics for the deep floats in $1^\circ \times 1^\circ$ boxes. Number of floats \times days, \bar{u} ($\text{cm}\cdot\text{s}^{-1}$), \bar{v} ($\text{cm}\cdot\text{s}^{-1}$) and EKE ($\text{cm}^2\cdot\text{s}^{-2}$) are given in each box.

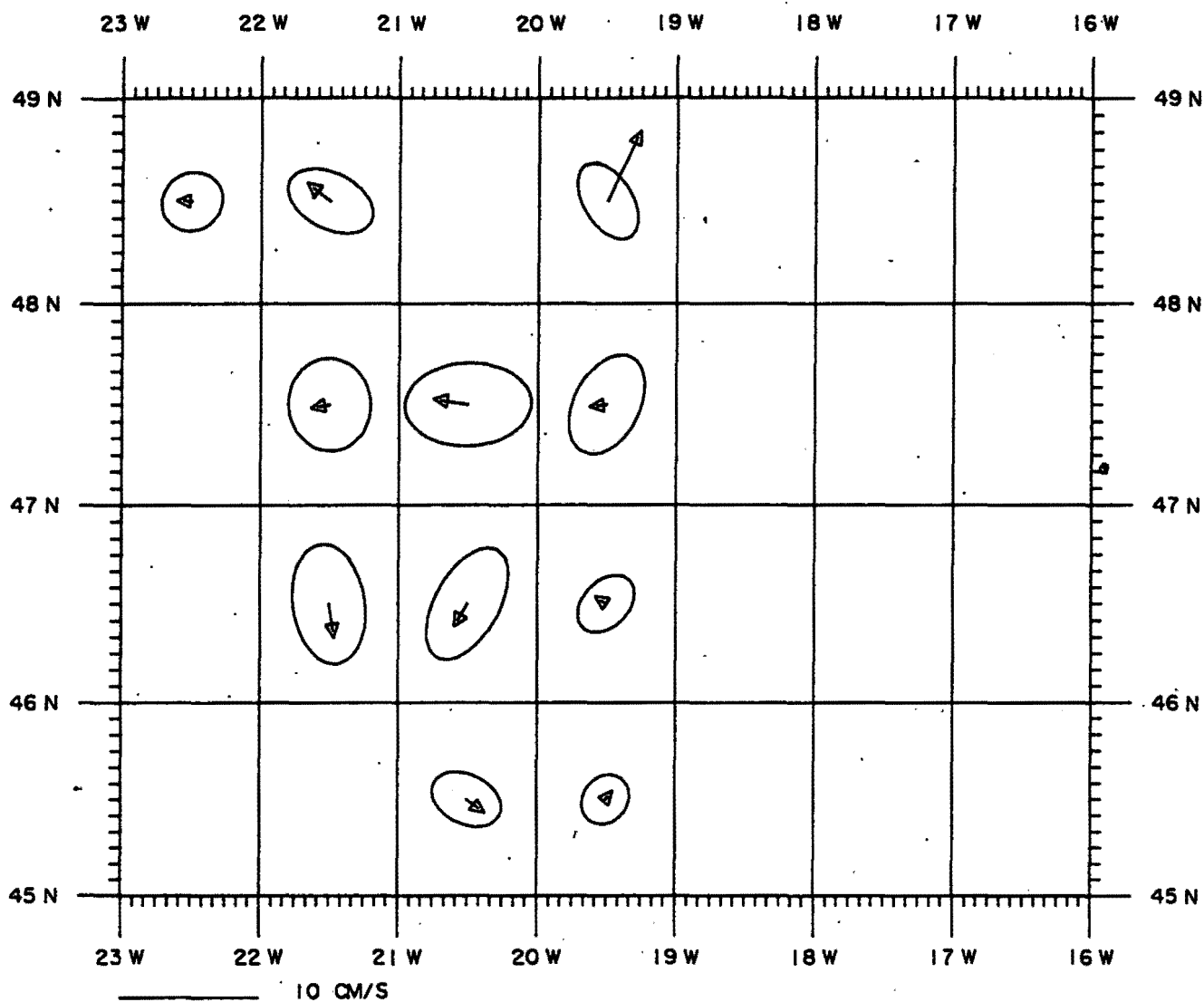


Figure 18 : Mean velocity and r.m.s. ellipses for the deep floats in $1^\circ \times 1^\circ$ boxes with more than 50 floats \times days (see Figure 17). Axes of these ellipses are principal standard deviations (square root of principal variances) and the probability that eddy current be inside the ellipse is 0.4 (under a Gaussian hypothesis).

Lat N	45.5	45.5	46.5	46.5	46.5	47.5	47.5	47.5	48.5	48.5	48.5
Long W	20.5	19.5	21.5	20.5	19.5	21.5	20.5	19.5	22.5	21.5	19.5
Number of floats × days	424	781	243	263	204	377	307	425	157	65	67
\bar{u} cm.s ⁻¹	.88	.19	.29	-.69	-.40	-.84	-1.96	-.73	-.61	-1.26	2.17
Error on \bar{u}	±.60	±.32	±.82	±.88	±.68	±.75	±1.17	±.63	±.93	±1.92	±1.28
\bar{v} cm.s ⁻¹	-.67	.22	-1.97	-1.21	.27	-.15	.32	-.08	.04	1.03	4.67
Error on \bar{v}	±.49	±.33	±1.35	±1.23	±.69	±.86	±.78	±.83	±.92	±1.48	±1.63
Var(u) cm ² .s. ⁻²	6.16	3.00	7.14	8.69	4.30	8.94	20.76	7.67	4.85	9.57	4.88
Var(v) cm ² .s. ⁻²	4.08	3.31	19.46	16.89	4.38	11.61	9.33	13.24	4.74	5.68	7.89
Covar cm ² .s. ⁻²	-1.52	.48	-1.88	6.24	1.55	-.23	.59	3.78	.39	-2.85	-2.82
σ max cm.s ⁻¹	2.64	1.91	4.44	4.50	2.43	3.41	4.56	3.89	2.28	3.33	3.10
σ min cm.s ⁻¹	1.81	1.63	2.62	2.31	1.67	2.99	3.05	2.40	2.10	2.04	1.79
Lower bound on σ (%)	86	89	83	83	82	85	85	86	78	72	73
Upper bound on σ (%)	121	115	127	127	130	122	122	120	142	171	165
Direction degrees	-28	54	99	62	46	95	3	63	41	-28	121
Isotropy (yes or no)	no	yes	no	no	no	yes	no	no	yes	yes	yes
EKE cm ² .s. ⁻²	5.1	3.2	13.3	12.8	4.3	10.3	15.0	10.5	4.8	7.6	6.4
EKE/MKE	8	74	7.	13	37	28	8	39	26	6	0.5

Table 4 : "Eulerian" statistics for the deep floats in 1° × 1° boxes with more than 50 floats × days.

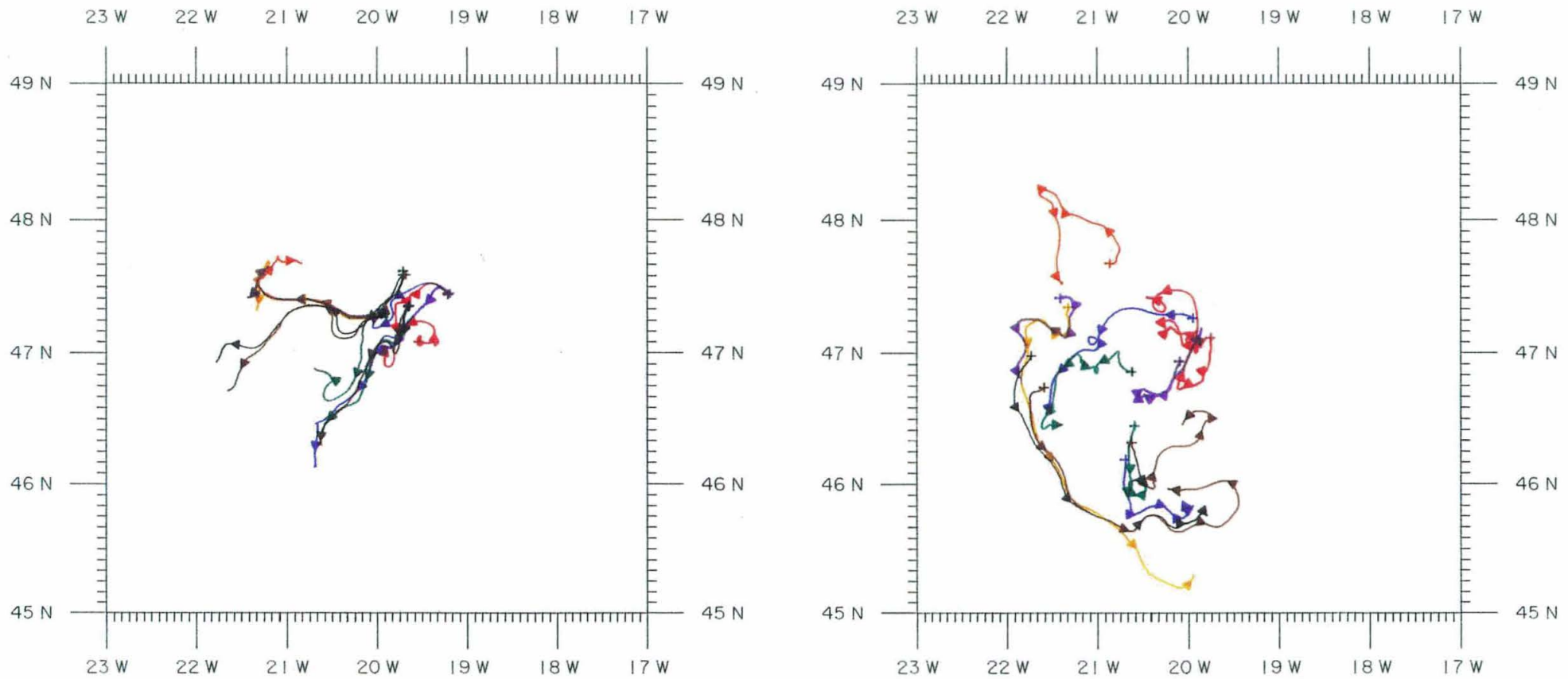


Figure 19 : Deep float trajectories for days n° 12917 to 12950 (left frame), and days n° 12950 to 13000 (right frame). There is an arrow every 10 days.

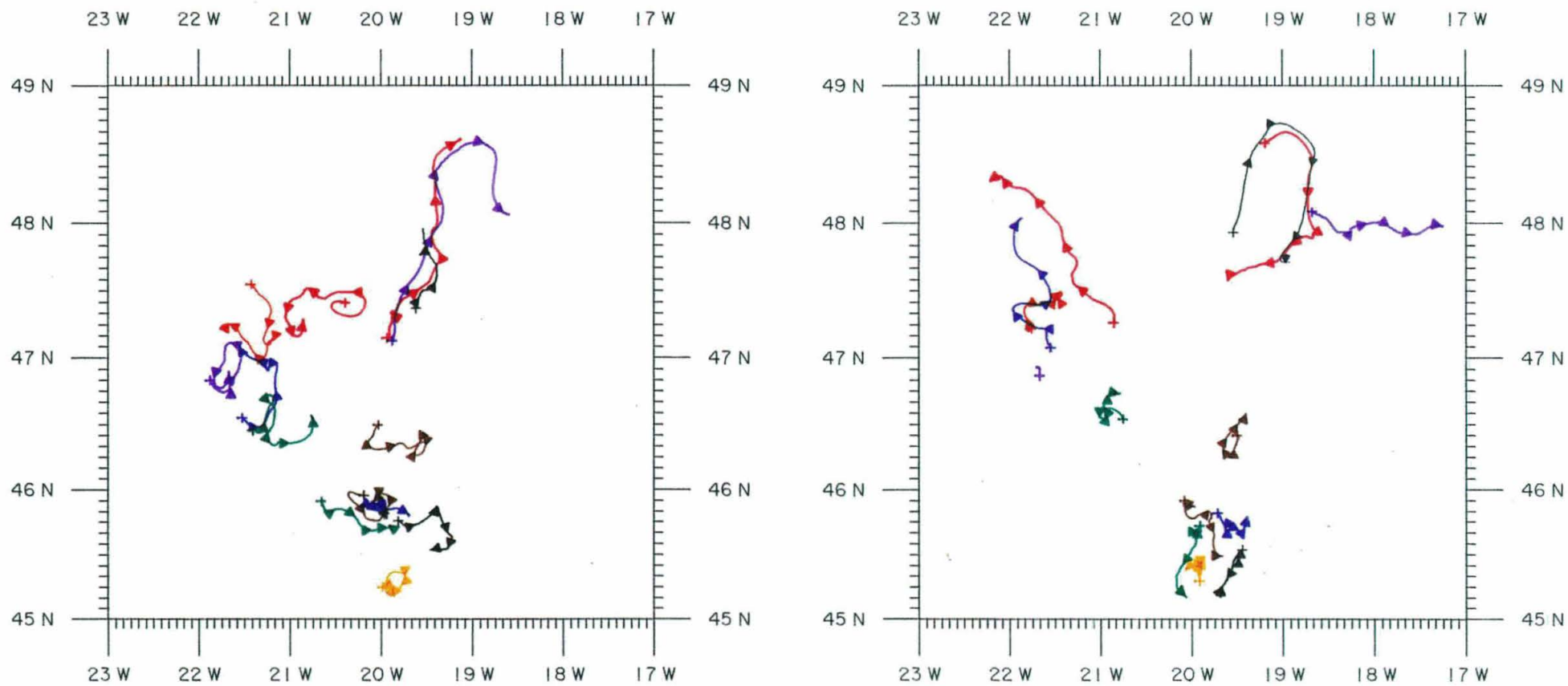


Figure 19 bis : Deep float trajectories for days n° 13000 to 13050 (left) and days n° 13050 to 13100 (right).

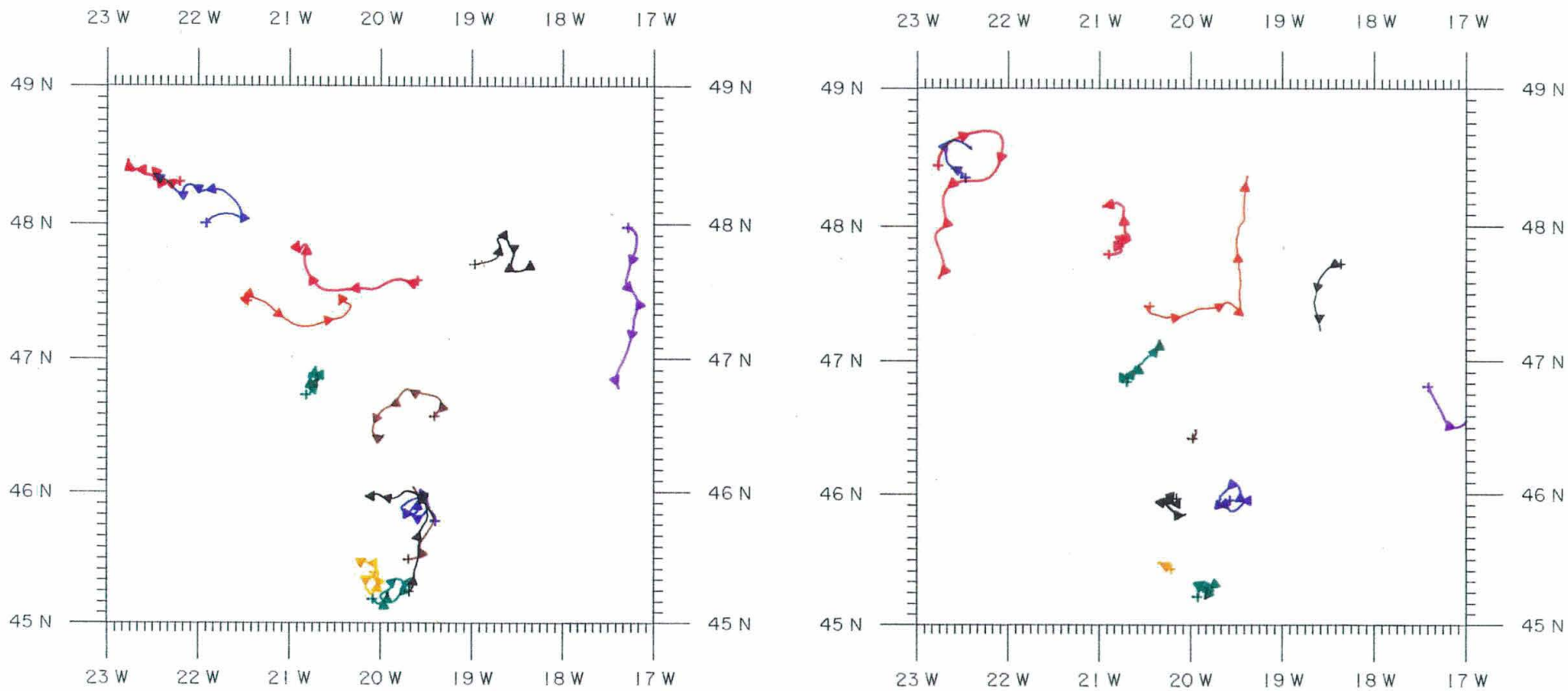
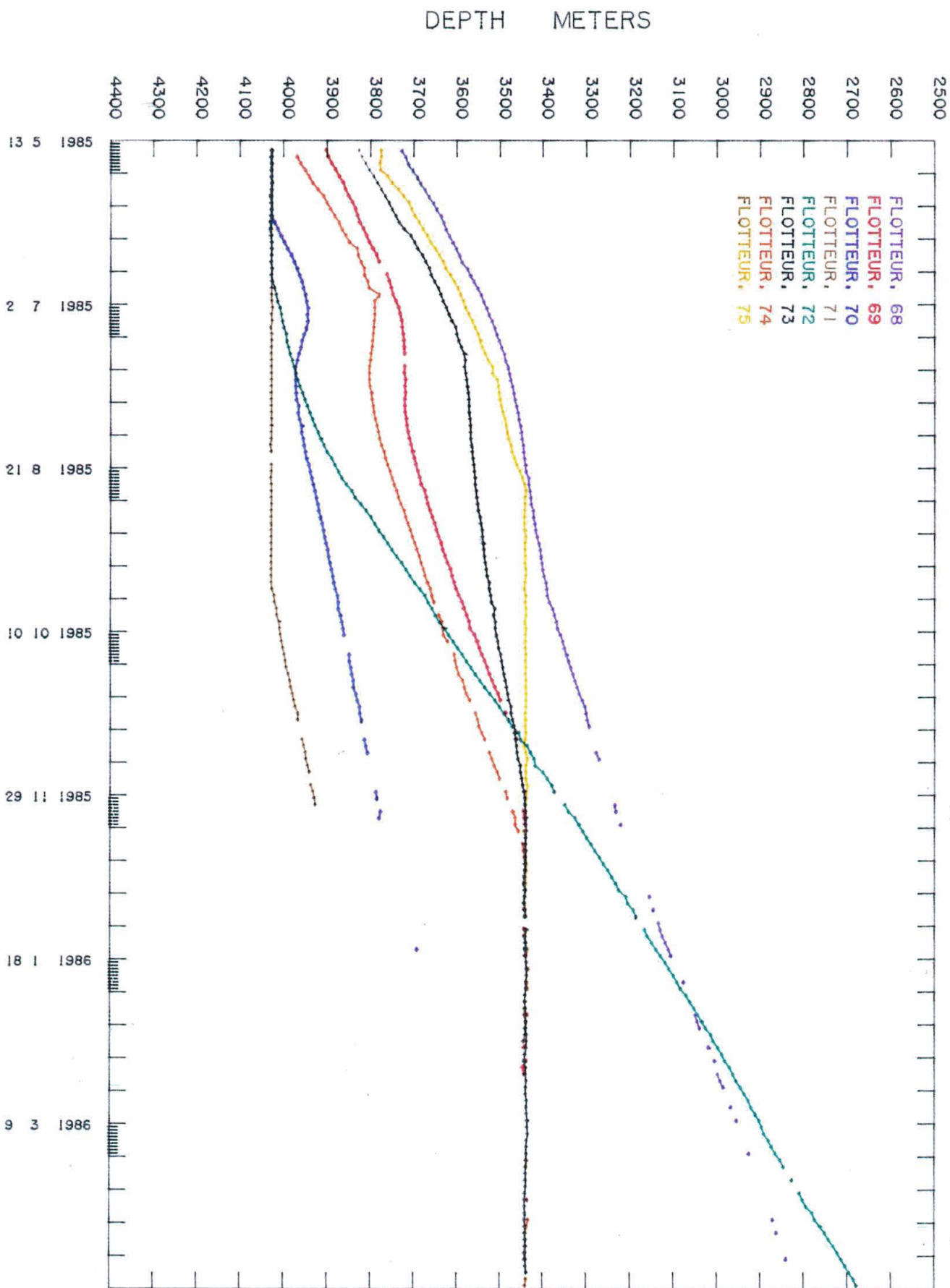


Figure 19 ter : Deep float trajectories for days n° 13100 to 13150 (left) and days n° 13150 to 13200 (right).

Figure 20 : Depth history for deep floats 68, 69, 70, 71, 72, 73, 74 and 75.



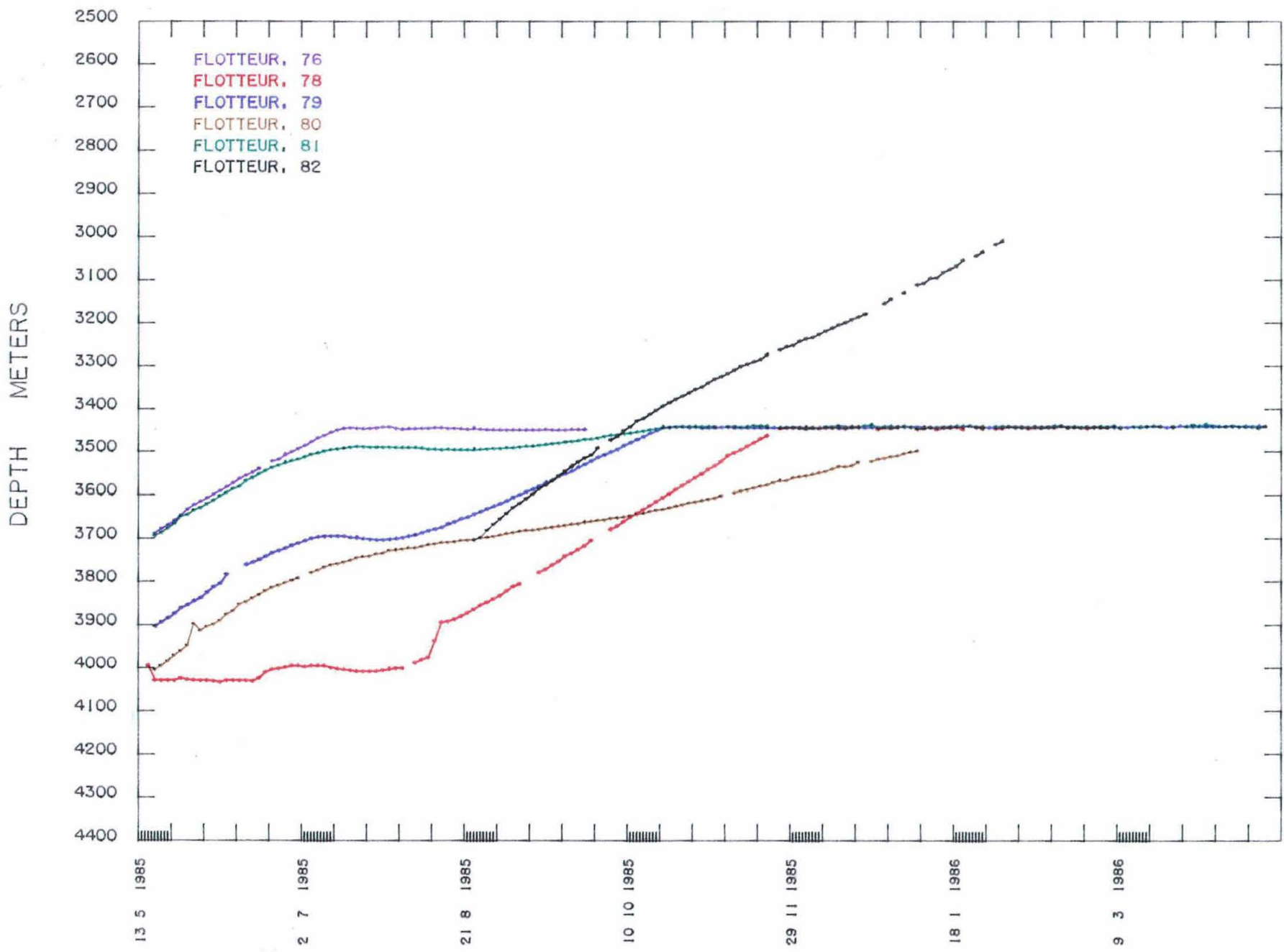
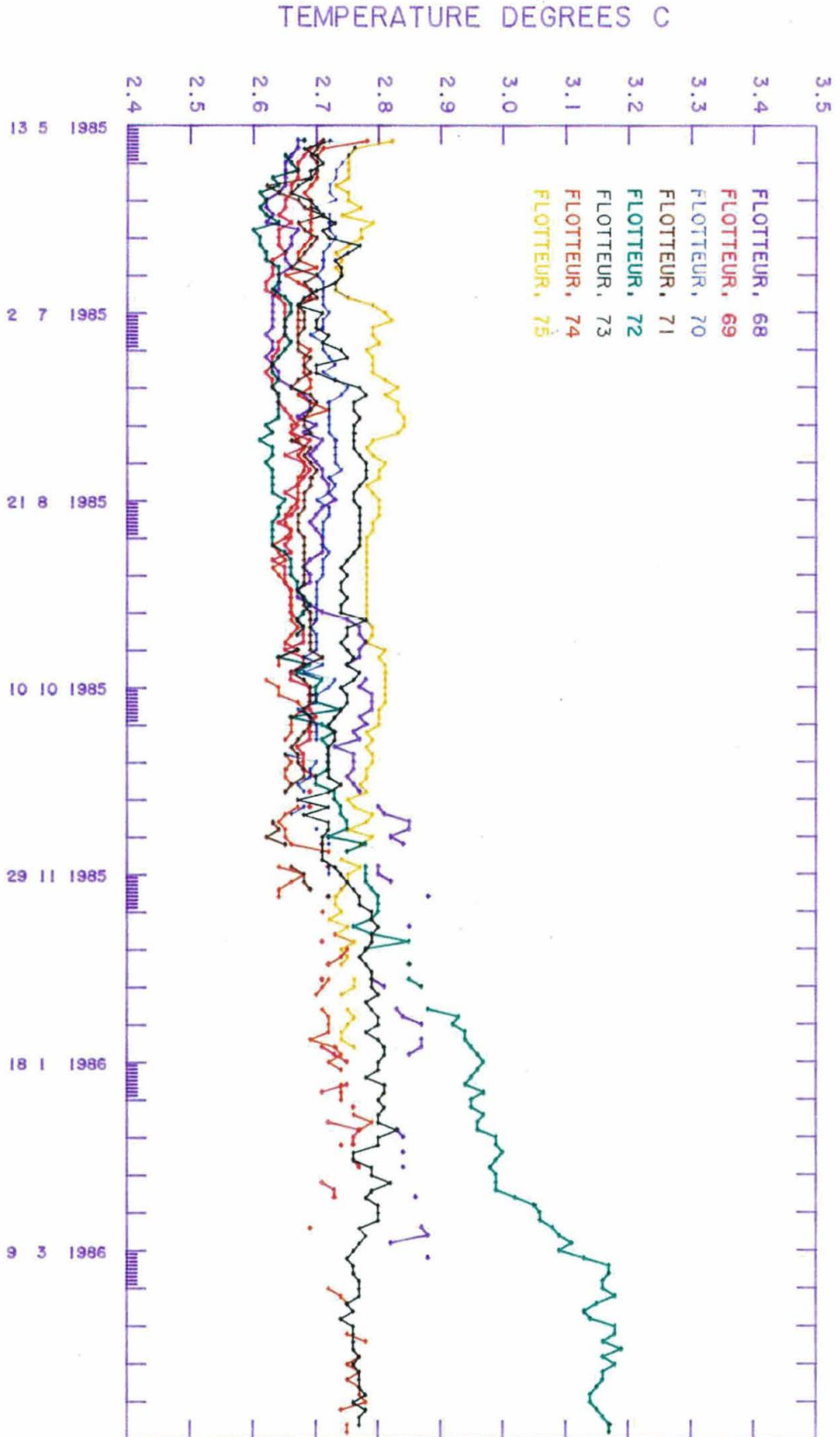


Figure 20 bis : Depth history for deep floats 76, 78, 79, 80, 81 and 82.

Figure 21 : Temperature as seen by floats 68, 69, 70, 71, 72, 73, 74 and 75.



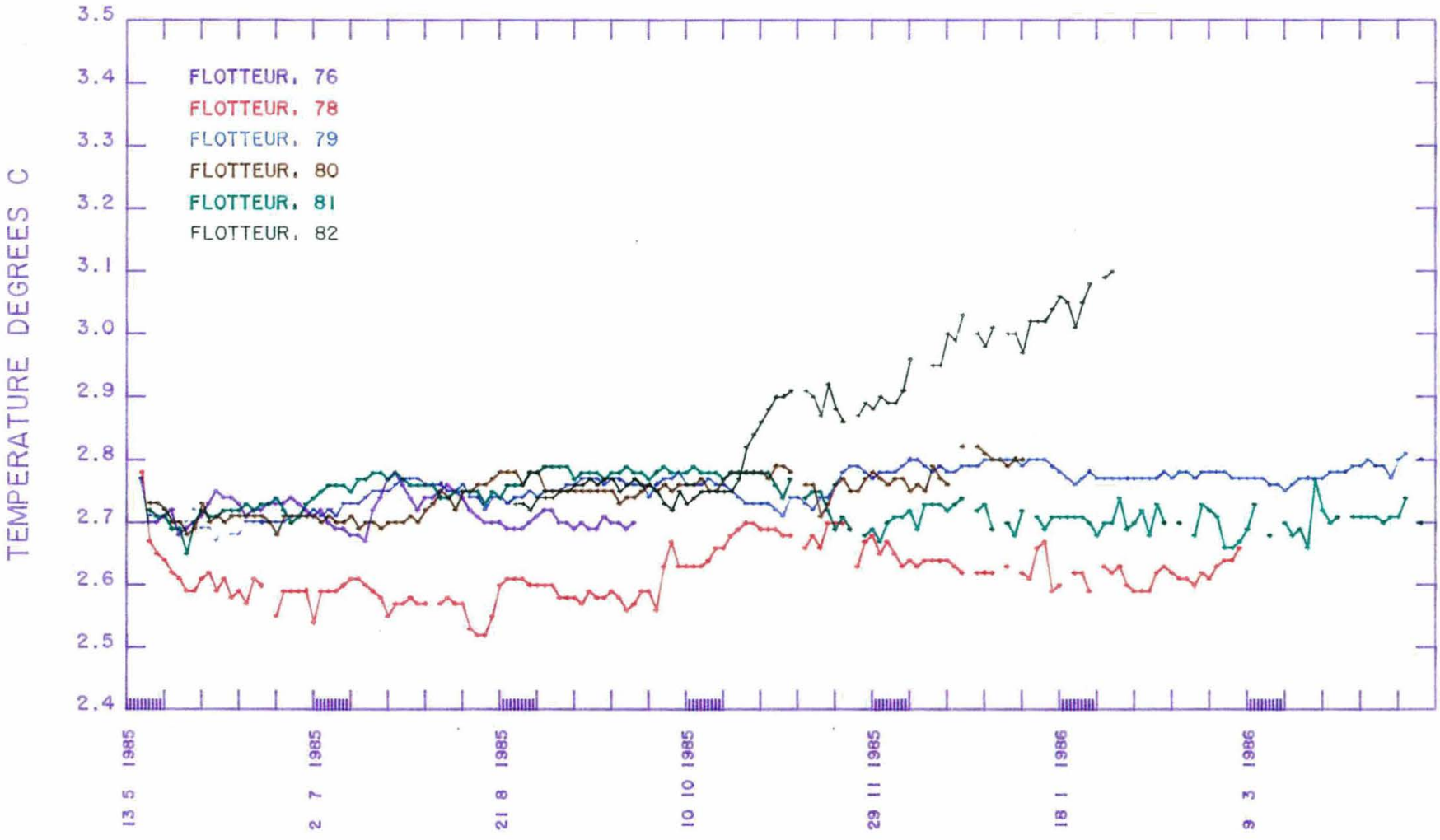


Figure 21 bis : Temperature as seen by floats 76, 78, 79, 80, 81 and 82.

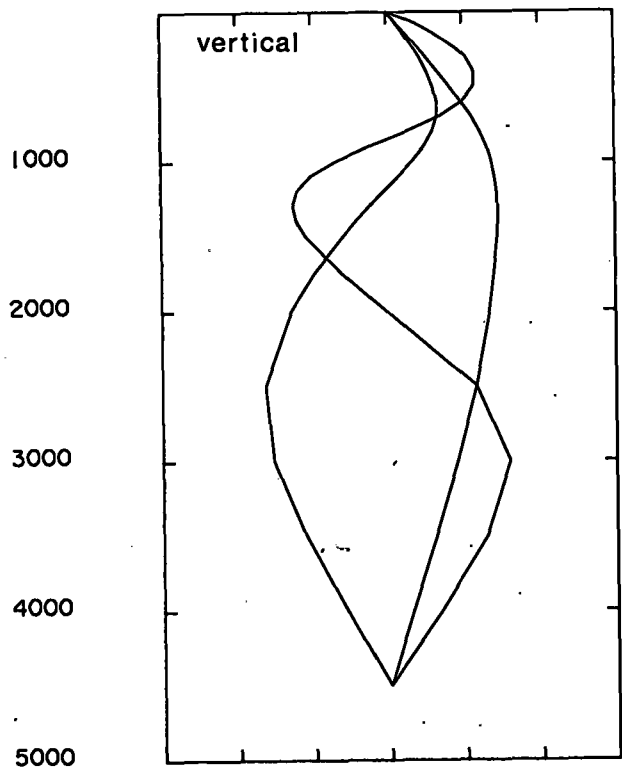
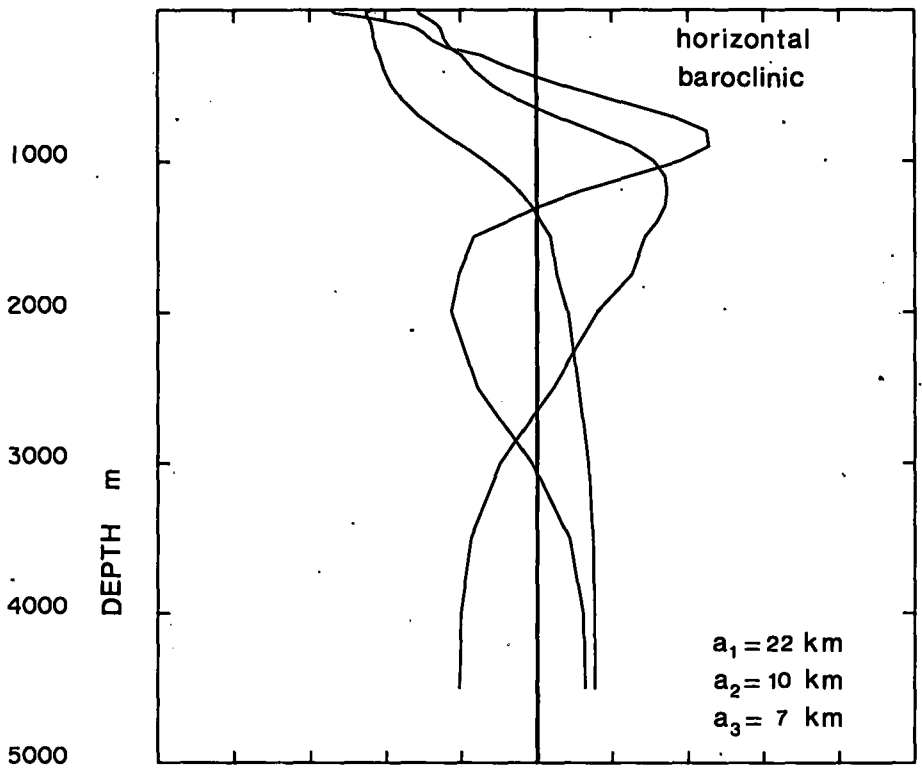


Figure 22 : Normal modes for the Levitus profile centered at 46°5N, 19°5W.

H. Heinrich: Bathymetrie und Geomorphologie des NOAMP-Gebietes, Westeuropäisches Becken (17° W bis 22° W, 46° N bis 49° N)

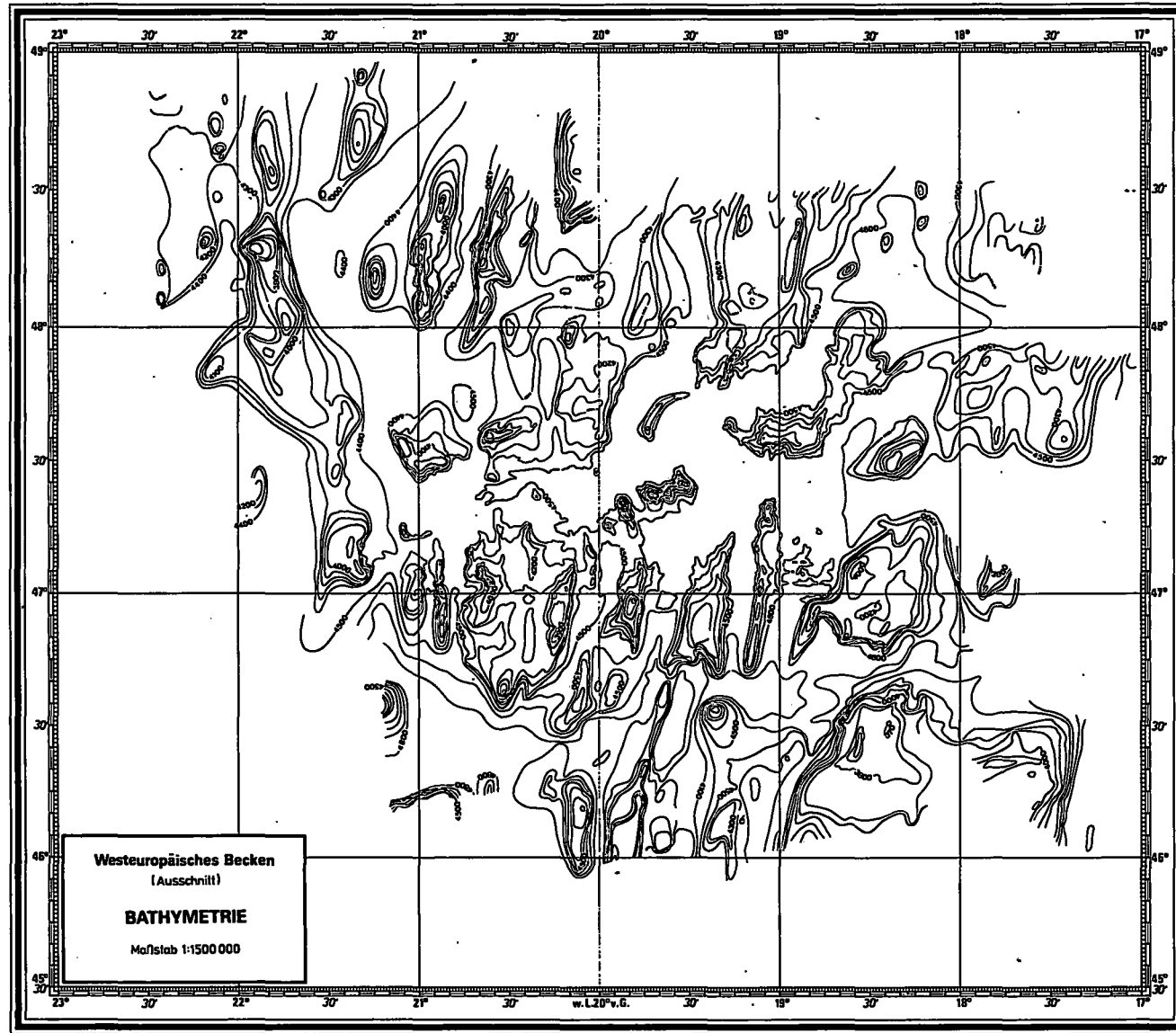


Figure 23 : Bathymetric map of the NOAMP region obtained by H. Heinrich (1986).

5 STATISTICS AND PLOTS OF INDIVIDUAL FLOATS

Lagrangian statistics, a trajectory plot, a velocity stick diagram, temperature and pressure plots are presented for each float.

The trajectory for each float is plotted on a Mercator projection using the same scale as the bathymetric map given in Figure 23 or in the transparency.

Along the trajectories, crosses denote the first float position, arrows mark the positions every 50 days, numbered with their Julian days referred to 1950 (Appendix B).

Stick plots show velocity every day, obtained by averaging over six 4 h sampling intervals.

NOAMP experiment

float no: 57

launch date	launch lat	launch long			
1985 5 19 5h UT	48.59 N	-21.34 W			
date of first pos	first lat	first long	init. pres.	init. temp.	
1985 5 19 7h UT	48.62 N	-21.34 W	933.	5.22	
date of last pos	last lat	last long	last pres.	last temp.	life (days)
1986 2 22 15h UT	50.31 N	-21.89 W	801.	7.48	279.3

total displacement 279.4 days after launching

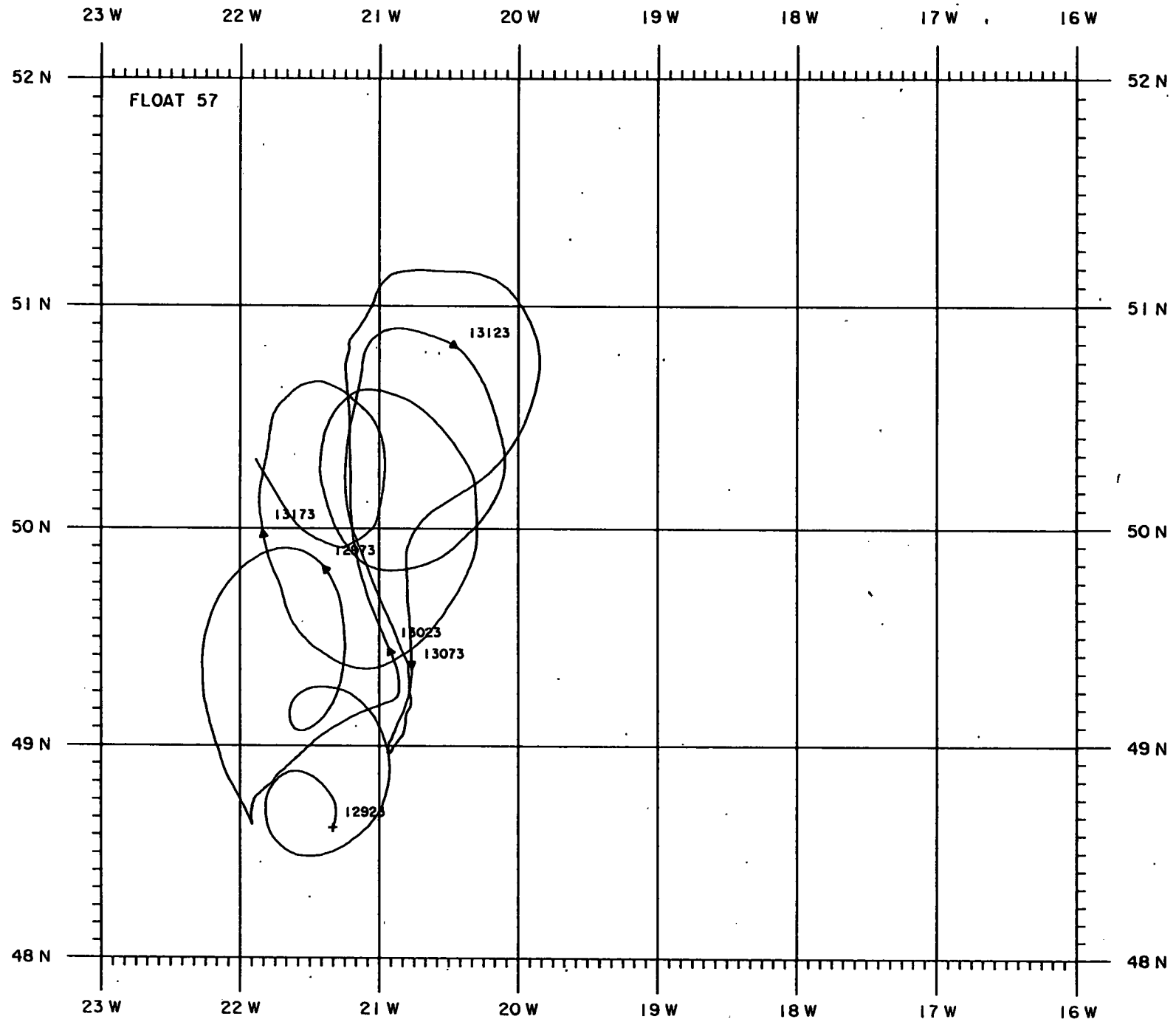
eastward displacement= -39.3 km mean eastward velocity= -0.14 cm/s
northward displacement= 221.7 km mean northward velocity= 0.79 cm/s

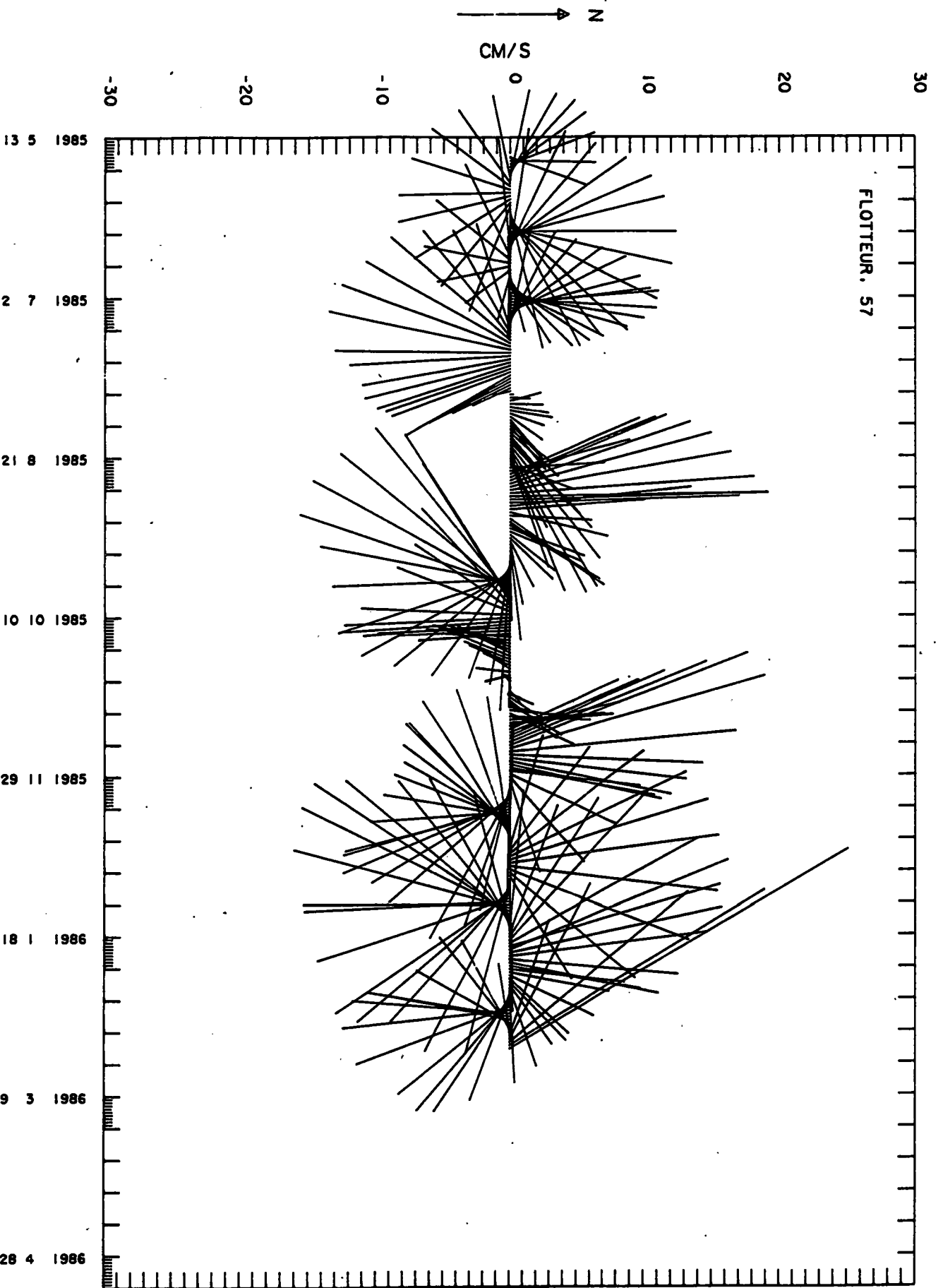
velocity time series statistics:

number of samples= 1677
average east velocity comp.= -0.18 cm/s
average north velocity comp.= 0.79 cm/s
variance of east velocity comp.= 33.50 cm²/s²
variance of north velocity comp.= 76.54 cm²/s²
covariance= -2.51 cm²/s²

EKE= 55.02 cm²/s²
MKE= 0.33 cm²/s²

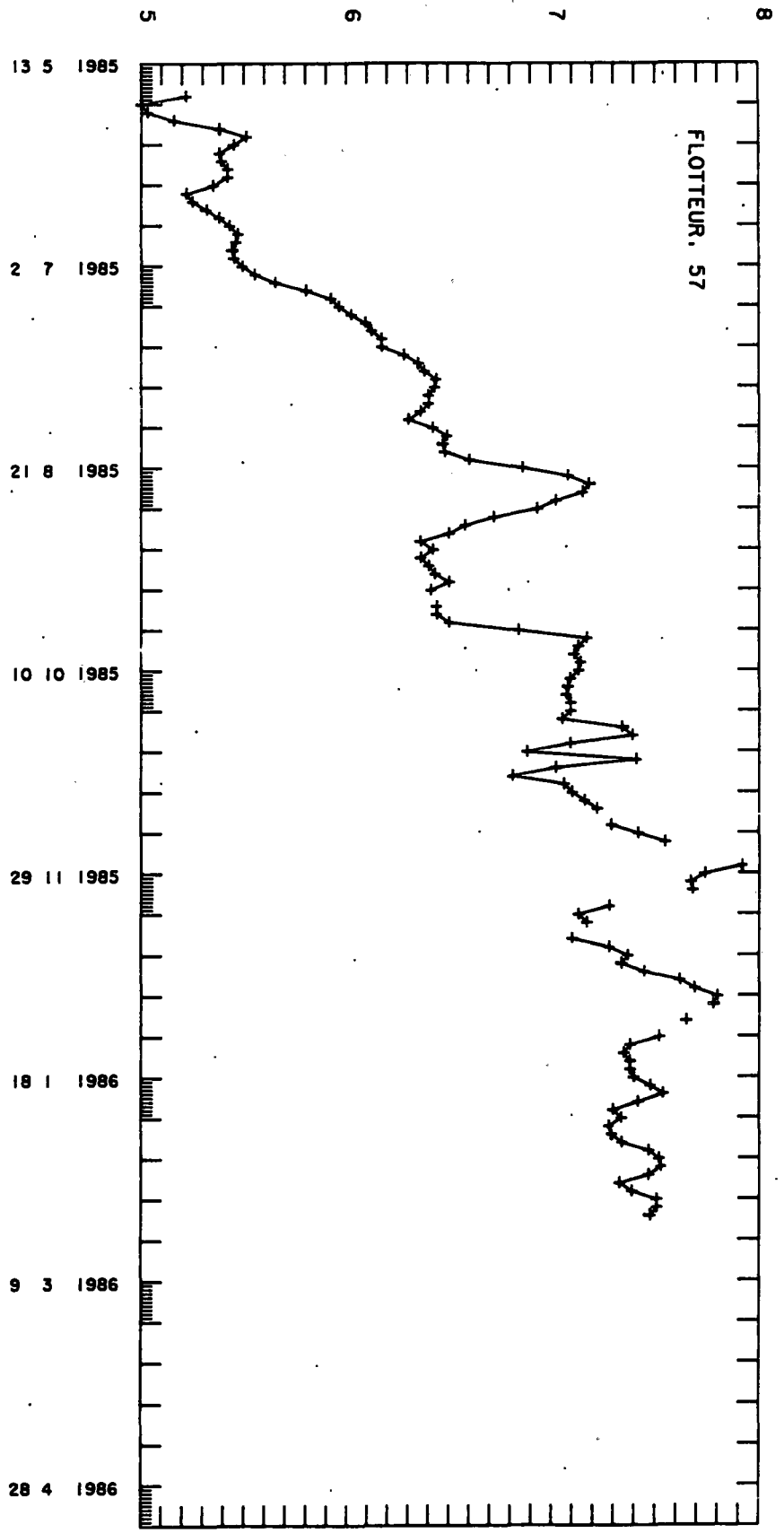
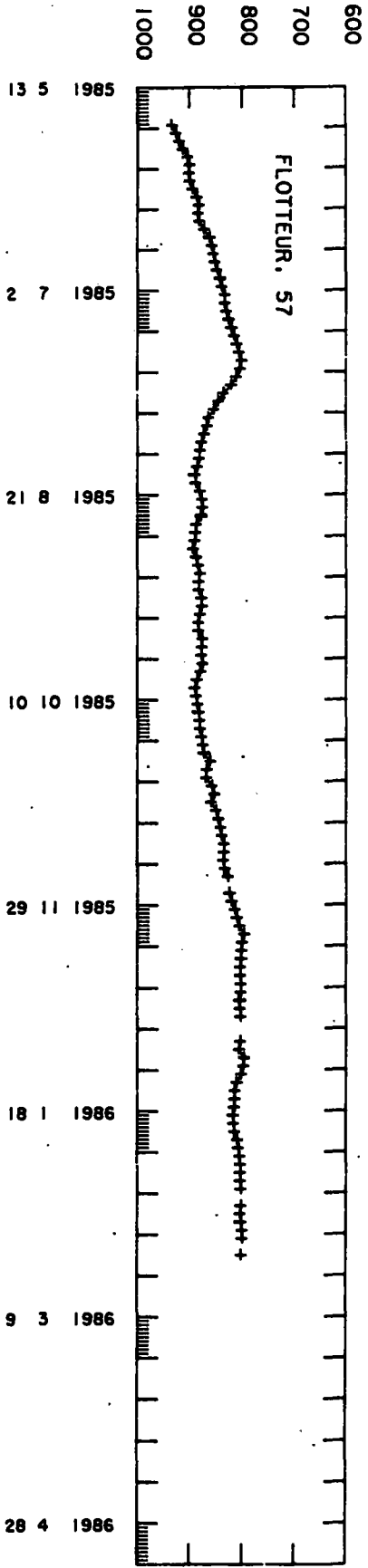
covar(u,temp)= -0.29 cm.degreeC/s
covar(v,temp)= -0.18 cm.degreeC/s





PRESSURE DBARS

TEMPERATURE DEGREES C



NOAMP experiment

float no: 68

launch date	launch lat	launch long			
1985 5 13 18h UT	47.44 N	-19.23 W			
date of first pos	first lat	first long	init. pres.	init. temp.	
1985 5 14 4h UT	47.45 N	-19.21 W	3787.	2.67	
date of last pos	last lat	last long	last pres.	last temp.	life (days)
1986 4 24 16h UT	47.44 N	-16.40 W	2880.	2.88	345.5

total displacement 345.9 days after launching

eastward displacement= 212.8 km mean eastward velocity= 0.62 cm/s
northward displacement= -0.1 km mean northward velocity= 0.00 cm/s

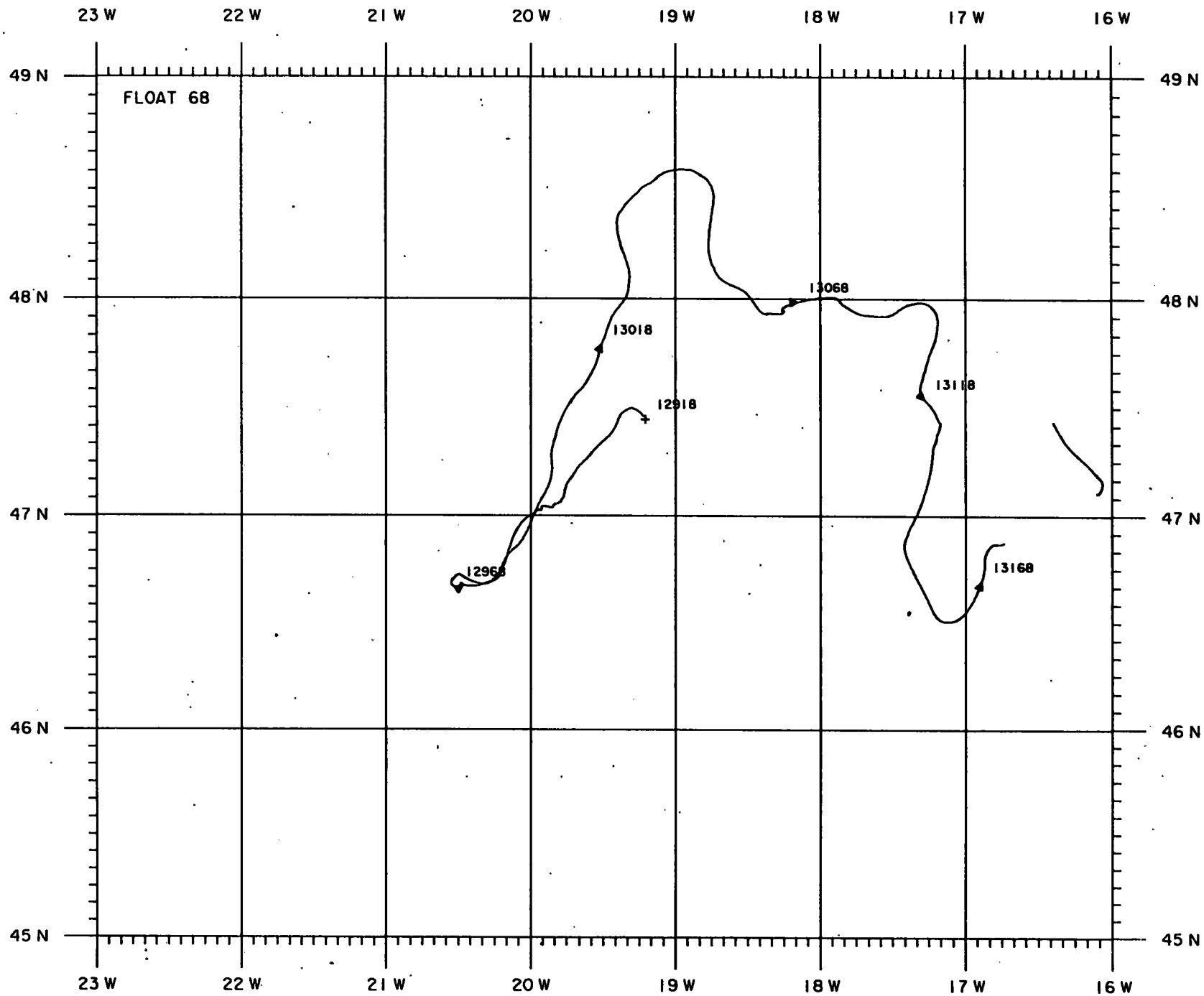
velocity time series statistics:

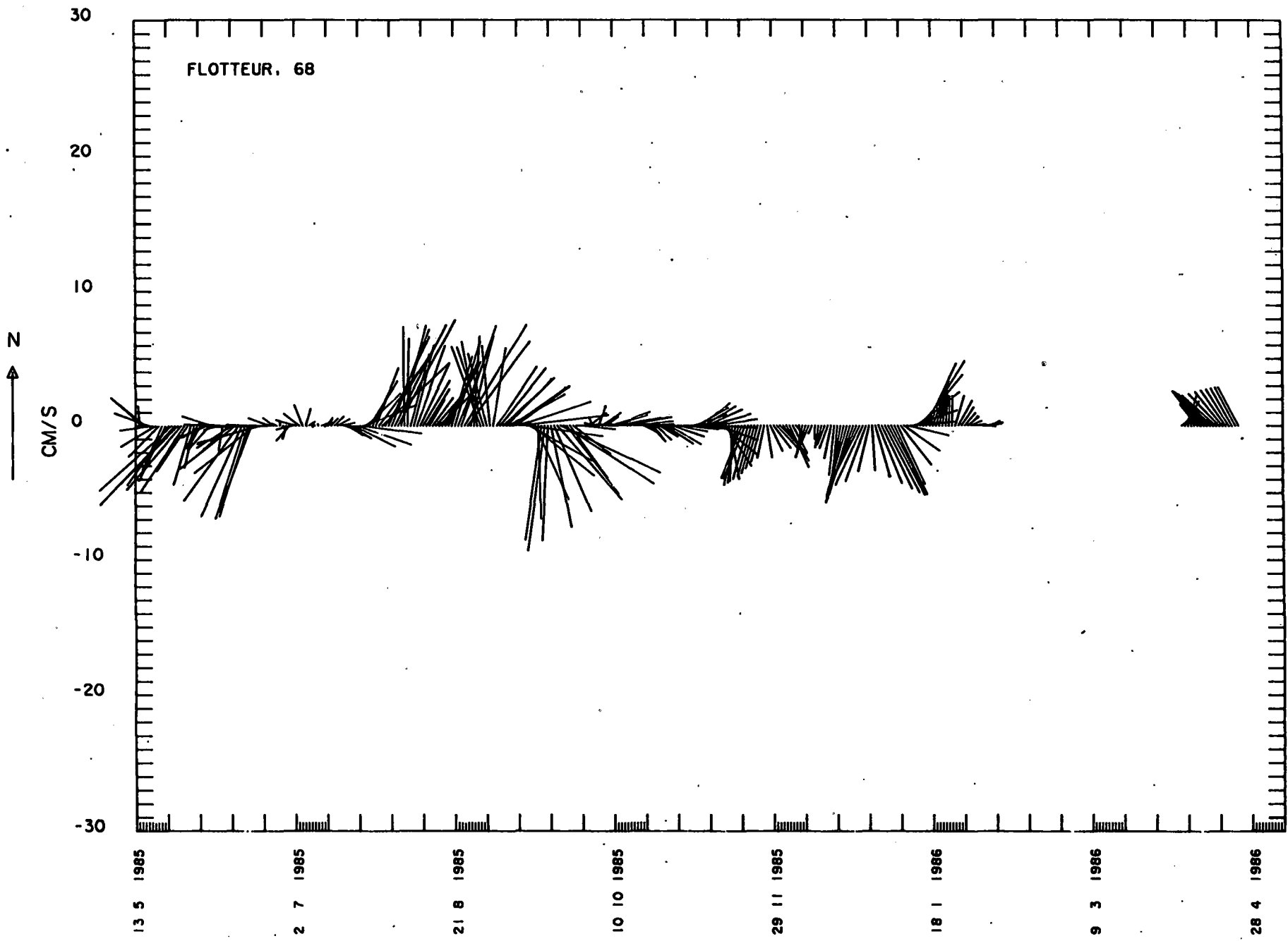
number of samples= 1726
average east velocity comp.= 0.65 cm/s
average north velocity comp.= -0.11 cm/s

variance of east velocity comp.= 5.43 cm²/s²
variance of north velocity comp.= 12.01 cm²/s²
covariance= 2.32 cm²/s²

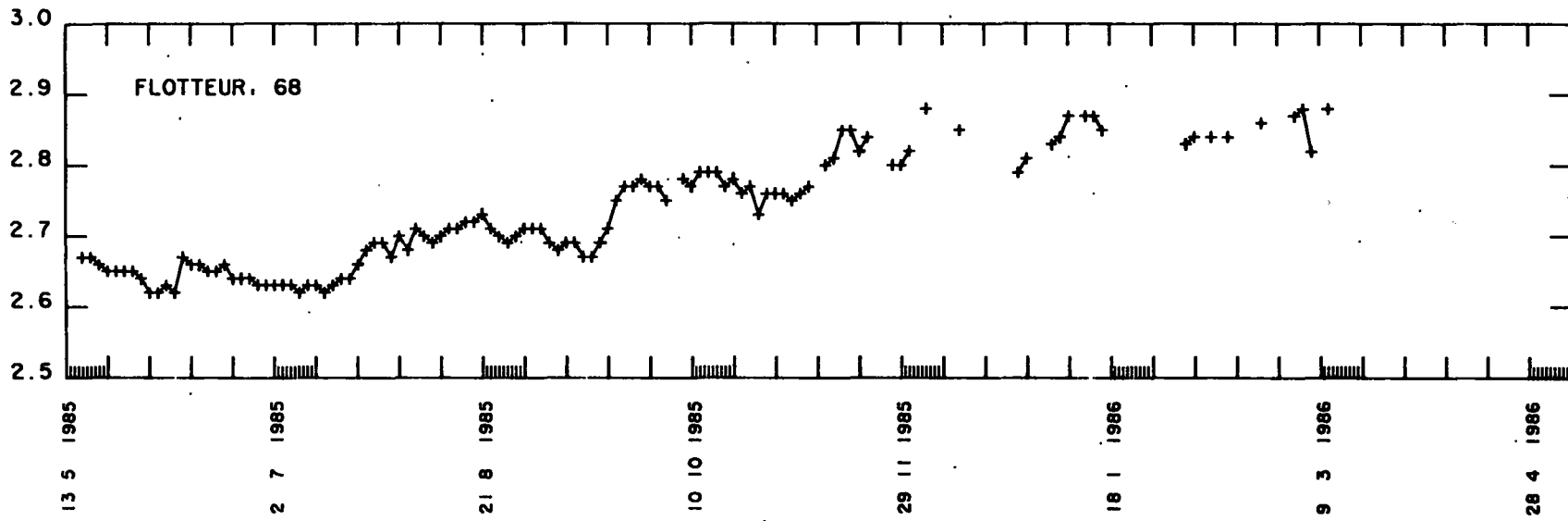
EKE= 8.72 cm²/s²
MKE= 0.22 cm²/s²

covar(u,temp)= 0.06 cm.degreeC/s
covar(v,temp)= -0.03 cm.degreeC/s

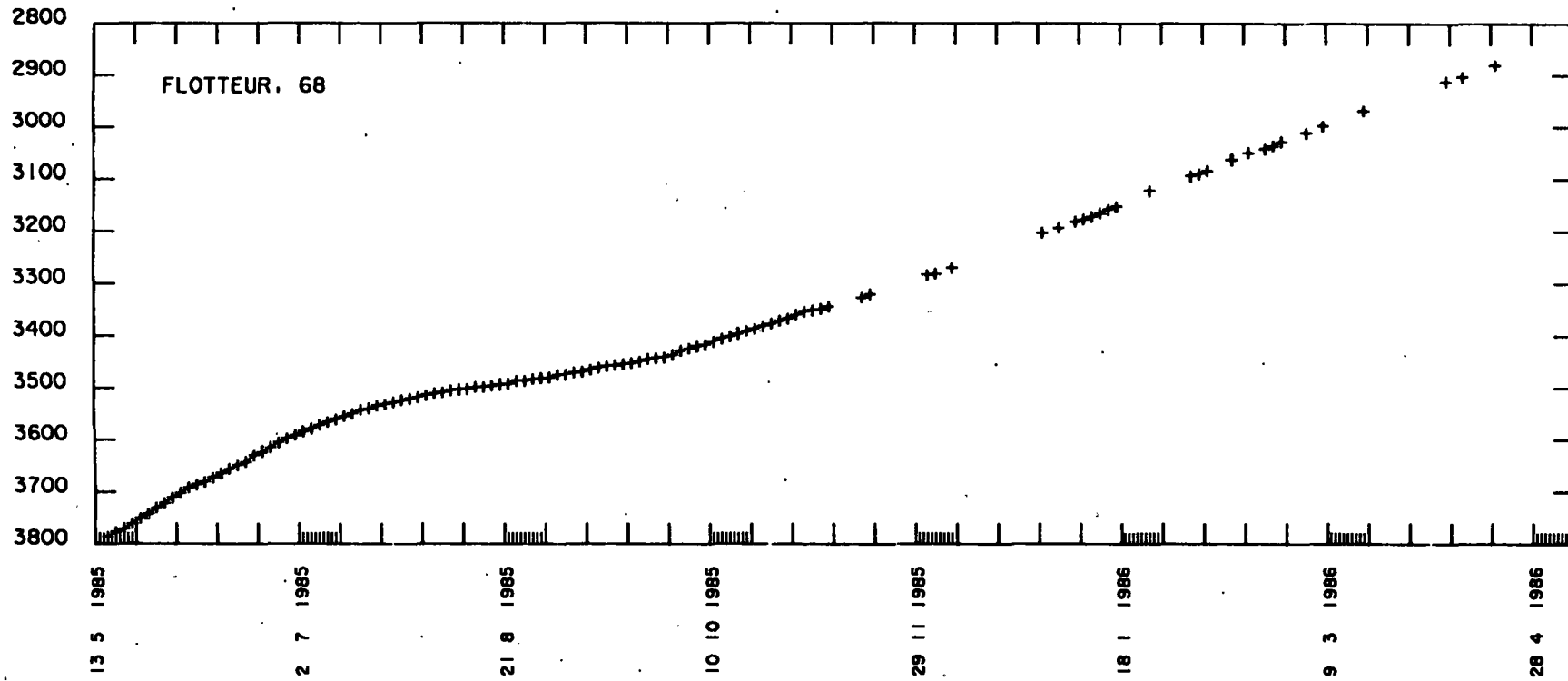




TEMPERATURE DEGREES C



PRESSURE DBARS



NOAMP experiment

float no: 69

launch date	launch lat	launch long			
1985 5 13 18h UT	47.44 N	-19.23 W			
date of first pos	first lat	first long	init. pres.	init. temp.	
1985 5 14 4h UT	47.45 N	-19.21 W	3966.	2.71	
date of last pos	last lat	last long	last pres.	last temp.	life (days)
1986 2 23 0h UT	47.54 N	-22.81 W	3496.	2.73	284.8

total displacement 285.3 days after launching

eastward displacement= -268.7 km mean eastward velocity= -0.94 cm/s
northward displacement= 13.1 km mean northward velocity= 0.05 cm/s

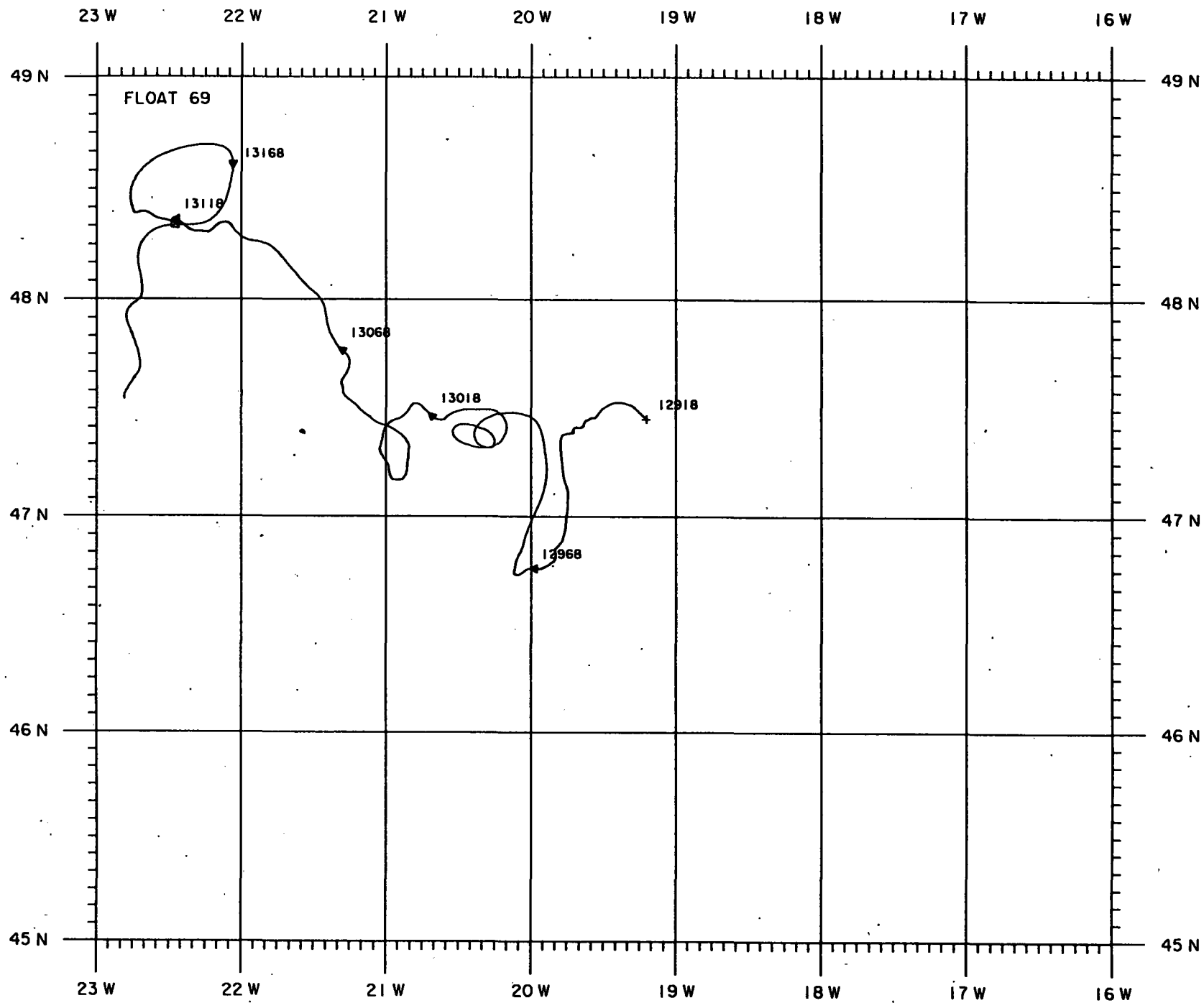
velocity time series statistics:

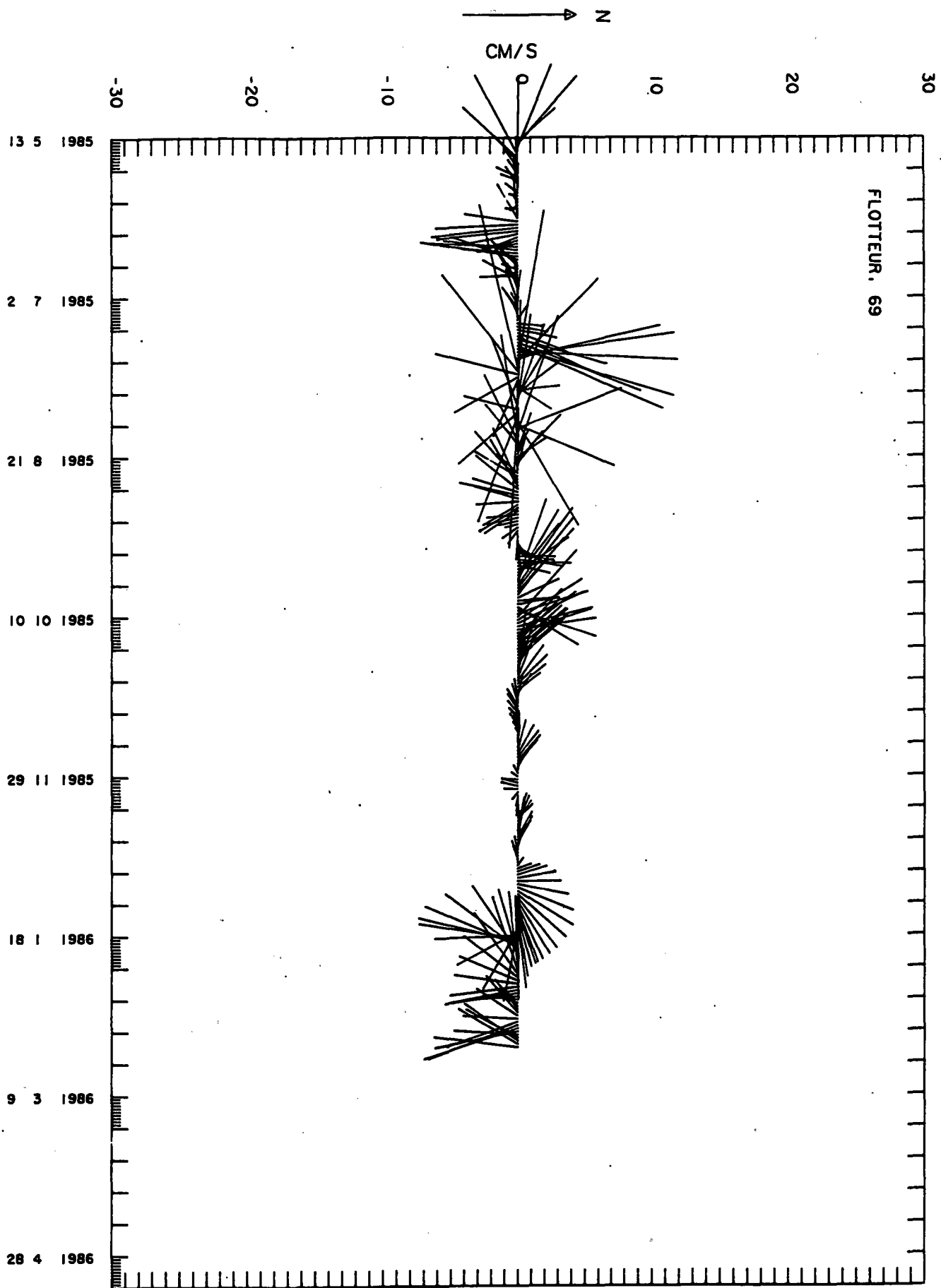
number of samples= 1710
average east velocity comp.= -1.09 cm/s
average north velocity comp.= 0.04 cm/s

variance of east velocity comp.= 8.19 cm²/s²
variance of north velocity comp.= 11.69 cm²/s²
covariance= -0.04 cm²/s²

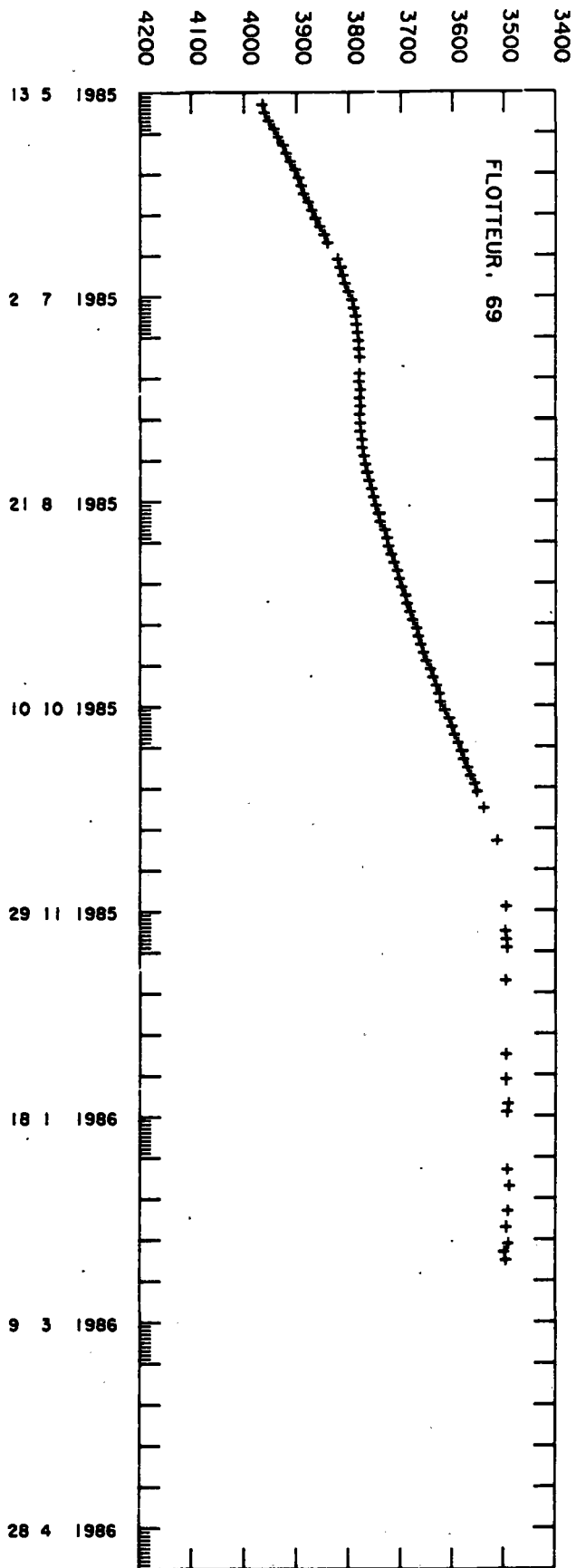
EKE= 9.94 cm²/s²
MKE= 0.60 cm²/s²

covar(u,temp)= 0.00 cm.degreeC/s
covar(v,temp)= -0.03 cm.degreeC/s

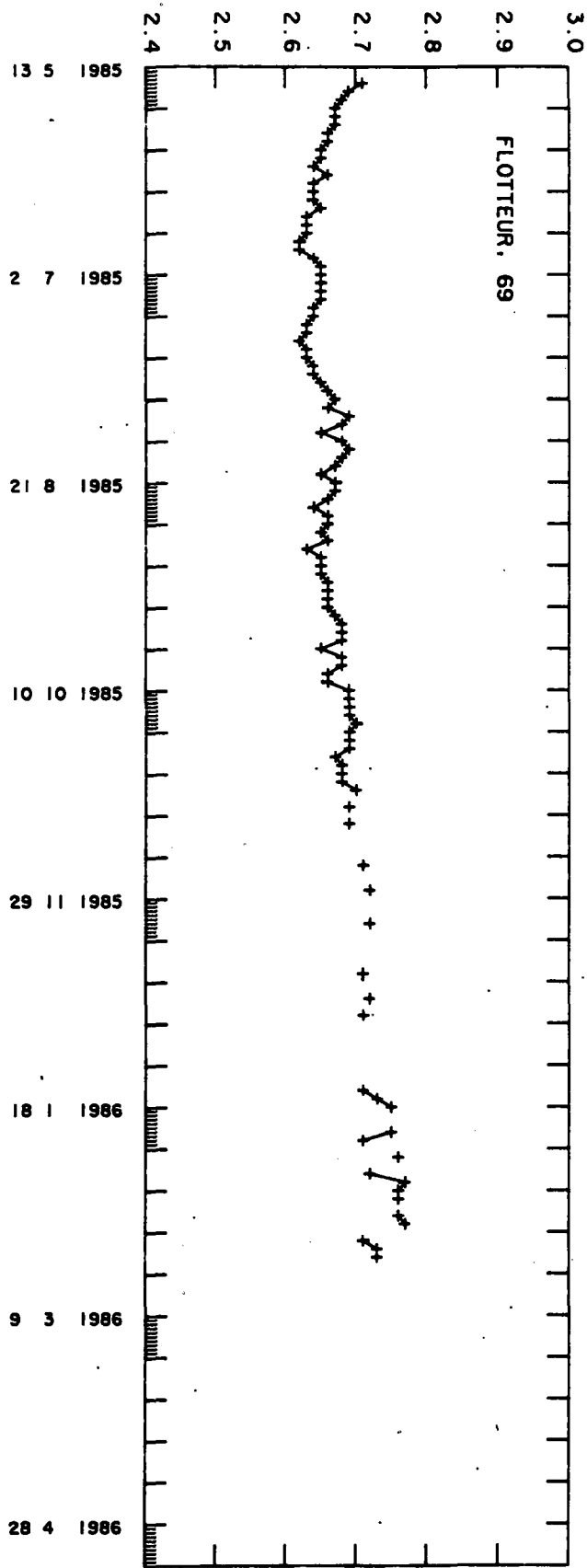




PRESSURE DBARS



TEMPERATURE DEGREES C



NOAMP experiment

float no: 70

launch date	launch lat	launch long			
1985 5 13 18h UT	47.44 N	-19.23 W			
date of first pos	first lat	first long	init. pres.	init. temp.	
1985 5 14 4h UT	47.46 N	-19.20 W	4095.	2.72	
date of last pos	last lat	last long	last pres.	last temp.	life (days)
1986 1 29 12h UT	48.56 N	-22.42 W	3749.	2.72	260.3

total displacement 260.8 days after launching

eastward displacement= -236.9 km mean eastward velocity= -0.91 cm/s
northward displacement= 144.6 km mean northward velocity= 0.55 cm/s

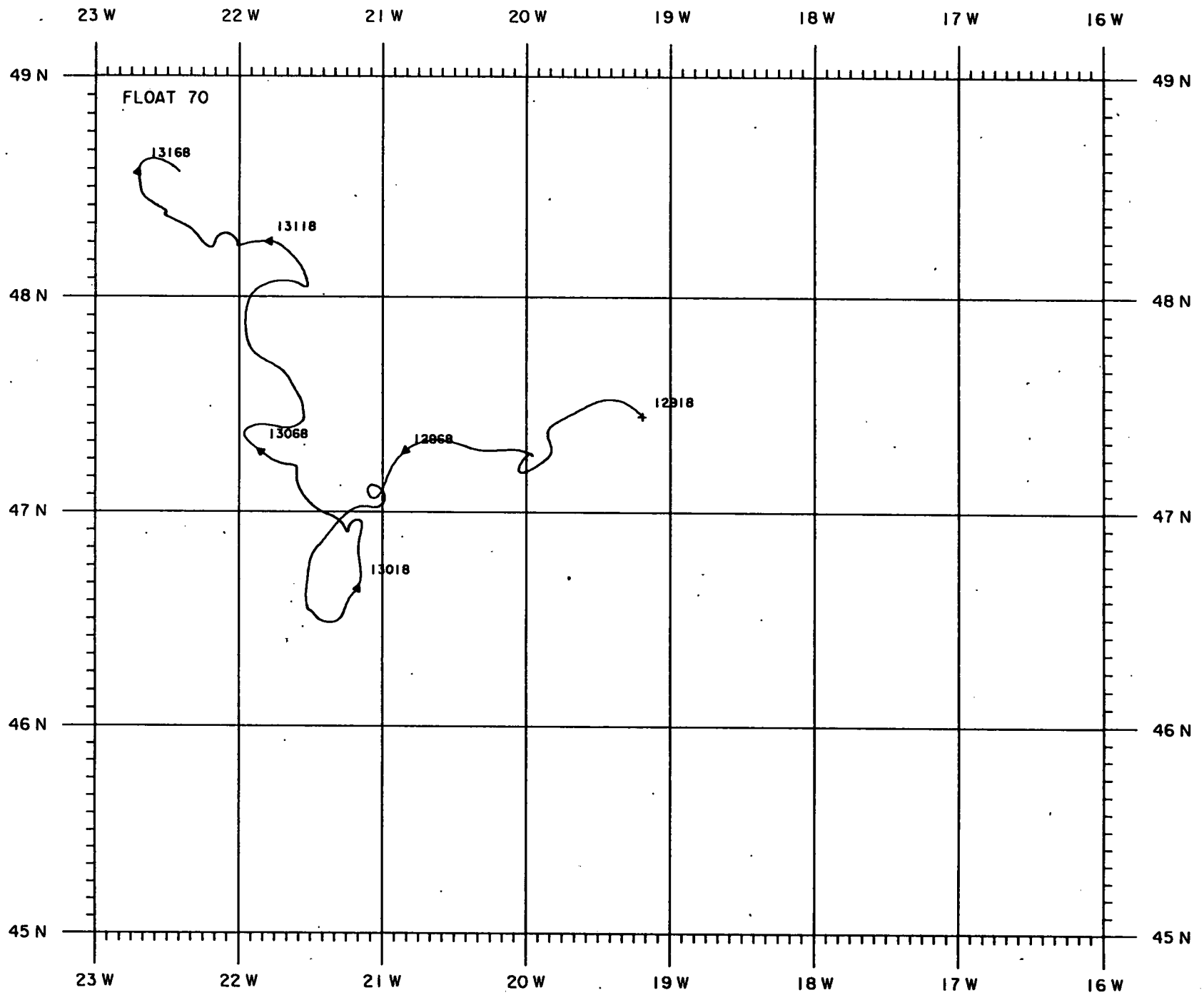
velocity time series statistics:

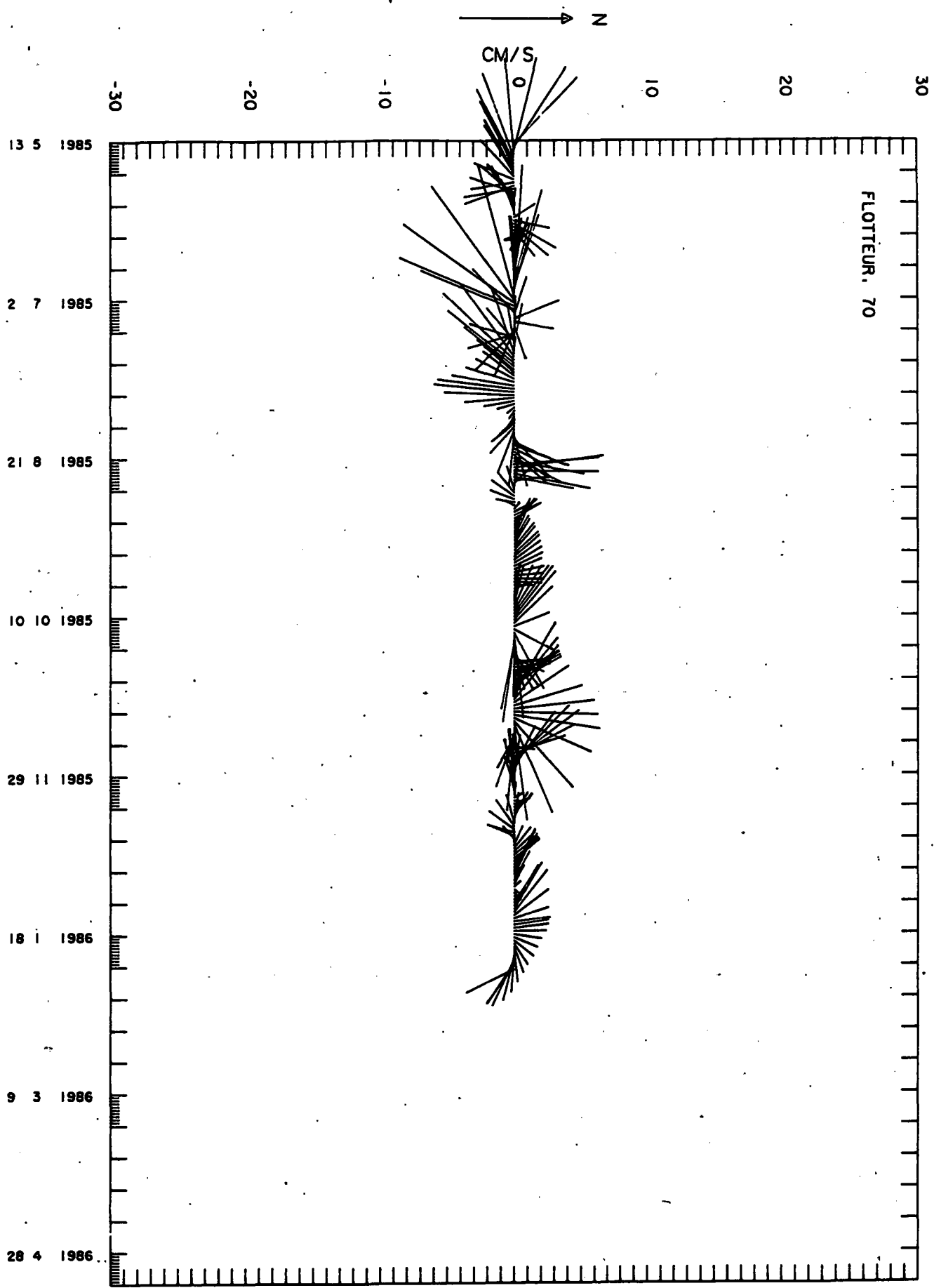
number of samples= 1563
average east velocity comp.= -1.08 cm/s
average north velocity comp.= 0.55 cm/s

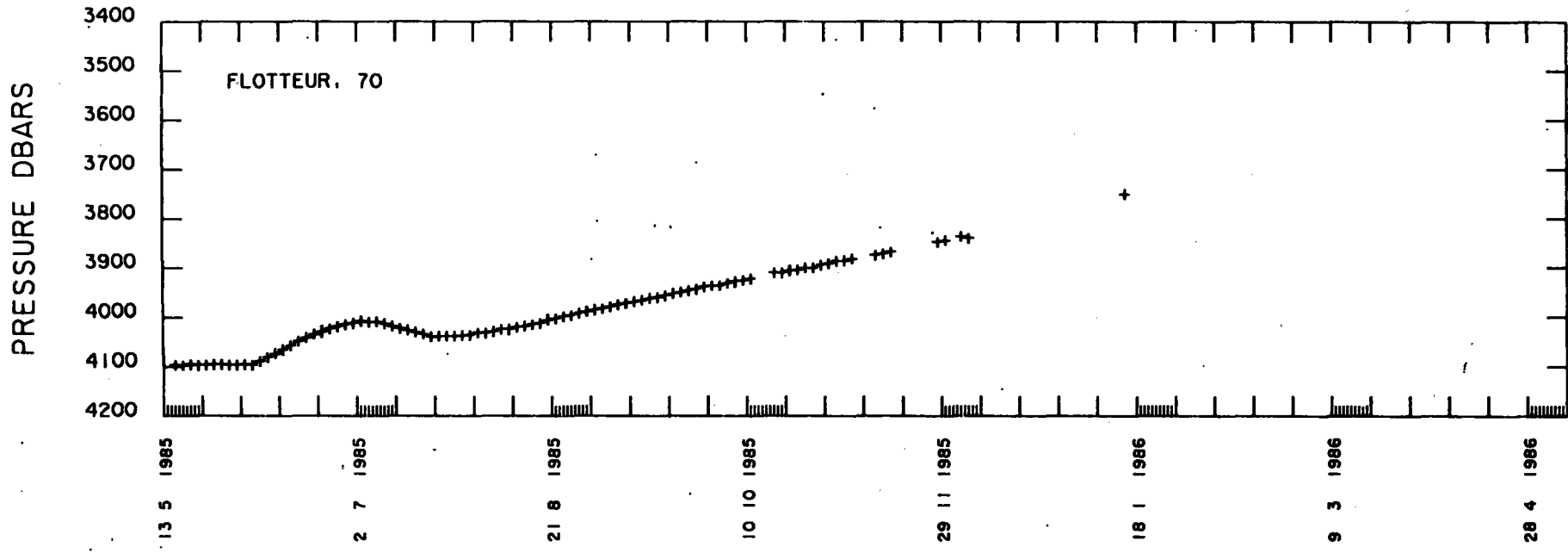
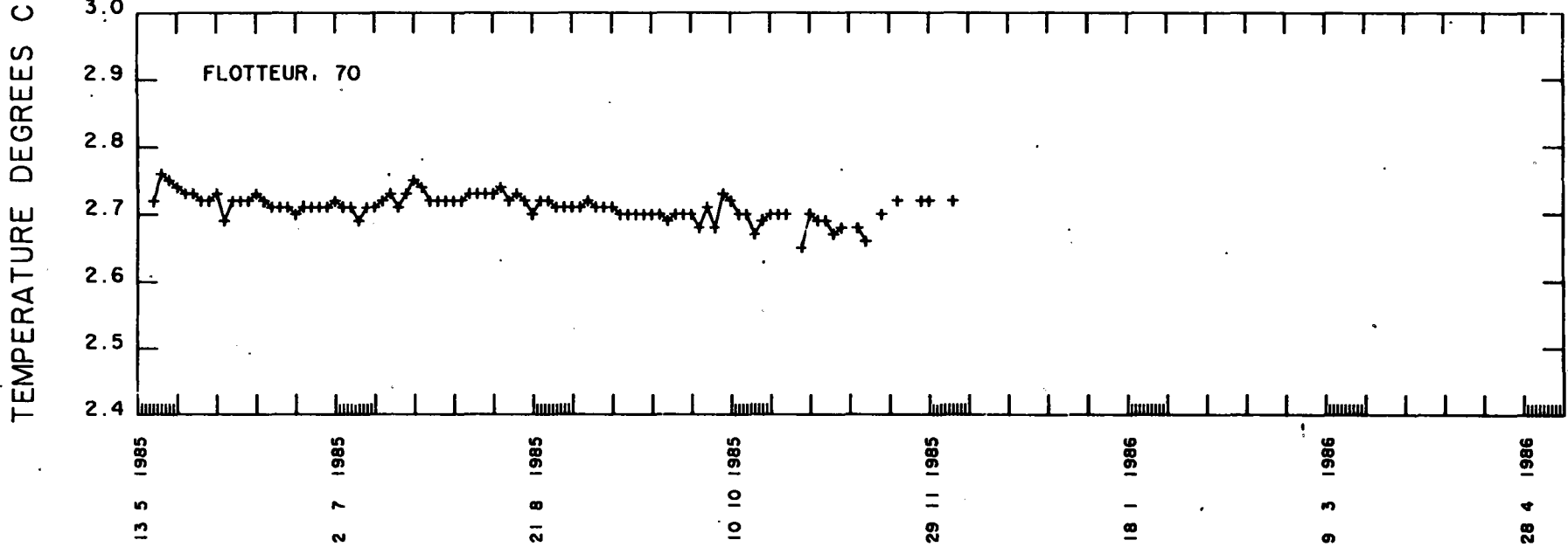
variance of east velocity comp.= 7.32 cm²/s²
variance of north velocity comp.= 6.68 cm²/s²
covariance= 0.83 cm²/s²

EKE= 7.00 cm²/s²
MKE= 0.73 cm²/s²

covar(u,temp)= -0.01 cm.degreeC/s
covar(v,temp)= -0.03 cm.degreeC/s







NOAMP experiment

float no: 71

launch date	launch lat	launch long			
1985 5 13 24h UT	47.62 N	-19.72 W			
date of first pos	first lat	first long	init. pres.	init. temp.	
1985 5 14 8h UT	47.59 N	-19.68 W	4095.	2.71	
date of last pos	last lat	last long	last pres.	last temp.	life (days)
1985 12 3 8h UT	46.04 N	-19.64 W	3989.	2.69	203.0

total displacement 203.3 days after launching

eastward displacement= 6.1 km mean eastward velocity= 0.03 cm/s
northward displacement= -203.4 km mean northward velocity= -1.00 cm/s

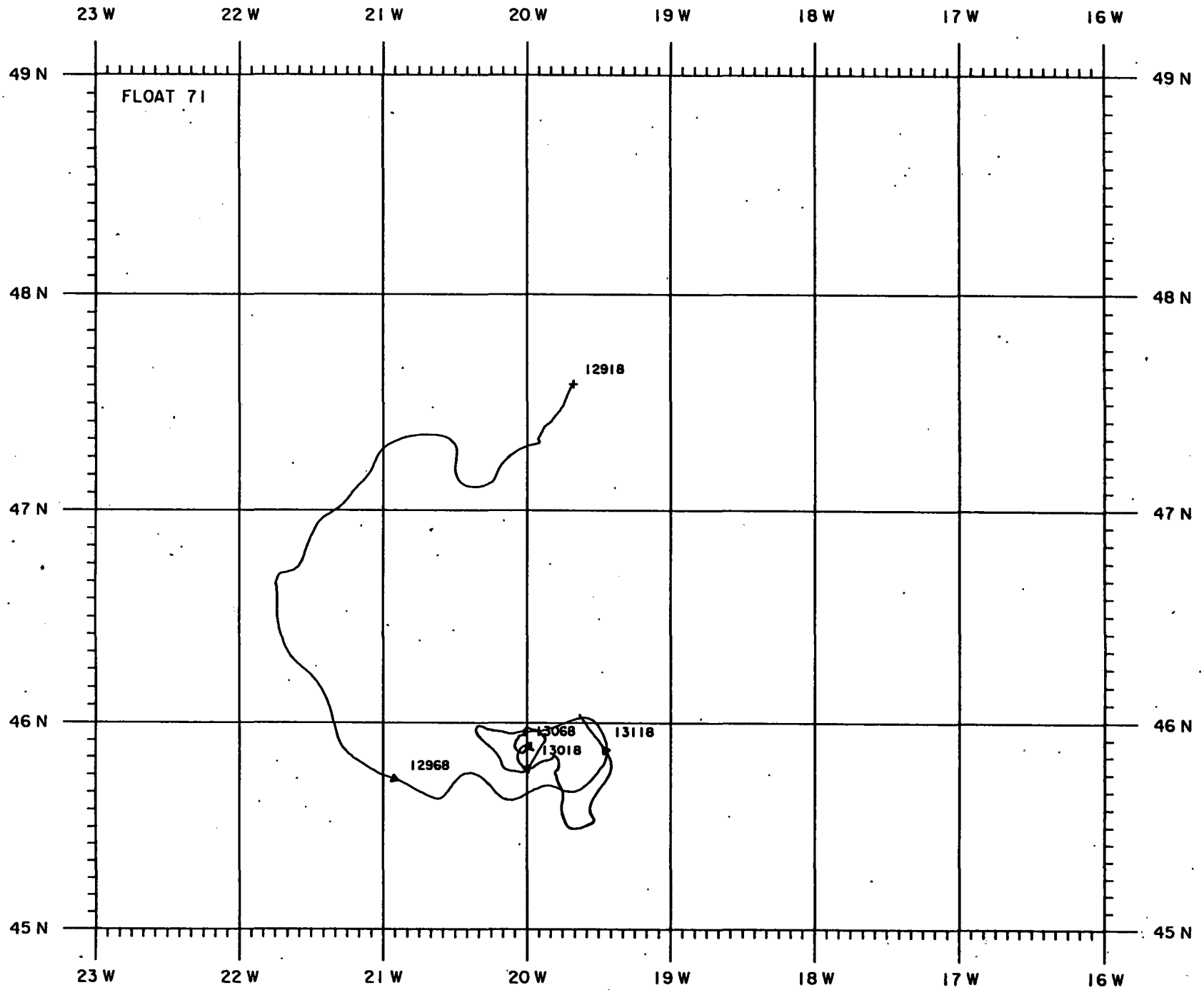
velocity time series statistics:

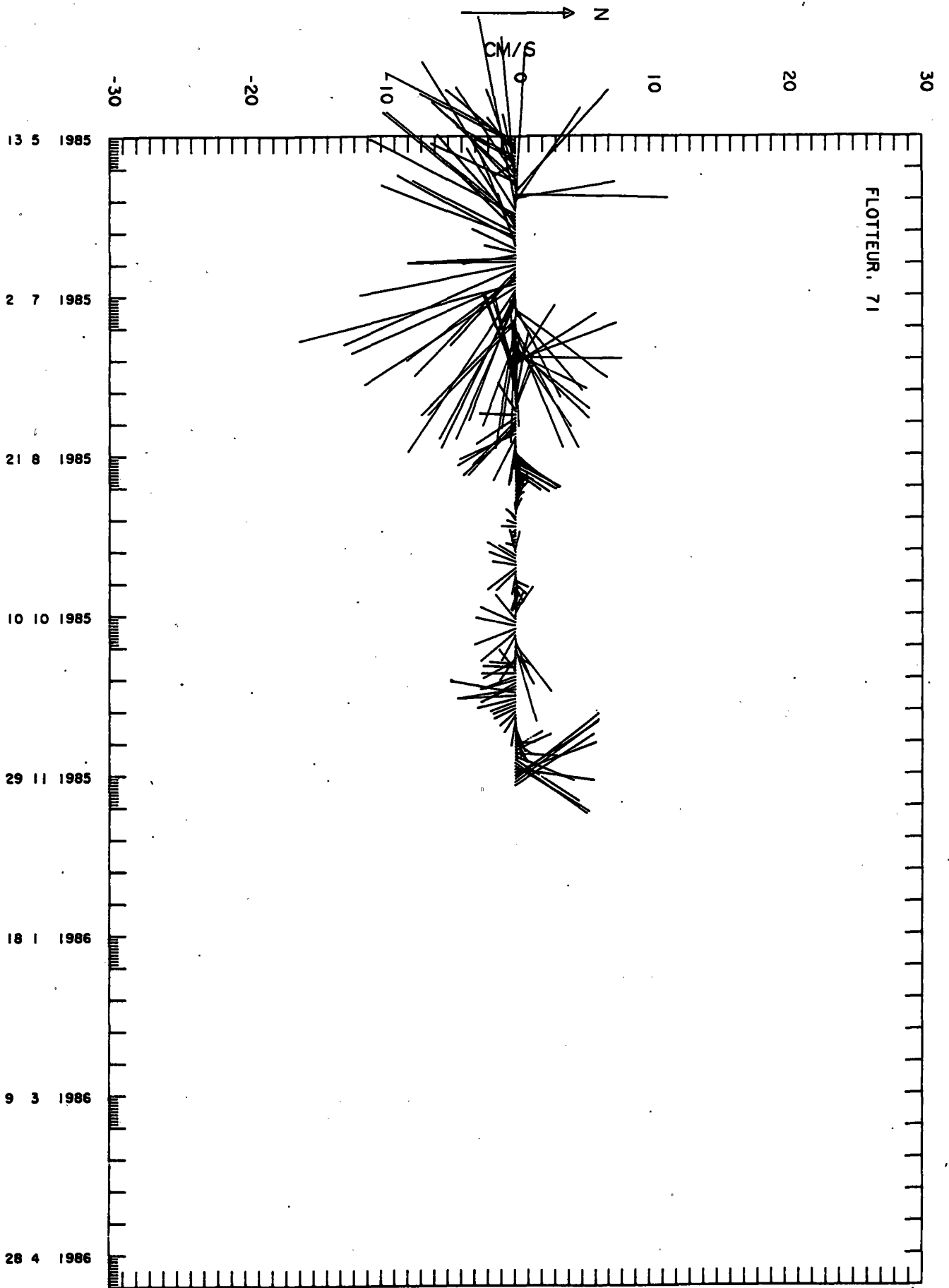
number of samples= 1219
average east velocity comp.= 0.04 cm/s
average north velocity comp.= -0.99 cm/s

variance of east velocity comp.= 18.93 cm²/s²
variance of north velocity comp.= 18.15 cm²/s²
covariance= -0.11 cm²/s²

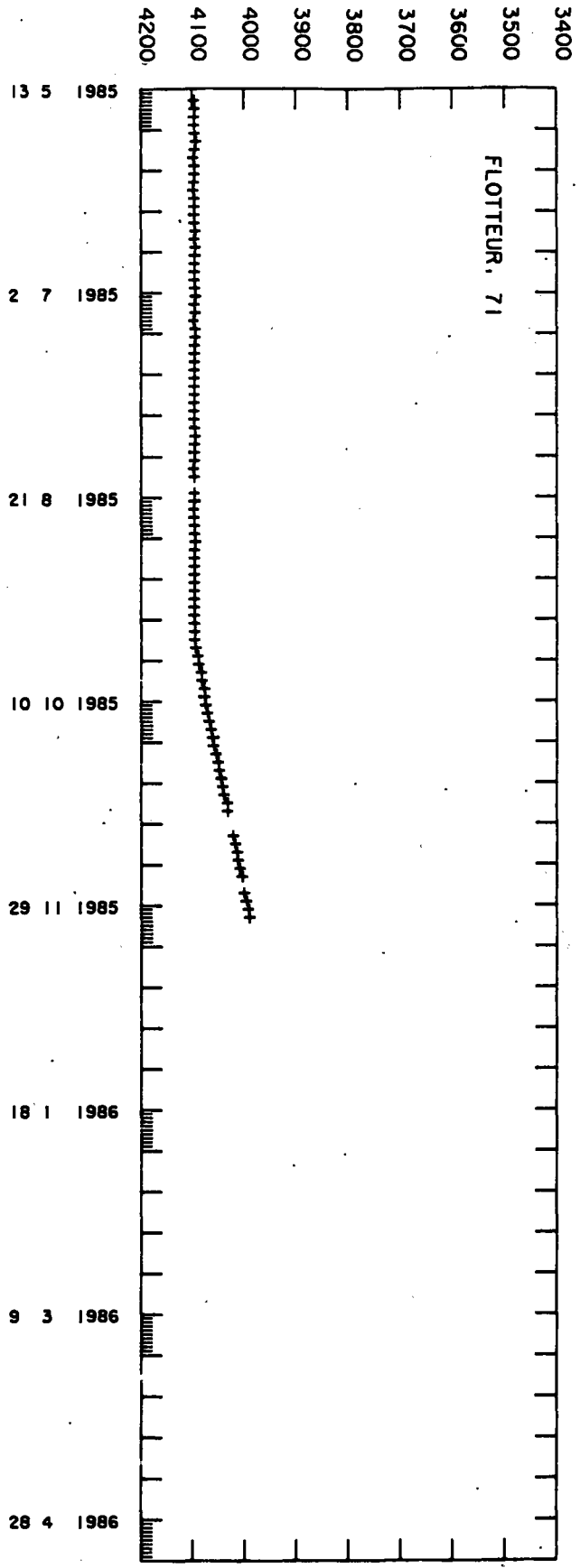
EKE= 18.54 cm²/s²
MKE= 0.49 cm²/s²

covar(u,temp)= 0.00 cm.degreeC/s
covar(v,temp)= -0.02 cm.degreeC/s

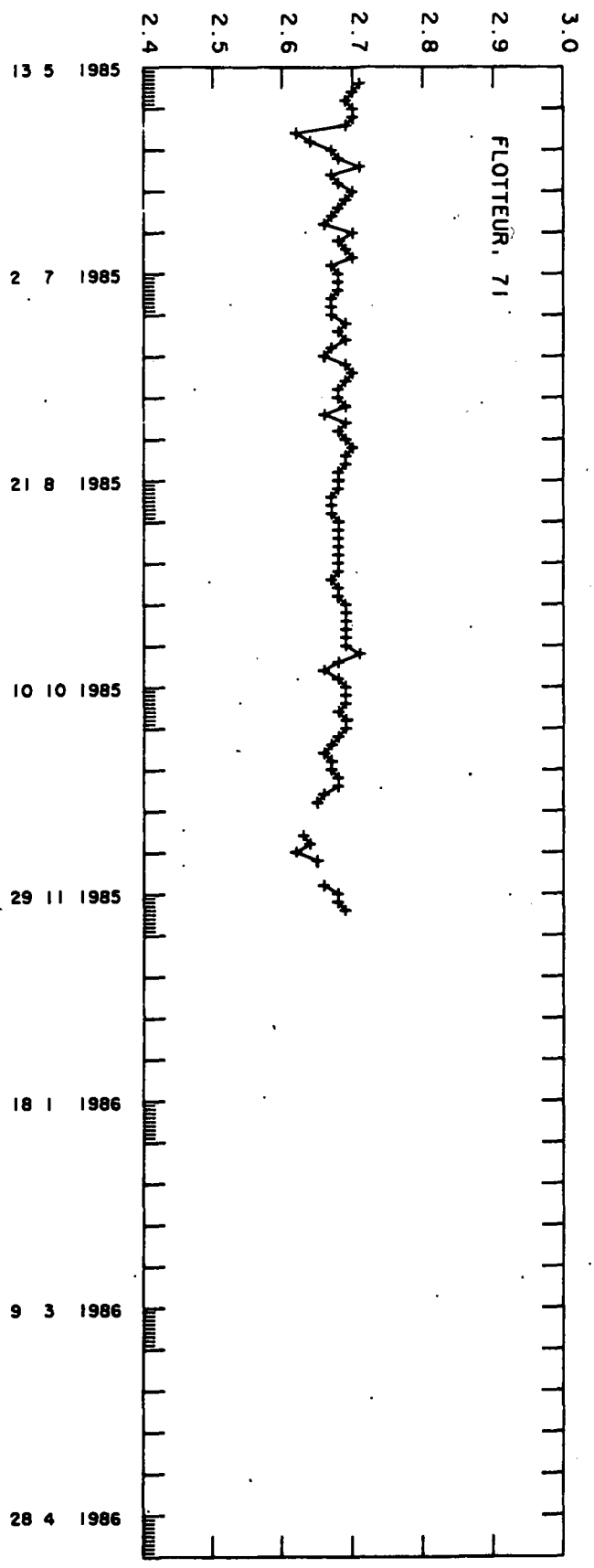




PRESSURE DBARS



TEMPERATURE DEGREES C



NOAMP experiment

float no: 72

launch date	launch lat	launch long			
1985 5 13 24h UT	47.62 N	-19.72 W			
date of first pos	first lat	first long	init. pres.	init. temp.	
1985 5 14 5h UT	47.62 N	-19.71 W	4094.	2.68	
date of last pos	last lat	last long	last pres.	last temp.	life (days)
1986 5 5 5h UT	47.03 N	-21.77 W	2678.	3.19	356.0

total displacement 356.2 days after launching

eastward displacement= -154.5 km mean eastward velocity= -0.43 cm/s
northward displacement= -75.8 km mean northward velocity= -0.21 cm/s

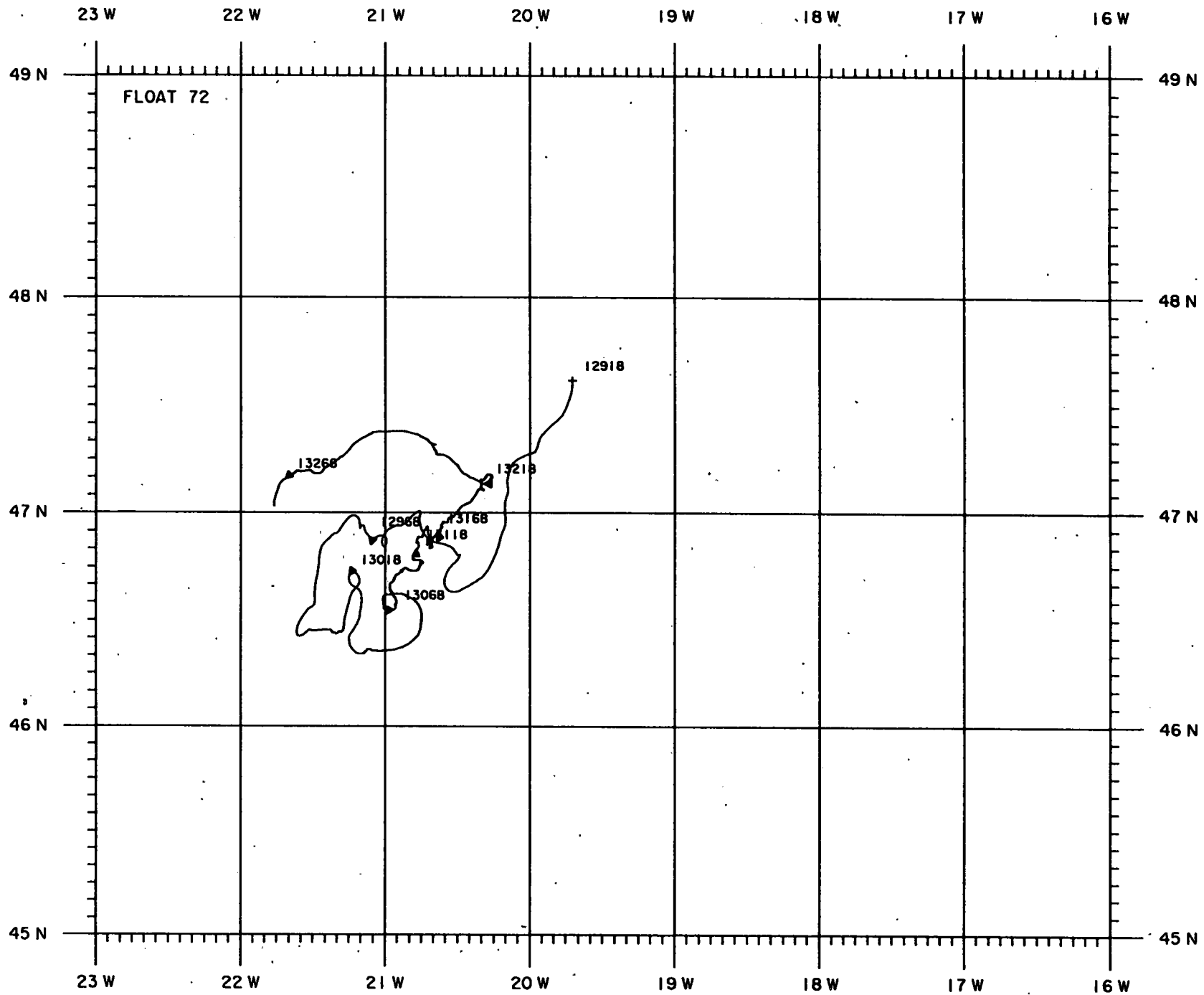
velocity time series statistics:

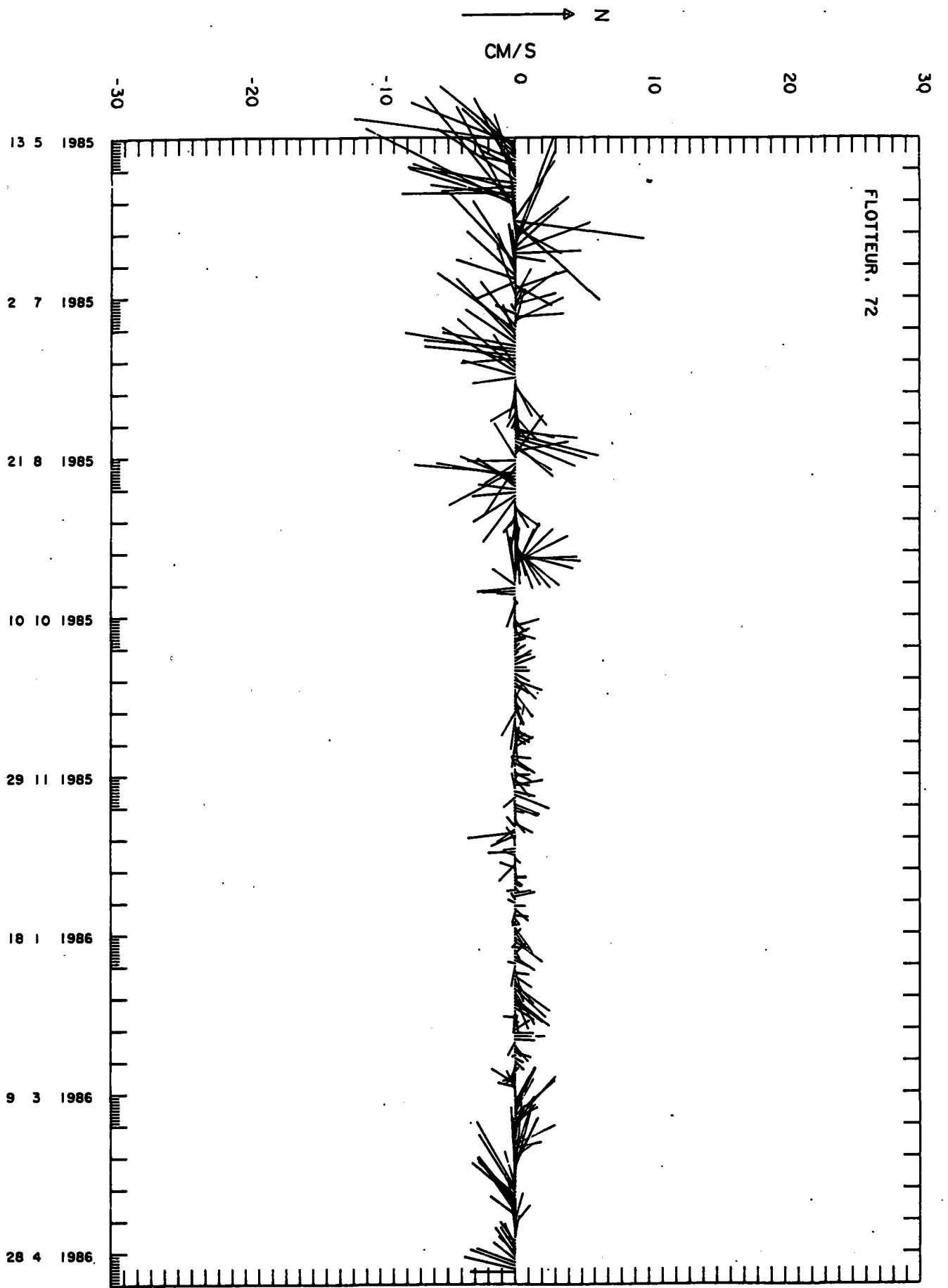
number of samples= 2137
average east velocity comp.= -0.50 cm/s
average north velocity comp.= -0.22 cm/s

variance of east velocity comp.= 4.63 cm²/s²
variance of north velocity comp.= 7.40 cm²/s²
covariance= 1.82 cm²/s²

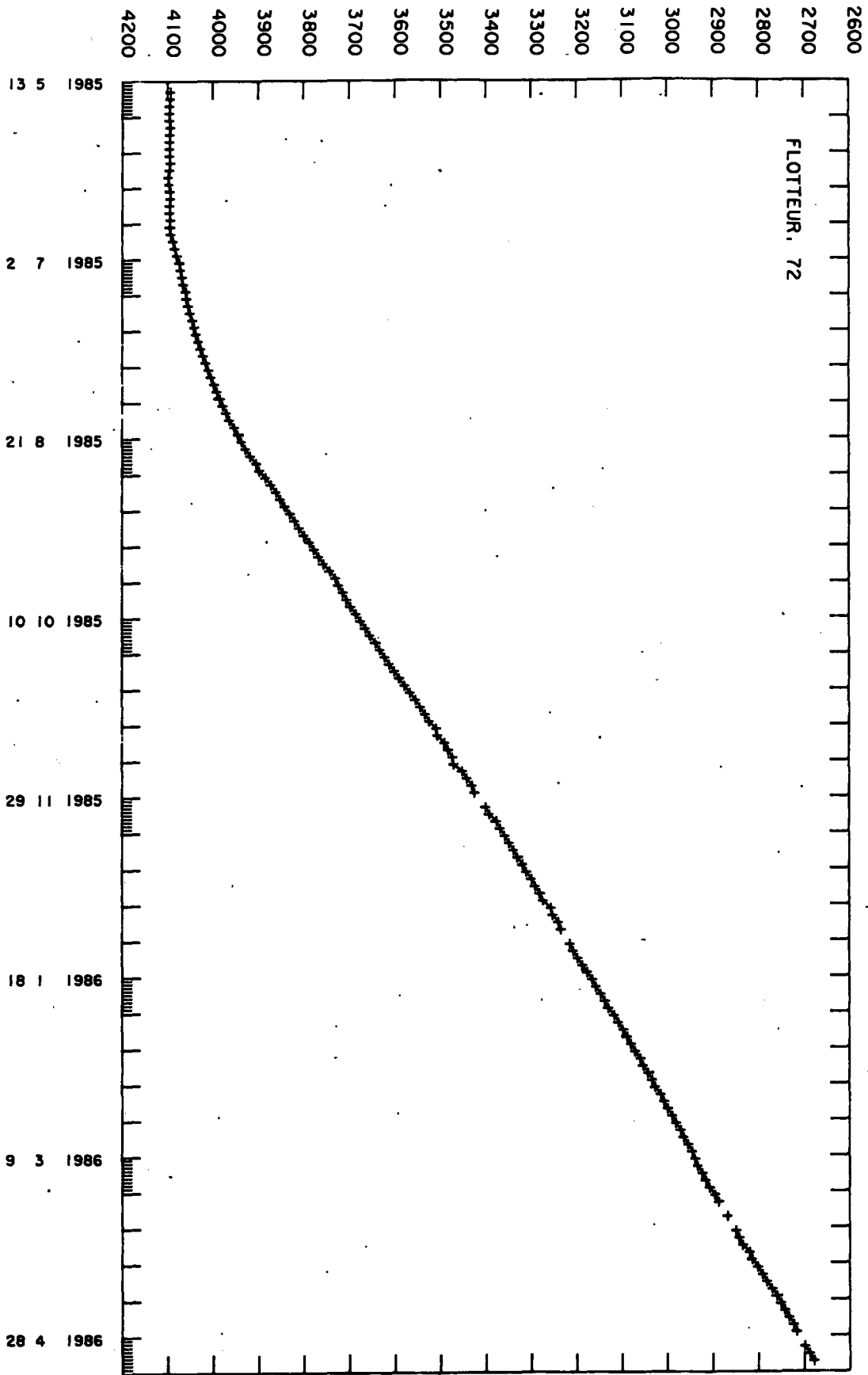
EKE= 6.01 cm²/s²
MKE= 0.15 cm²/s²

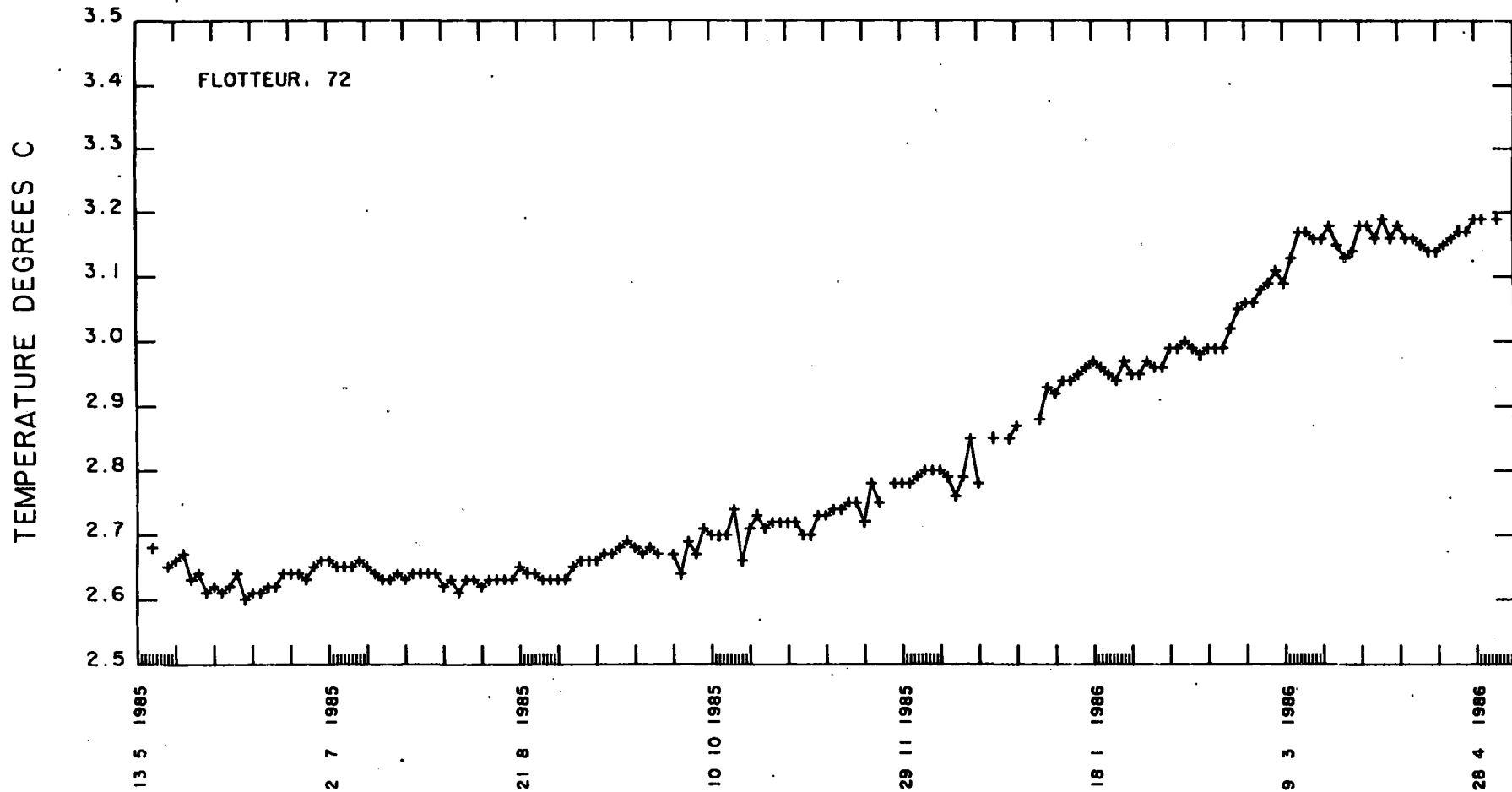
covar(u,temp)= -0.07 cm.degreeC/s
covar(v,temp)= 0.07 cm.degreeC/s





PRESSURE DBARS





NOAMP experiment

float no: 73

launch date	launch lat	launch long			
1985 5 13 24h UT	47.62 N	-19.72 W			
date of first pos	first lat	first long	init. pres.	init. temp.	
1985 5 14 13h UT	47.59 N	-19.71 W	3891.	2.72	
date of last pos	last lat	last long	last pres.	last temp.	life (days)
1986 4 24 17h UT	45.83 N	-19.52 W	3492.	2.77	345.2

total displacement 345.7 days after launching

eastward displacement= 14.8 km mean eastward velocity= 0.04 cm/s
northward displacement= -229.5 km mean northward velocity= -0.66 cm/s

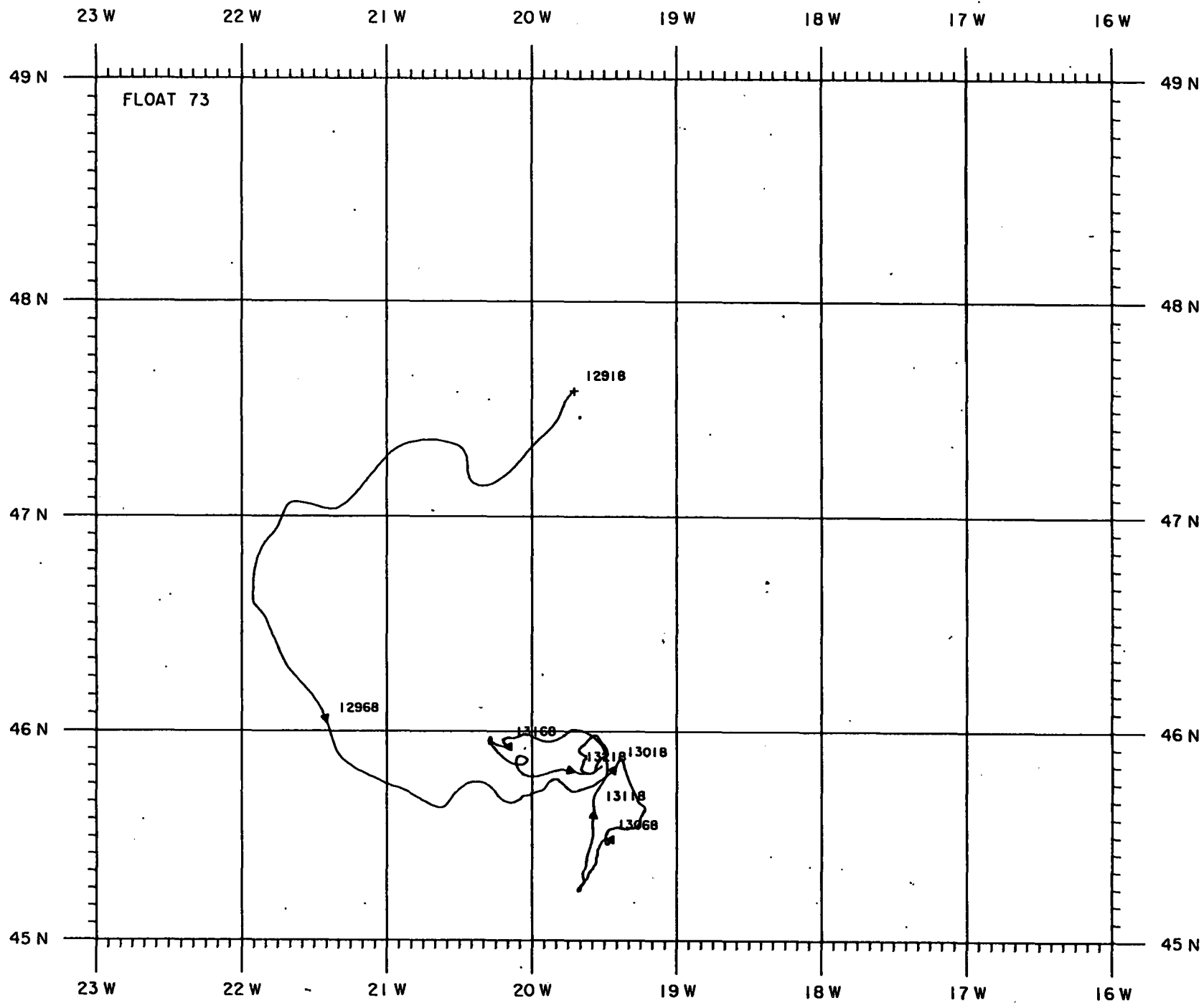
velocity time series statistics:

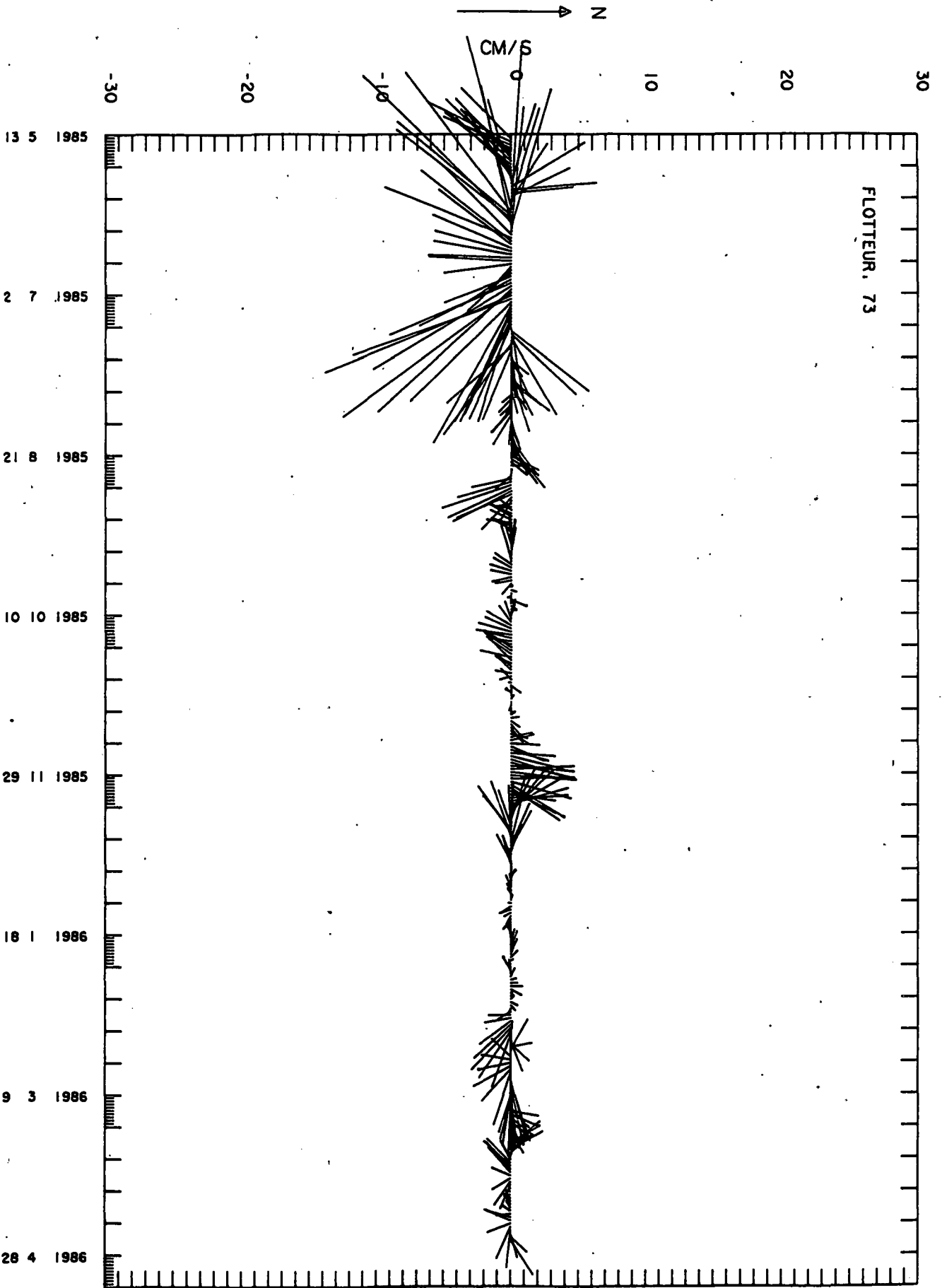
number of samples= 2072
average east velocity comp.= 0.06 cm/s
average north velocity comp.= -0.65 cm/s

variance of east velocity comp.= 9.60 cm²/s²
variance of north velocity comp.= 8.80 cm²/s²
covariance= -0.06 cm²/s²

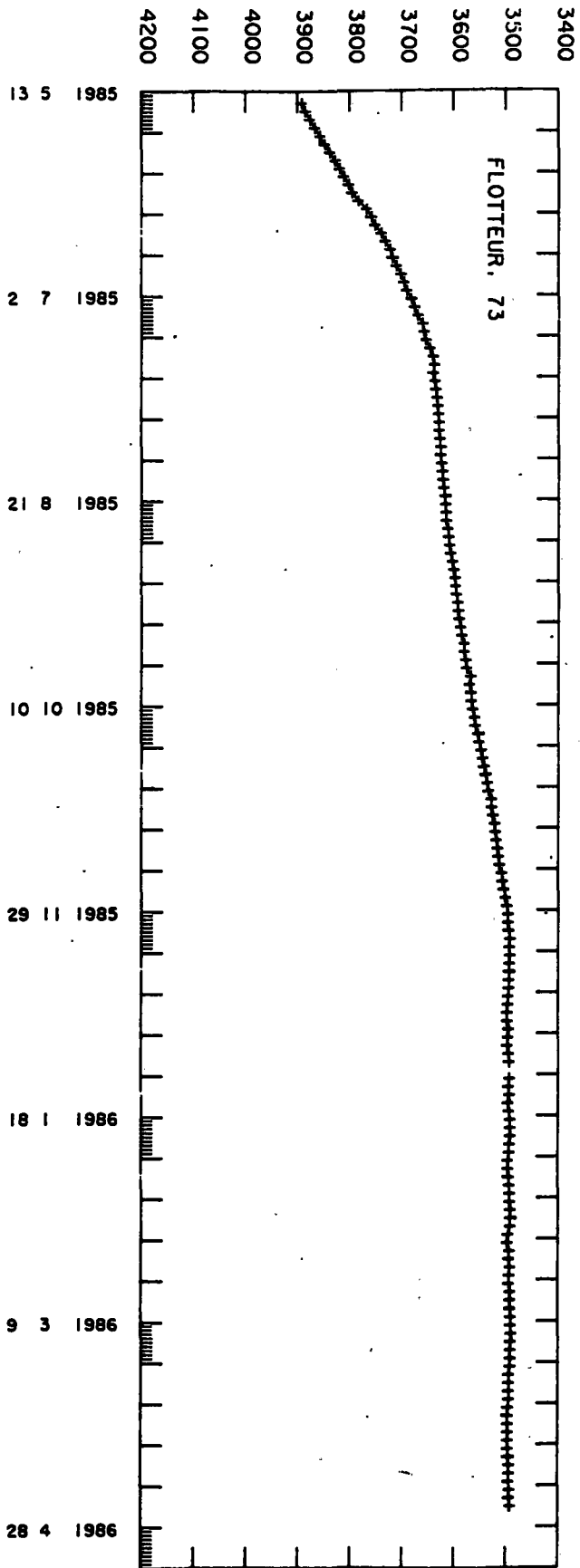
EKE= 9.20 cm²/s²
MKE= 0.22 cm²/s²

covar(u,temp)= 0.00 cm.degreeC/s
covar(v,temp)= 0.03 cm.degreeC/s

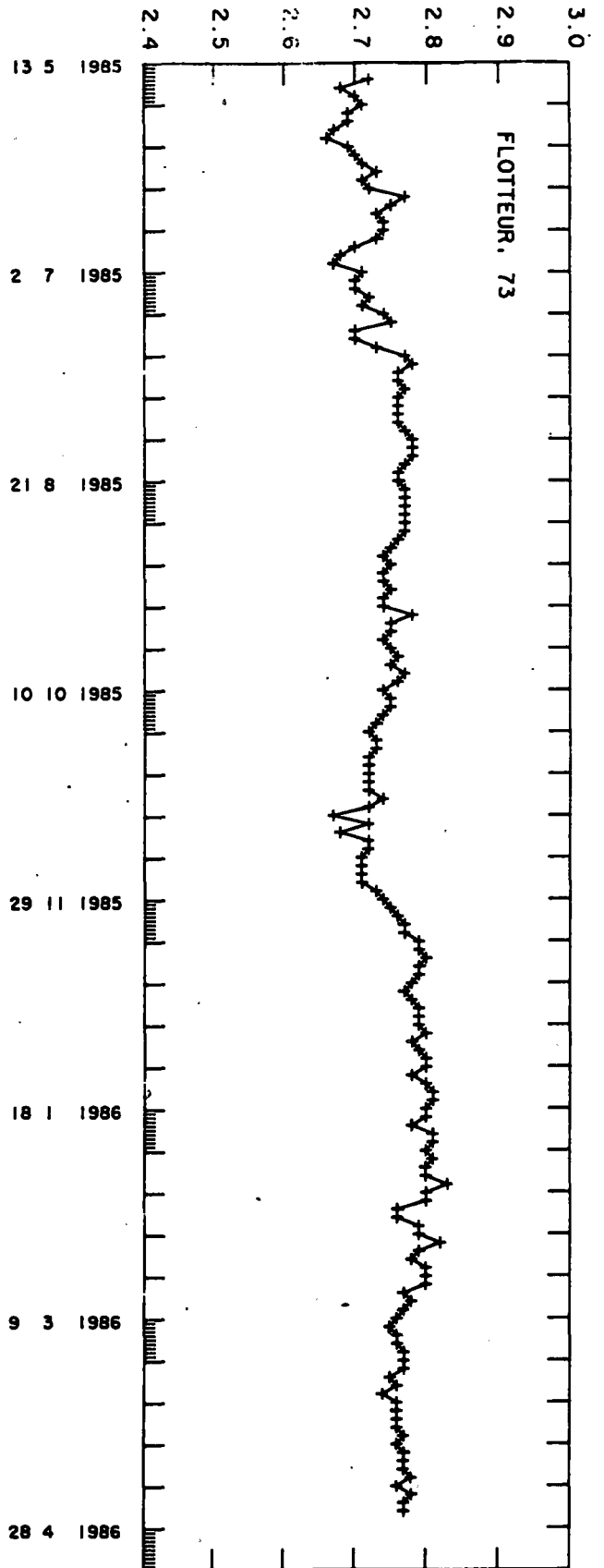




PRESSURE DBARS



TEMPERATURE DEGREES C



NOAMP experiment

float no: 74

launch date	launch lat	launch long			
1985 5 14 15h UT	47.27 N	-20.06 W			
date of first pos	first lat	first long	init. pres.	init. temp.	
1985 5 14 17h UT	47.27 N	-20.05 W	4036.	2.78	
date of last pos	last lat	last long	last pres.	last temp.	life (days)
1986 5 3 17h UT	47.44 N	-19.00 W	3490.	2.75	354.0

total displacement 354.1 days after launching

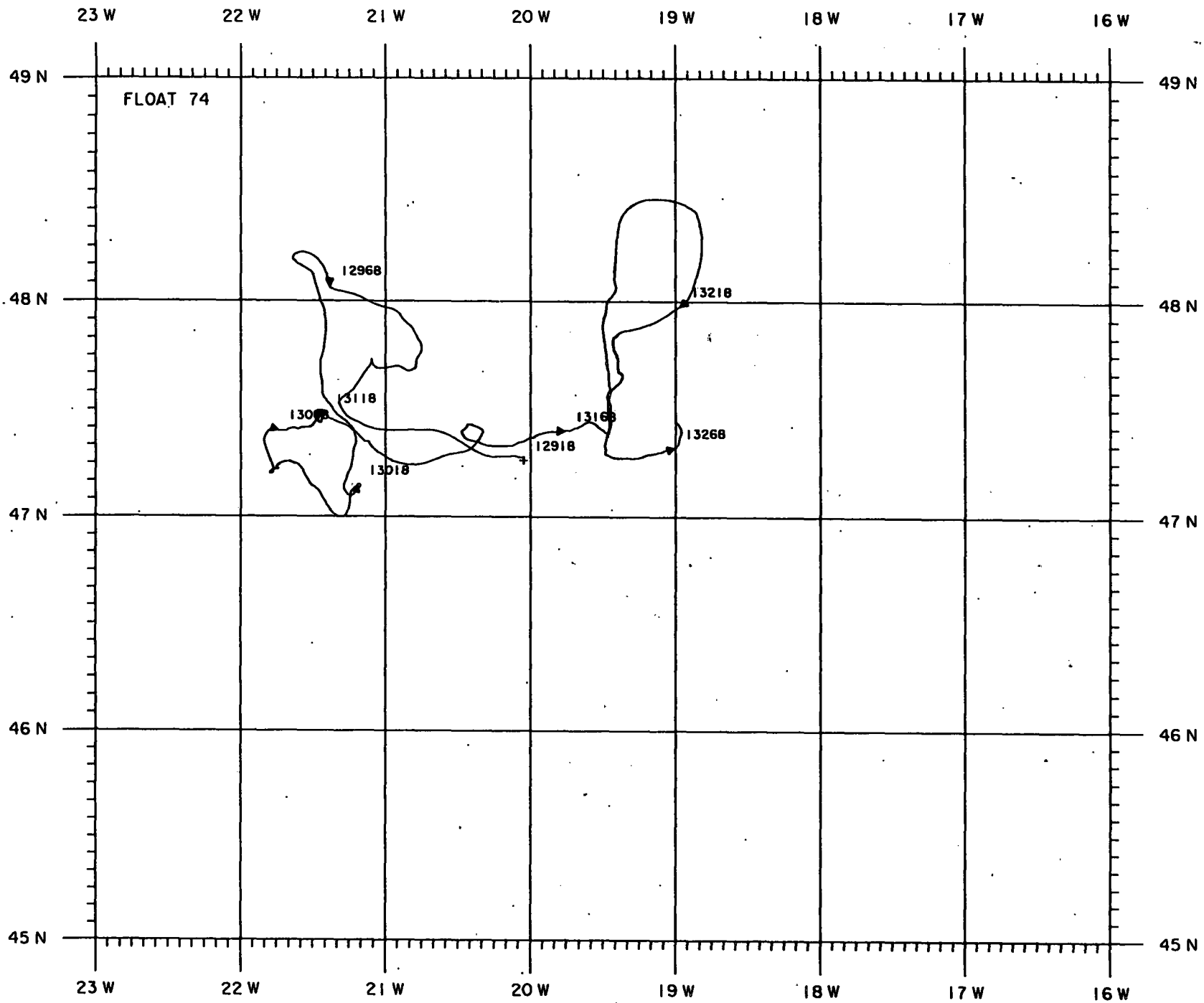
eastward displacement= 80.0 km mean eastward velocity= 0.23 cm/s
northward displacement= 21.6 km mean northward velocity= 0.06 cm/s

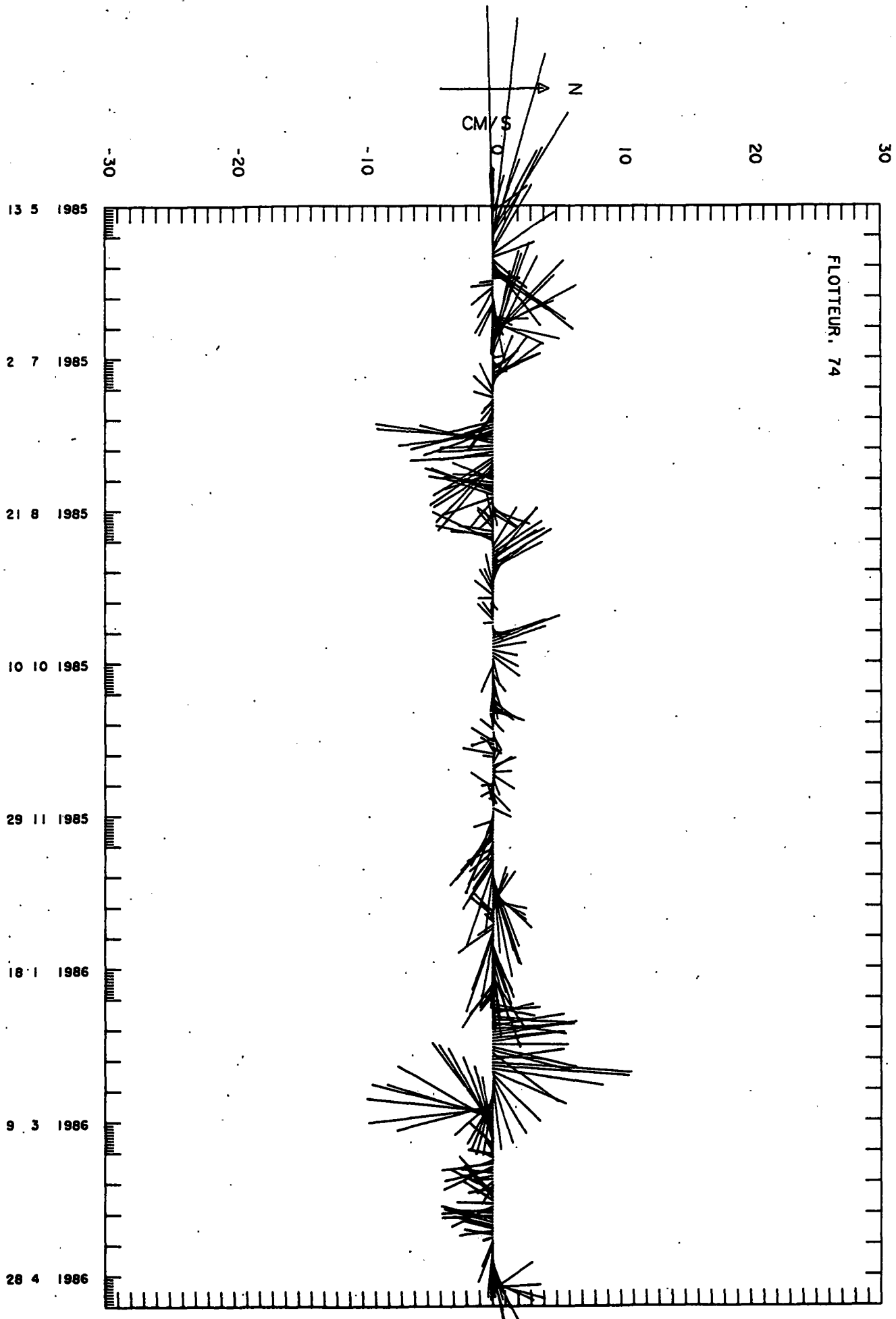
velocity time series statistics:

number of samples= 2125
average east velocity comp.= 0.26 cm/s
average north velocity comp.= 0.07 cm/s
variance of east velocity comp.= 10.60 cm²/s²
variance of north velocity comp.= 9.98 cm²/s²
covariance= -0.68 cm²/s²

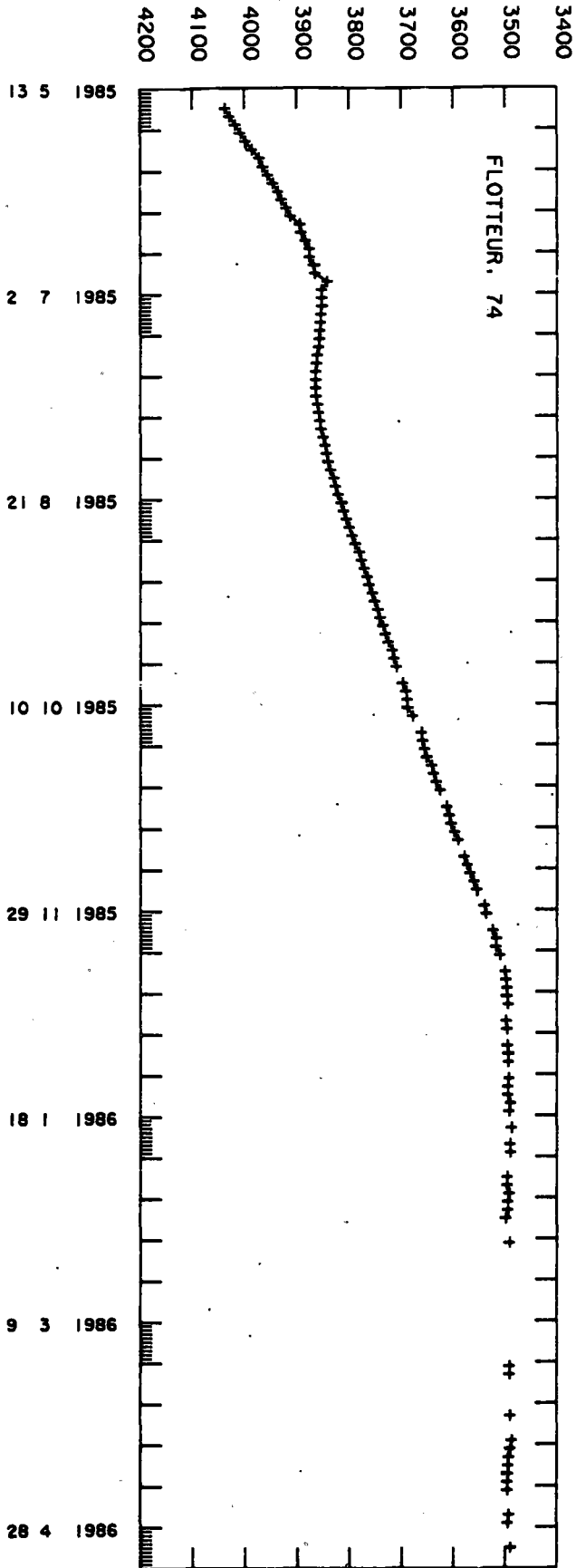
EKE= 10.29 cm²/s²
MKE= 0.04 cm²/s²

covar(u,temp)= 0.02 cm.degreeC/s
covar(v,temp)= -0.01 cm.degreeC/s

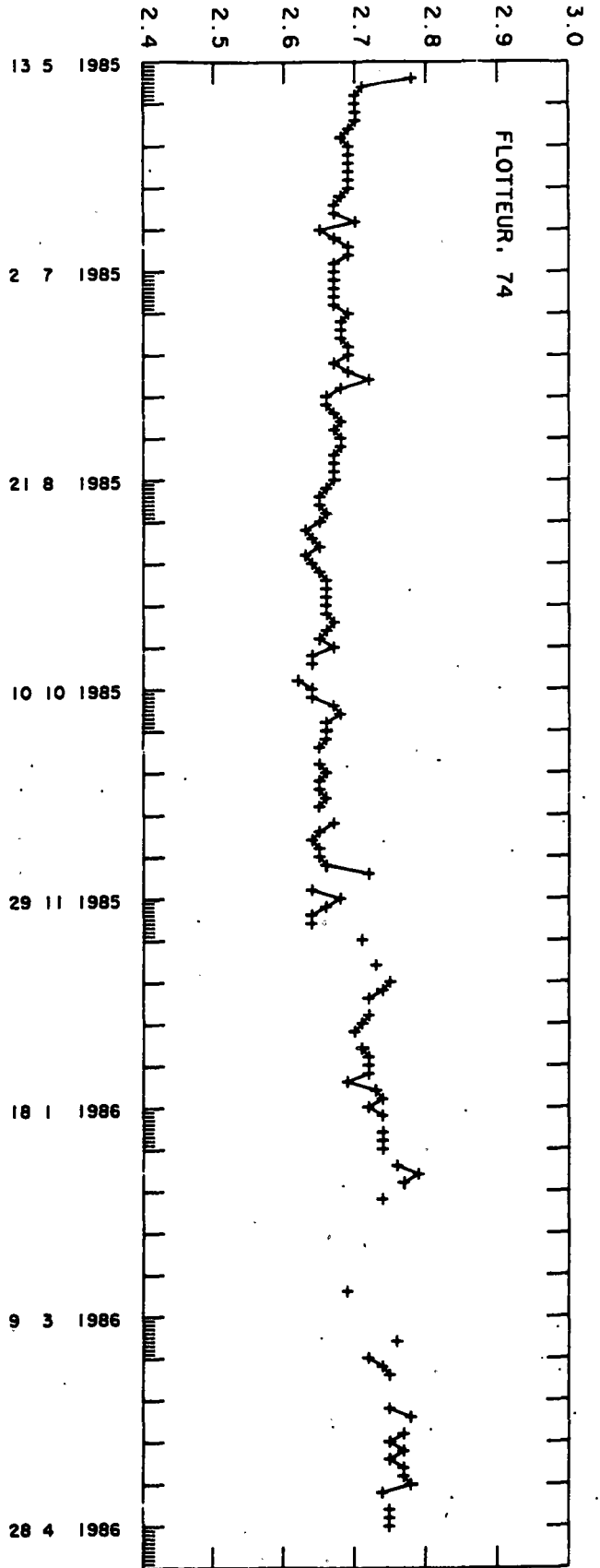




PRESSURE DBARS



TEMPERATURE DEGREES C



NOAMP experiment

float no: 75

launch date	launch lat	launch long			
1985 5 14 15h UT	47.27 N	-20.06 W			
date of first pos	first lat	first long	init. pres.	init. temp.	
1985 5 15 1h UT	47.27 N	-20.05 W	3839.	2.82	
date of last pos	last lat	last long	last pres.	last temp.	life (days)
1986 1 15 5h UT	45.48 N	-20.35 W	3494.	2.76	245.2

total displacement 245.6 days after launching

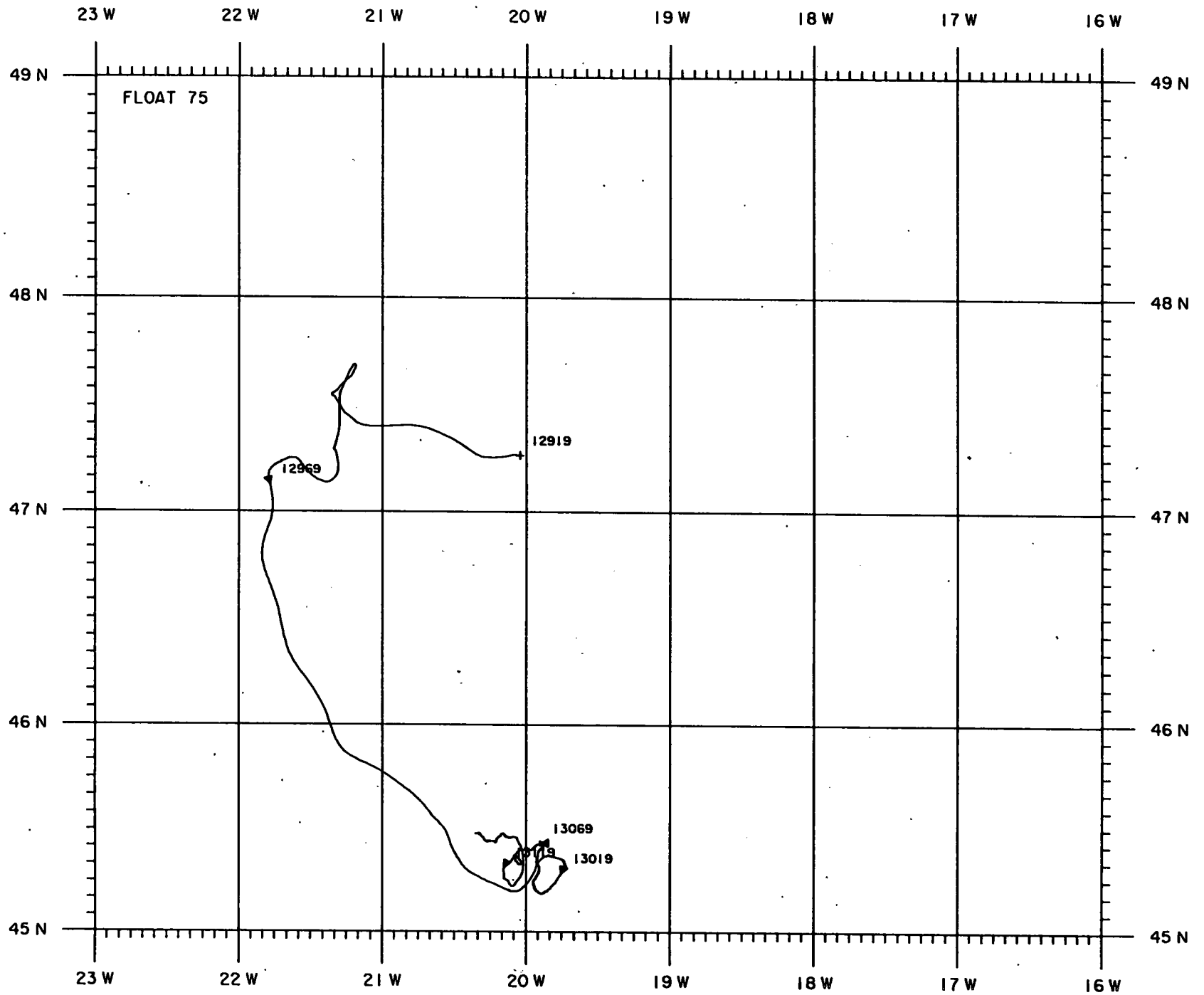
eastward displacement= -22.6 km mean eastward velocity= -0.09 cm/s
northward displacement= -230.7 km mean northward velocity= -0.94 cm/s

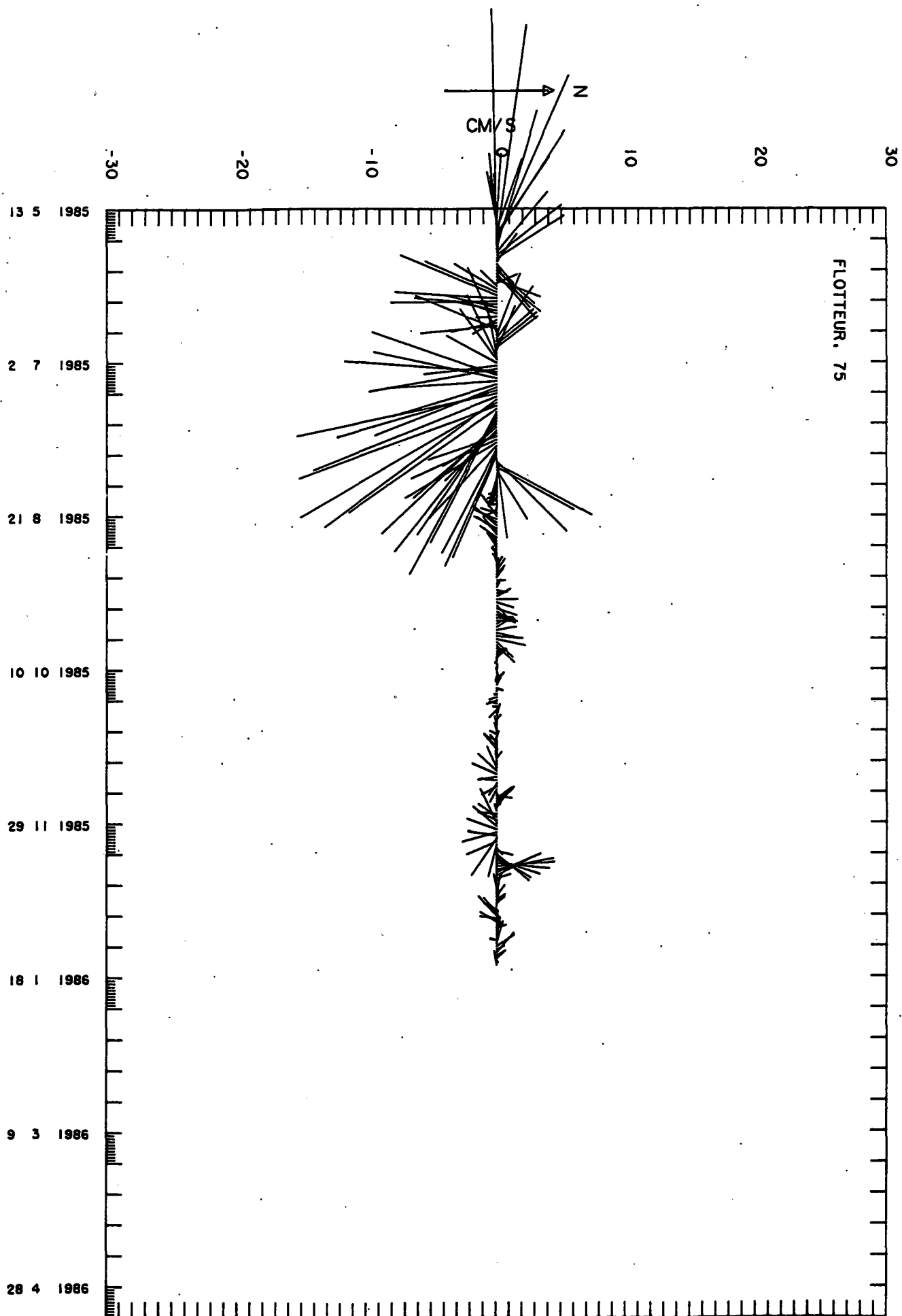
velocity time series statistics:

number of samples= 1472
average east velocity comp.= -0.10 cm/s
average north velocity comp.= -0.94 cm/s
variance of east velocity comp.= 12.19 cm²/s²
variance of north velocity comp.= 14.08 cm²/s²
covariance= -5.33 cm²/s²

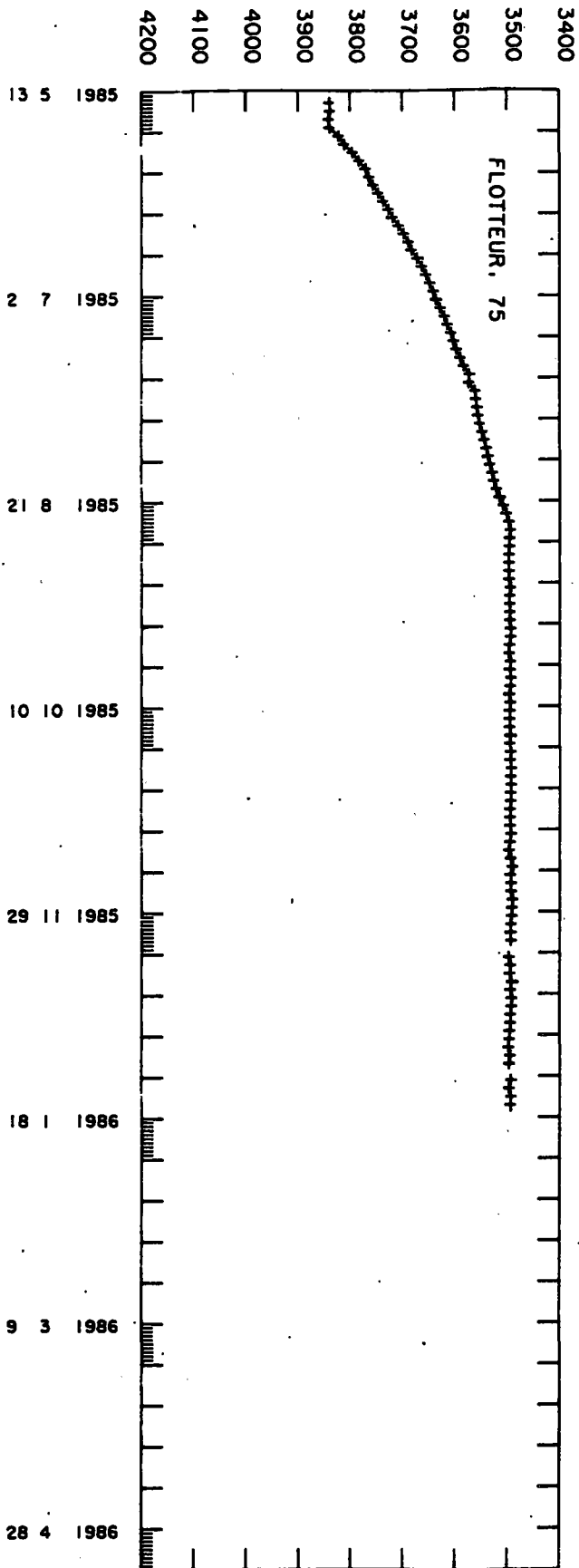
EKE= 13.14 cm²/s²
MKE= 0.45 cm²/s²

covar(u,temp)= 0.04 cm.degreeC/s
covar(v,temp)= -0.03 cm.degreeC/s

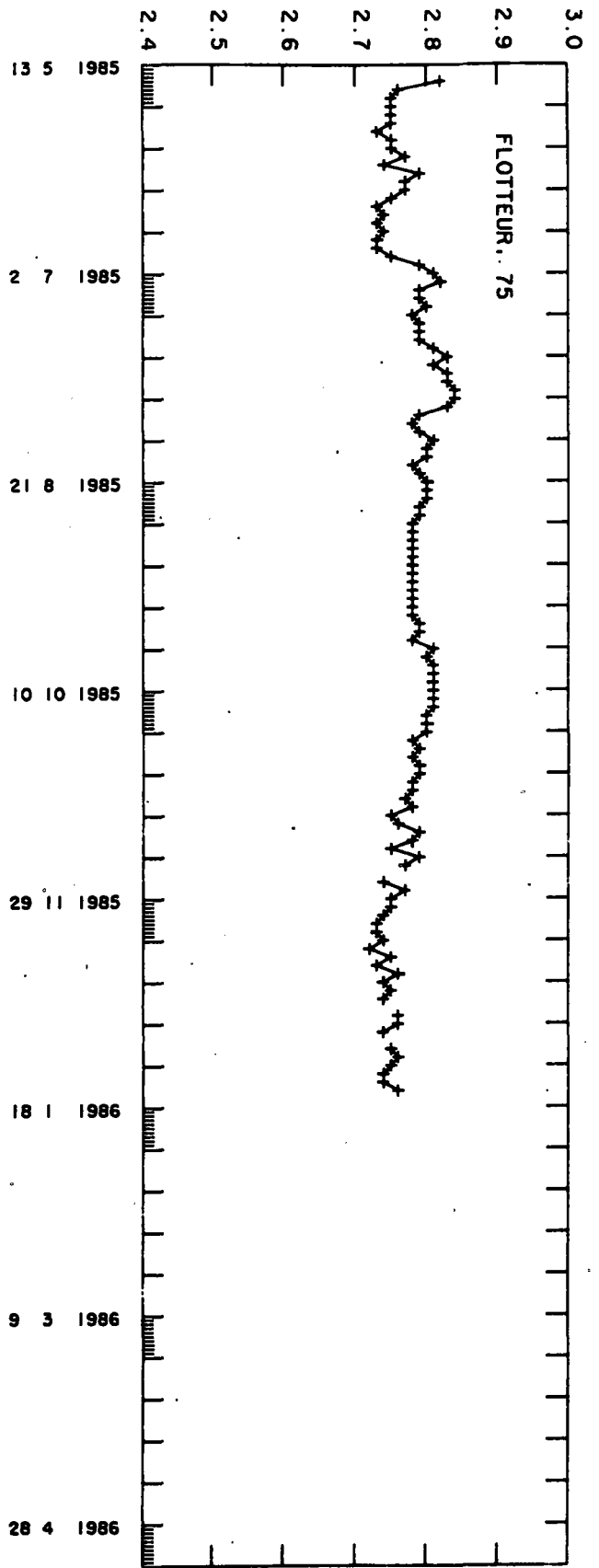




PRESSURE DBARS



TEMPERATURE DEGREES C



NOAMP experiment

float no: 76

launch date	launch lat	launch long			
1985 5 14 15h UT	47.27 N	-20.58 W			
date of first pos	first lat	first long	init. pres.	init. temp.	
1985 5 15 1h UT	47.28 N	-20.05 W	3747.	2.77	
date of last pos	last lat	last long	last pres.	last temp.	life (days)
1985 9 27 5h UT	46.93 N	-21.71 W	3501.	2.70	135.2

total displacement 135.6 days after launching

eastward displacement= -85.1 km mean eastward velocity= -0.63 cm/s
northward displacement= -43.7 km mean northward velocity= -0.32 cm/s

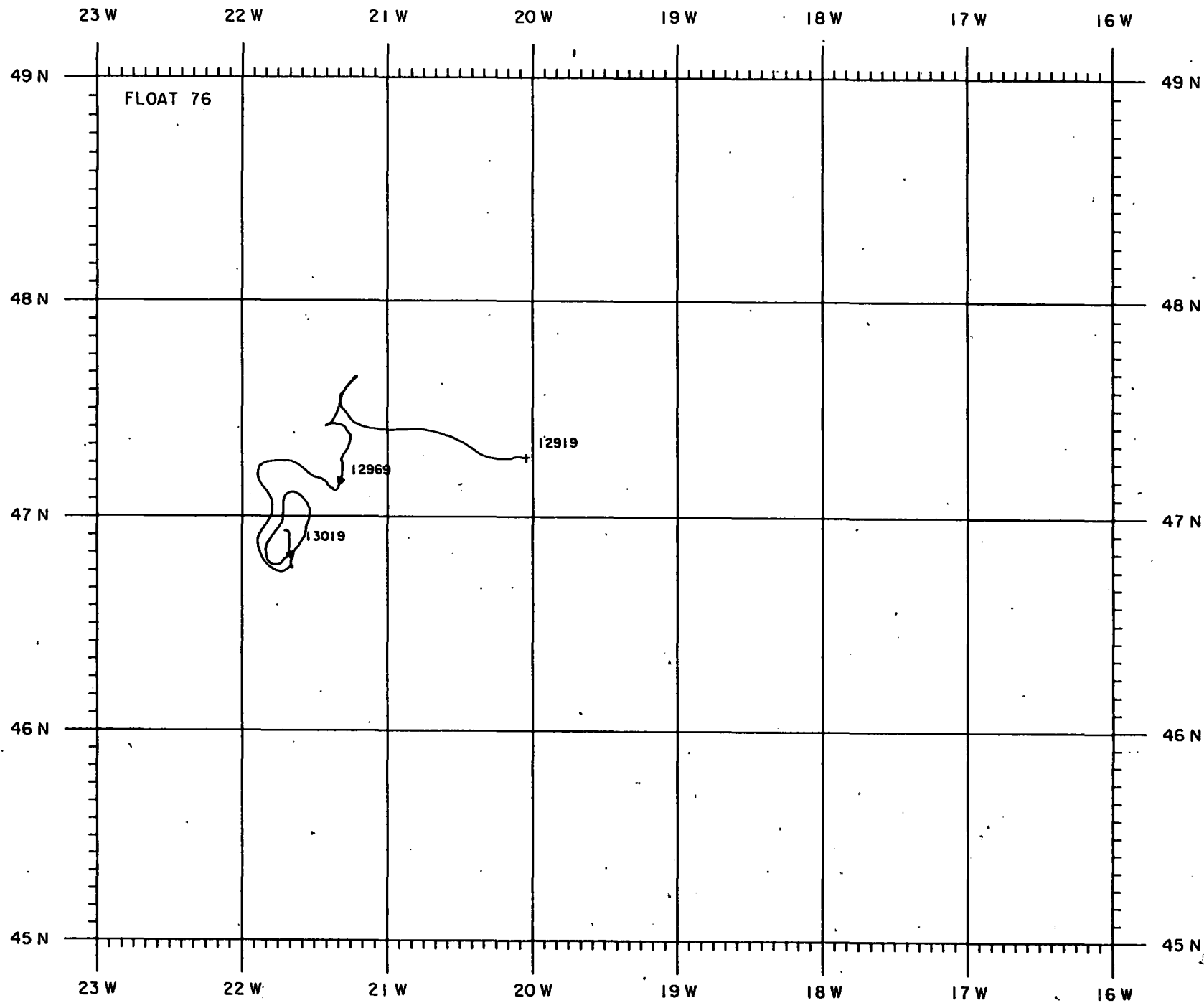
velocity time series statistics:

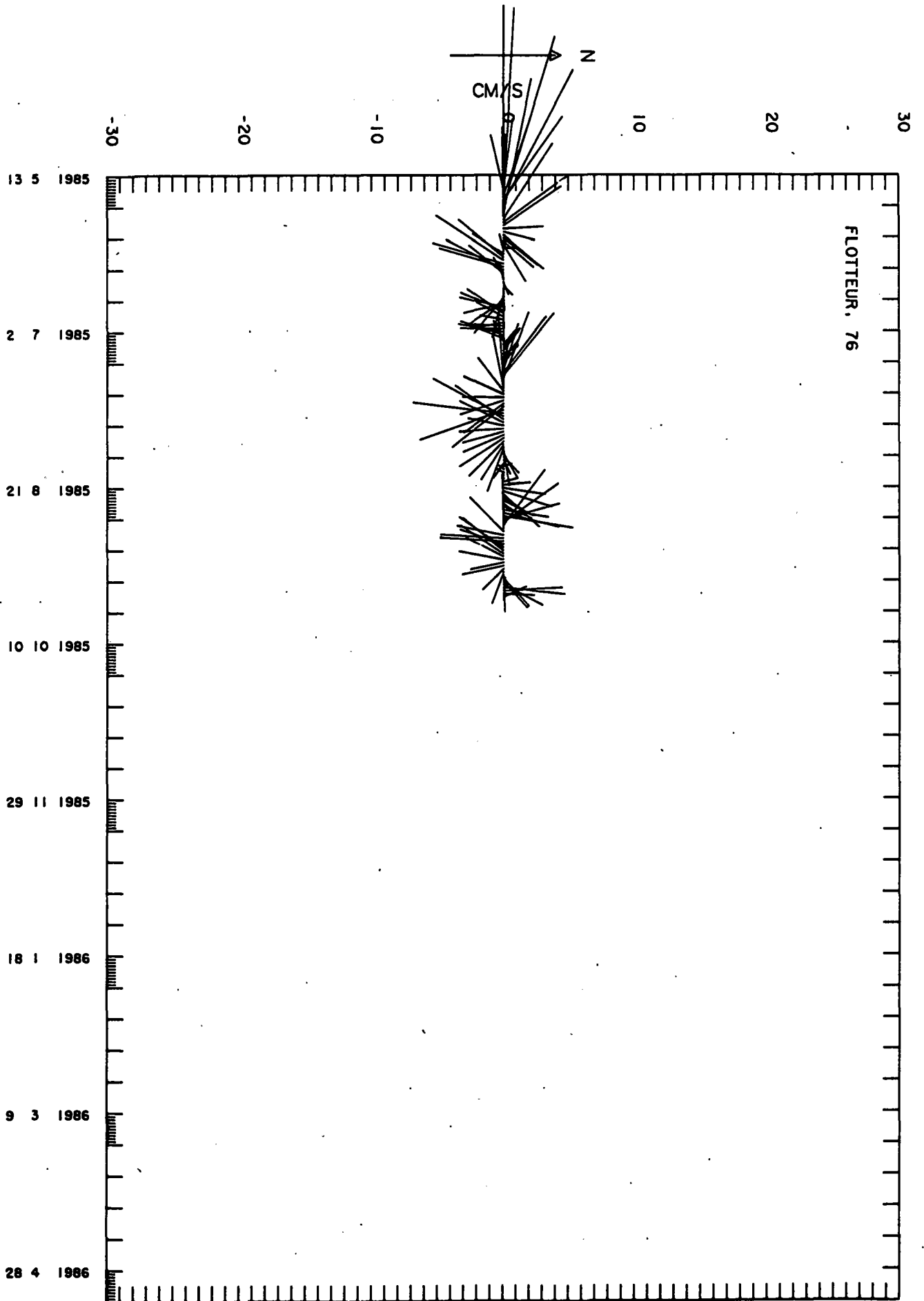
number of samples= 812
average east velocity comp.= -1.07 cm/s
average north velocity comp.= -0.33 cm/s

variance of east velocity comp.= 11.02 cm²/s²
variance of north velocity comp.= 8.14 cm²/s²
covariance= -1.49 cm²/s²

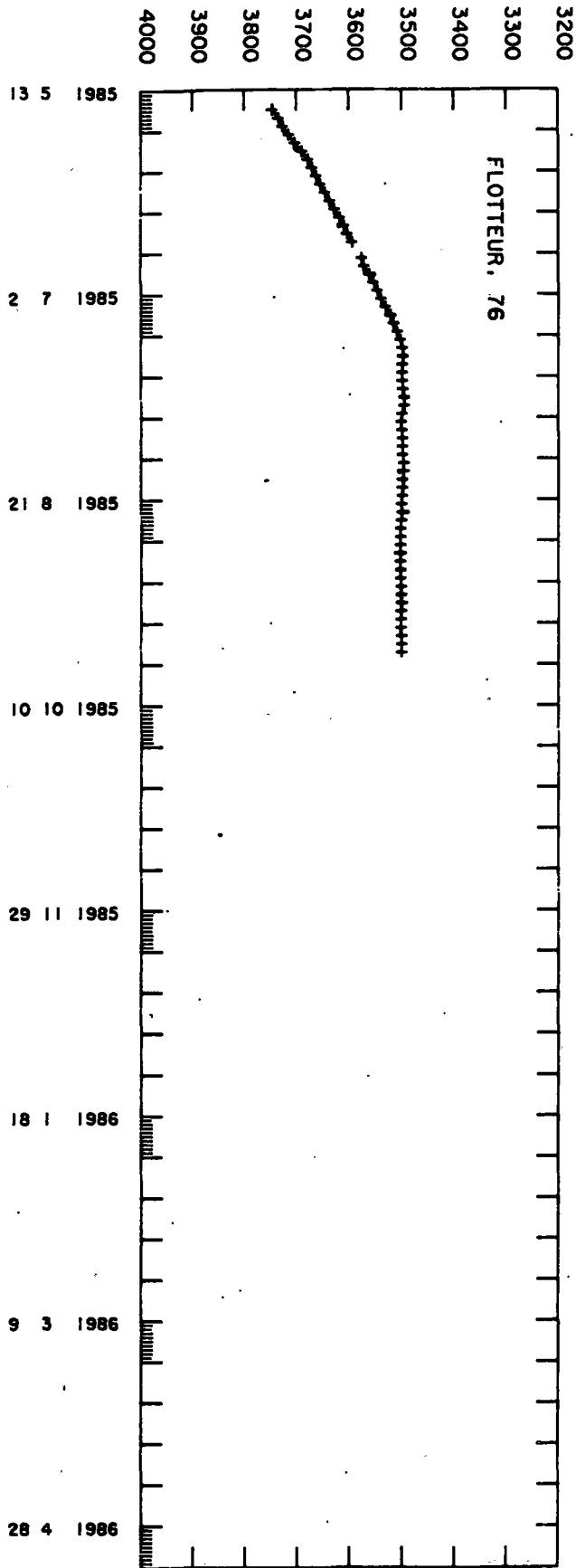
EKE= 9.58 cm²/s²
MKE= 0.63 cm²/s²

covar(u,temp)= 0.01 cm.degreeC/s
covar(v,temp)= -0.04 cm.degreeC/s

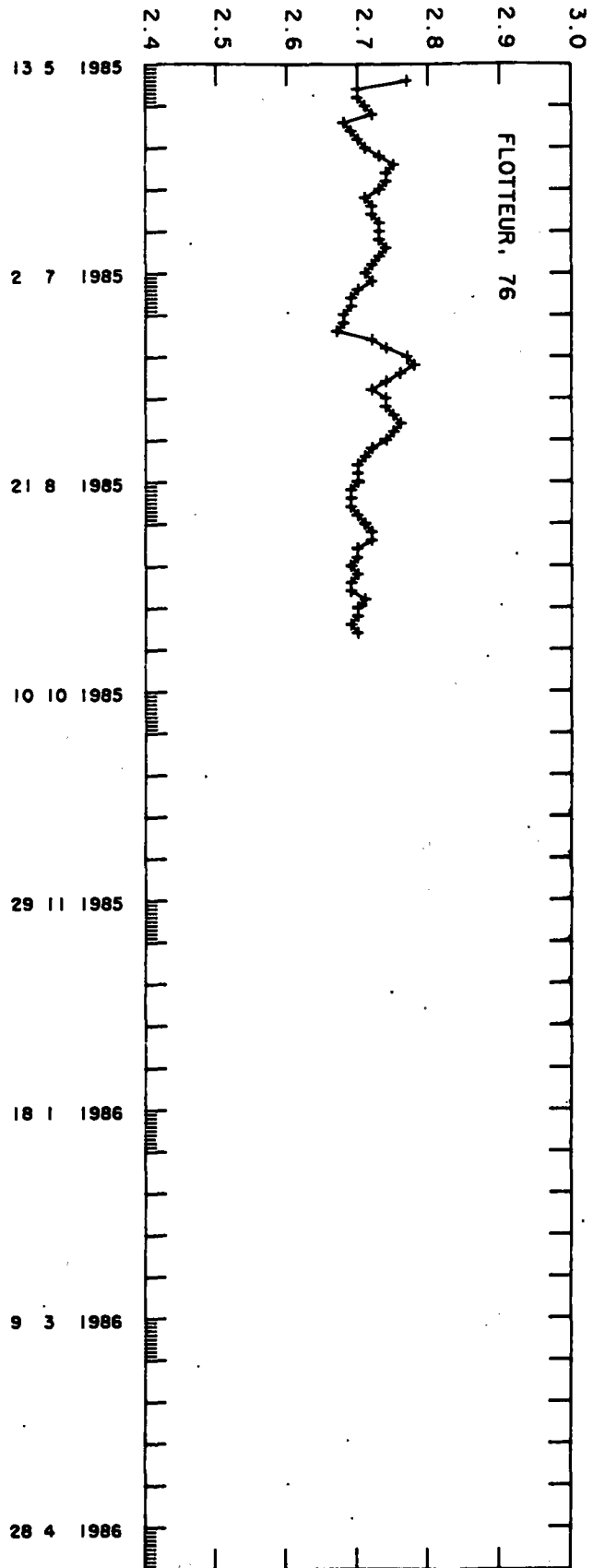




PRESSURE DBARS



TEMPERATURE DEGREES C



NOAMP experiment

float no: 78

launch date	launch lat	launch long			
1985 5 14 22h UT	47.06 N	-19.53 W			
date of first pos	first lat	first long	init. pres.	init. temp.	
1985 5 15 2h UT	47.09 N	-19.53 W	4059.	2.78	
date of last pos	last lat	last long	last pres.	last temp.	life (days)
1986 3 7 22h UT	48.40 N	-20.79 W	3496.	2.66	296.8

total displacement 297.0 days after launching

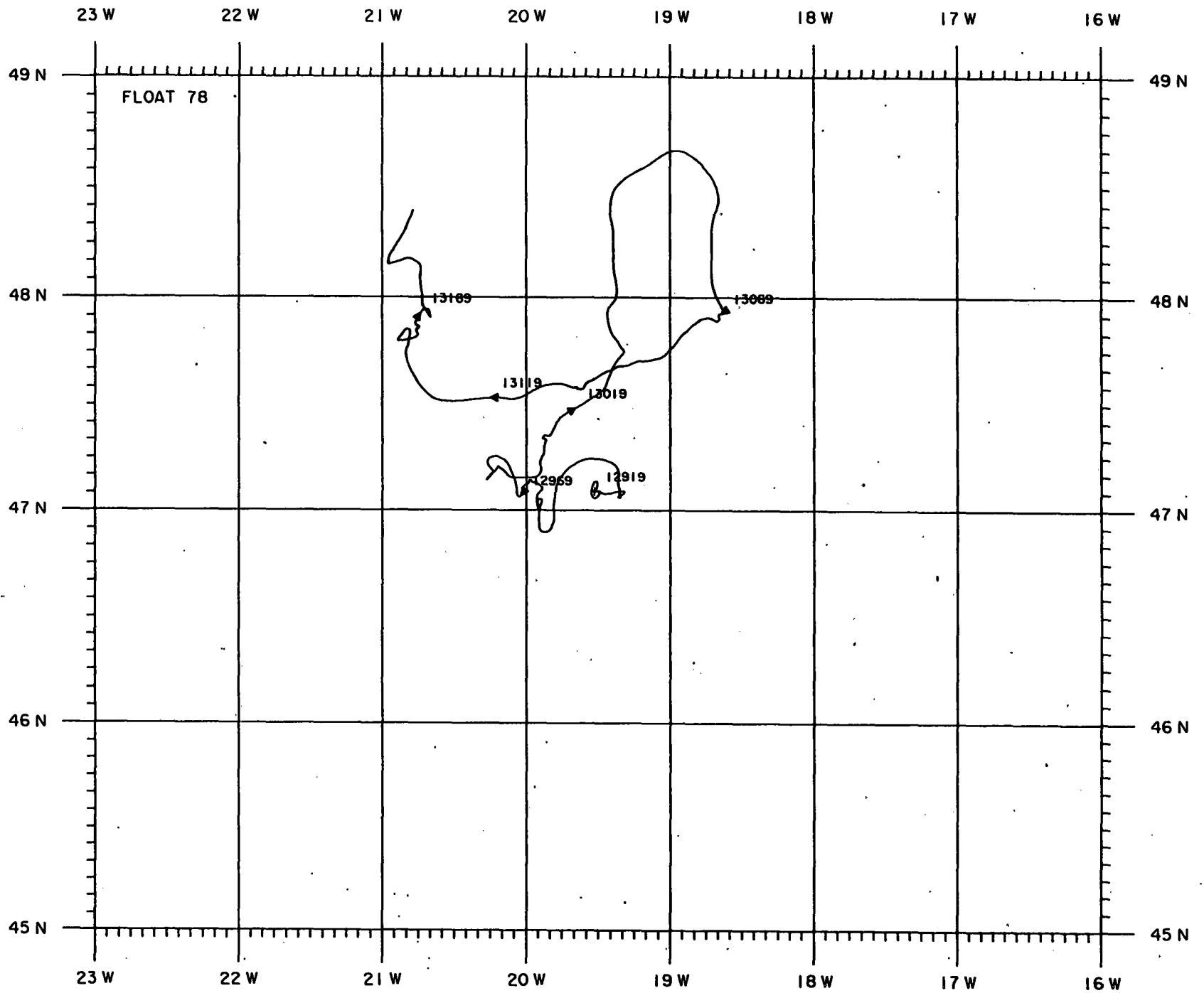
eastward displacement= -93.8 km mean eastward velocity= -0.32 cm/s
northward displacement= 171.5 km mean northward velocity= 0.58 cm/s

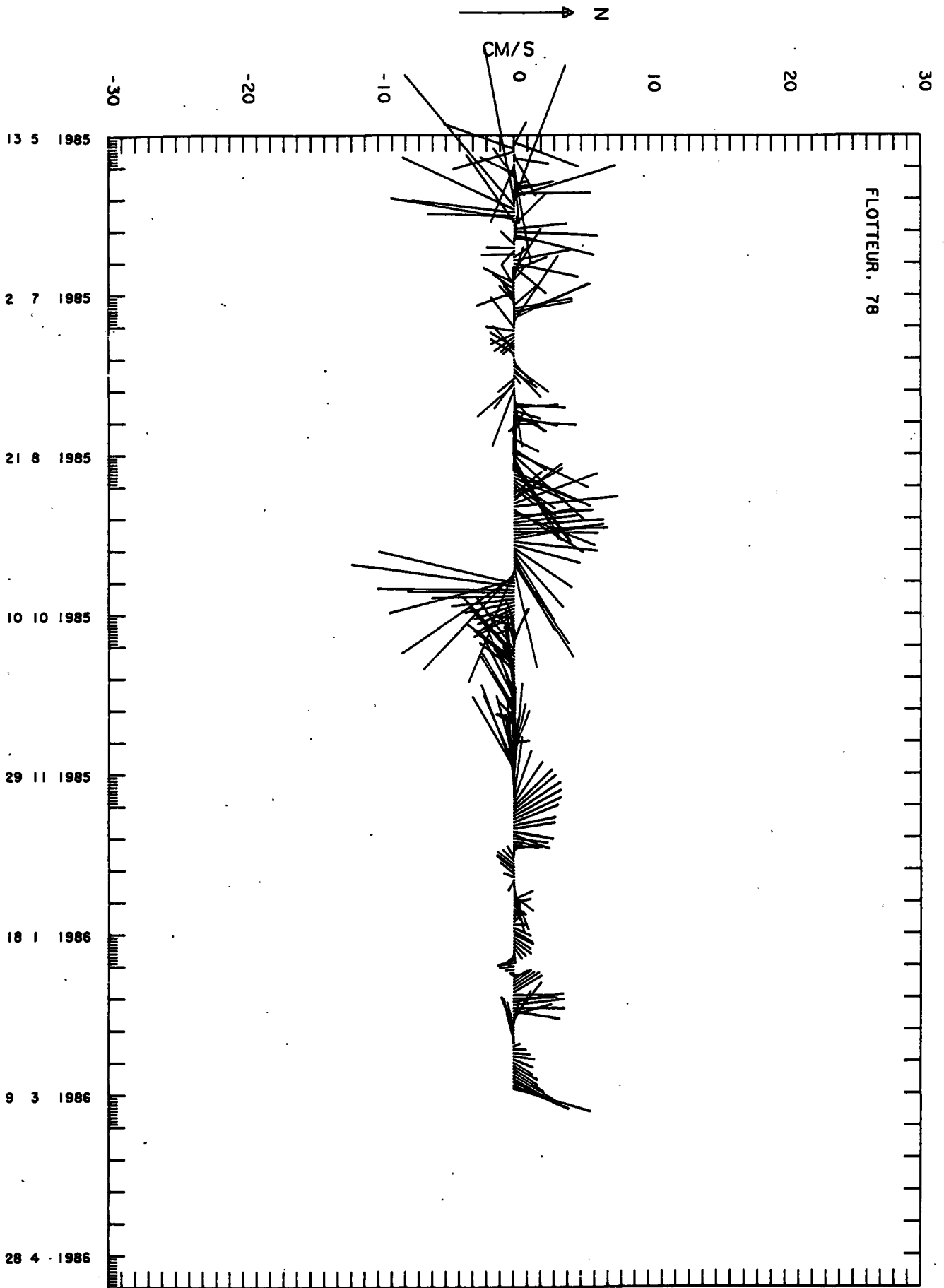
velocity time series statistics:

number of samples= 1782
average east velocity comp.= -0.37 cm/s
average north velocity comp.= 0.57 cm/s
variance of east velocity comp.= 7.77 cm²/s²
variance of north velocity comp.= 10.26 cm²/s²
covariance= 1.80 cm²/s²

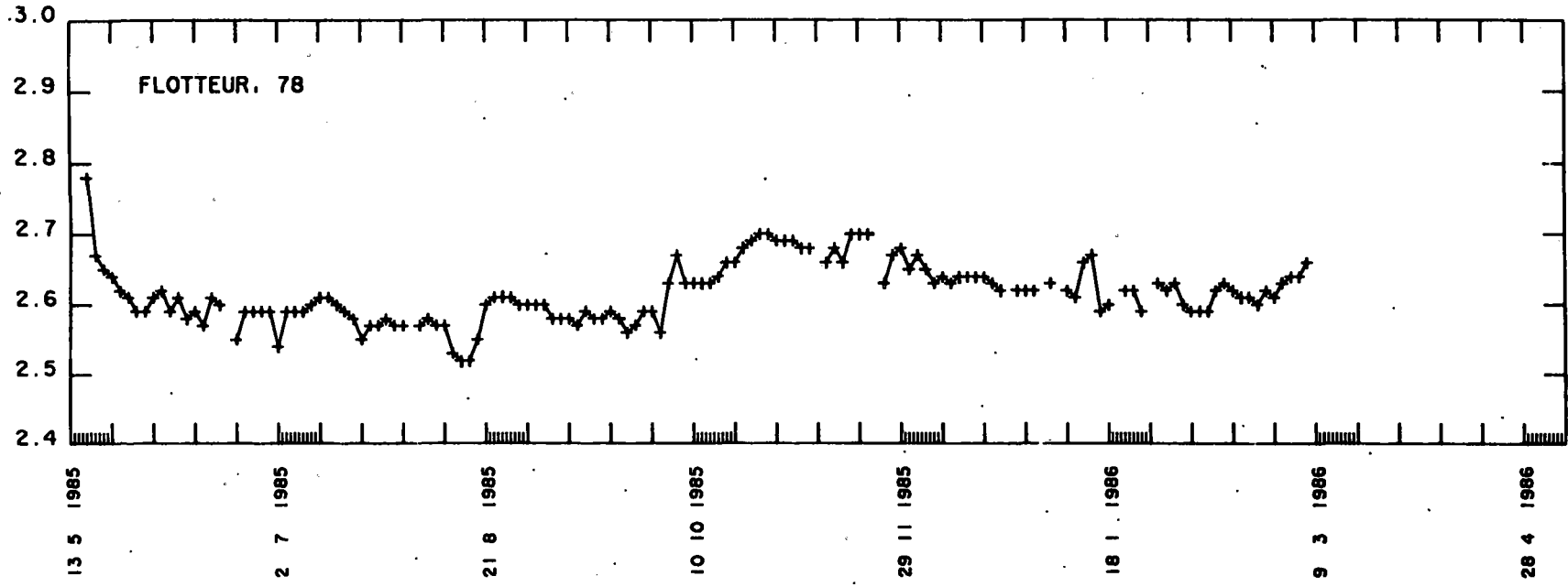
EKE= 9.02 cm²/s²
MKE= 0.23 cm²/s²

covar(u,temp)= -0.05 cm.degreeC/s
covar(v,temp)= -0.03 cm.degreeC/s

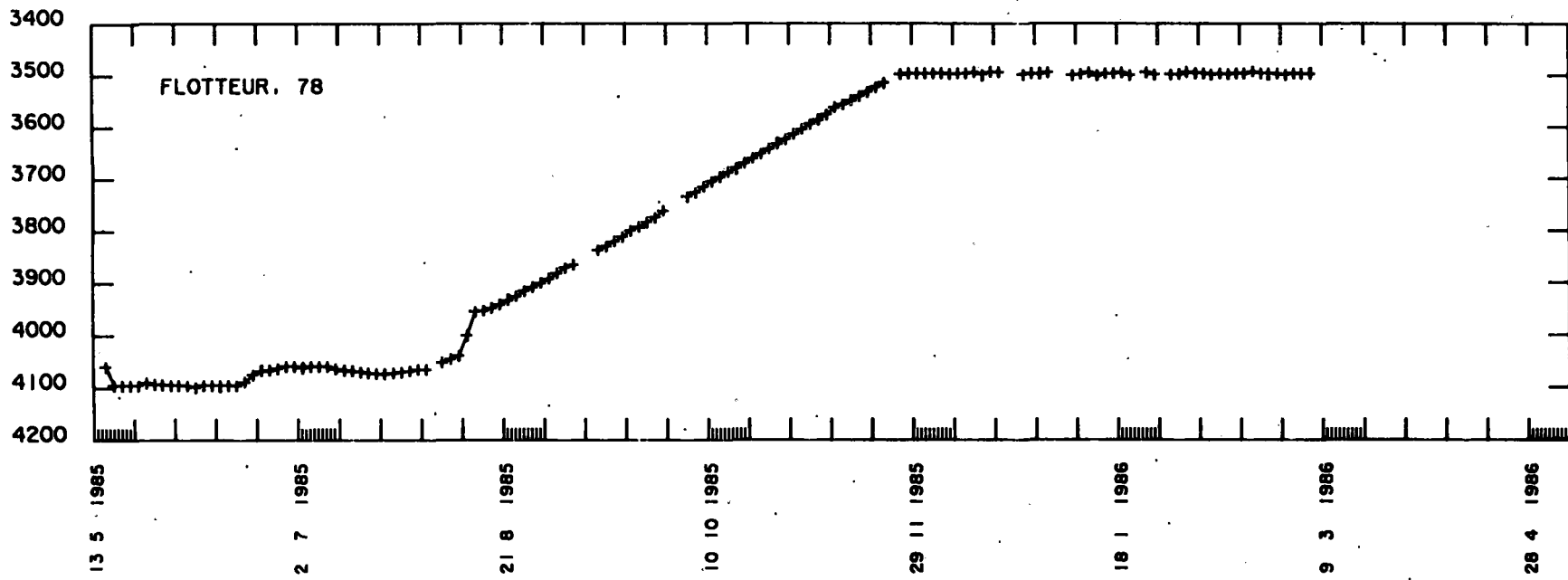




TEMPERATURE DEGREES C



PRESSURE DBARS



NOAMP experiment

float no: 79

launch date	launch lat	launch long			
1985 5 15 5h UT	47.35 N	-19.65 W			
date of first pos	first lat	first long	init. pres.	init. temp.	
1985 5 15 6h UT	47.36 N	-19.65 W	3966.	2.71	
date of last pos	last lat	last long	last pres.	last temp.	life (days)
1986 4 24 10h UT	45.75 N	-20.06 W	3493.	2.80	344.2

total displacement 344.2 days after launching

eastward displacement= -31.6 km mean eastward velocity= -0.09 cm/s
northward displacement= -204.7 km mean northward velocity= -0.59 cm/s

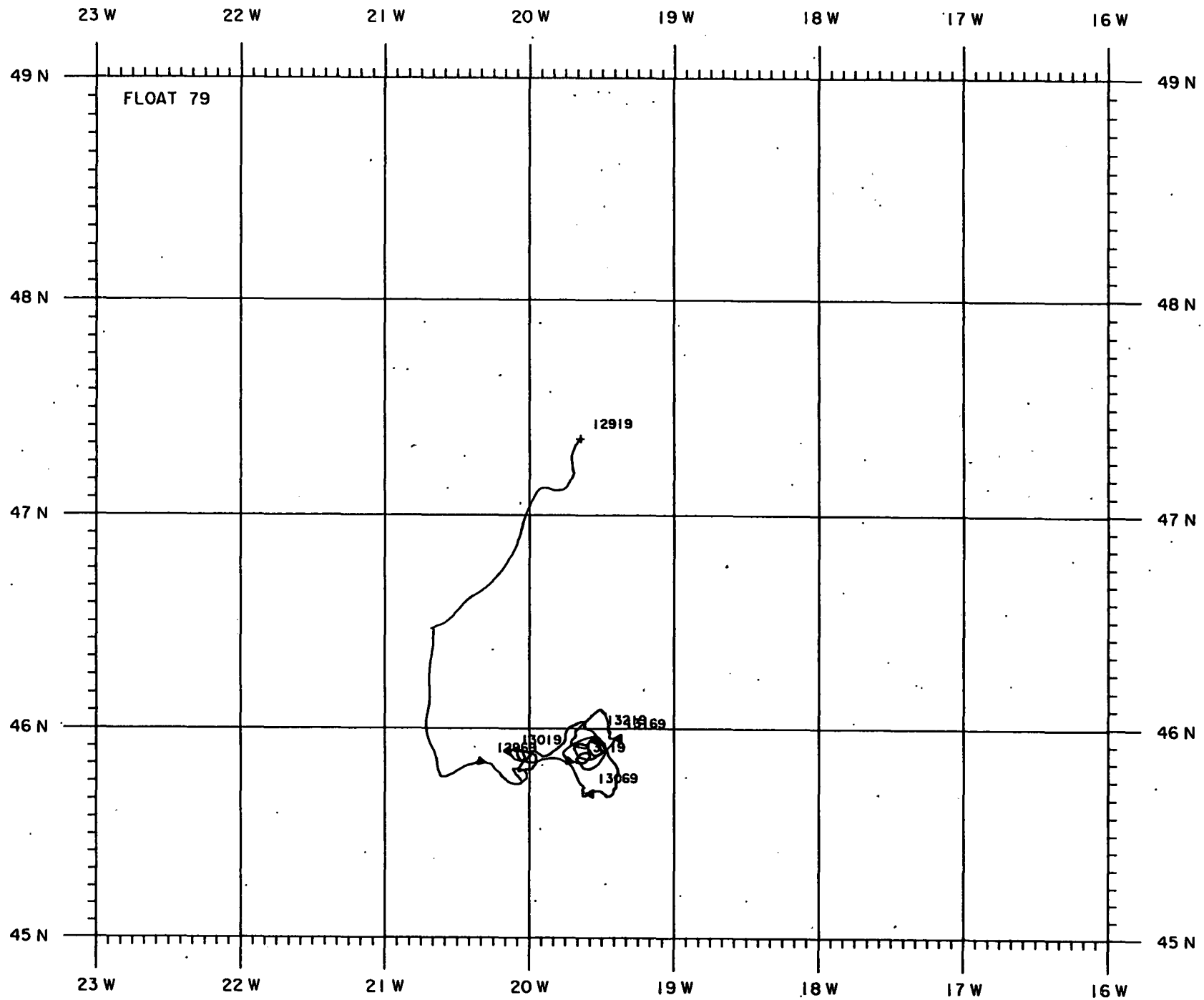
velocity time series statistics:

number of samples= 2066
average east velocity comp.= -0.10 cm/s
average north velocity comp.= -0.60 cm/s

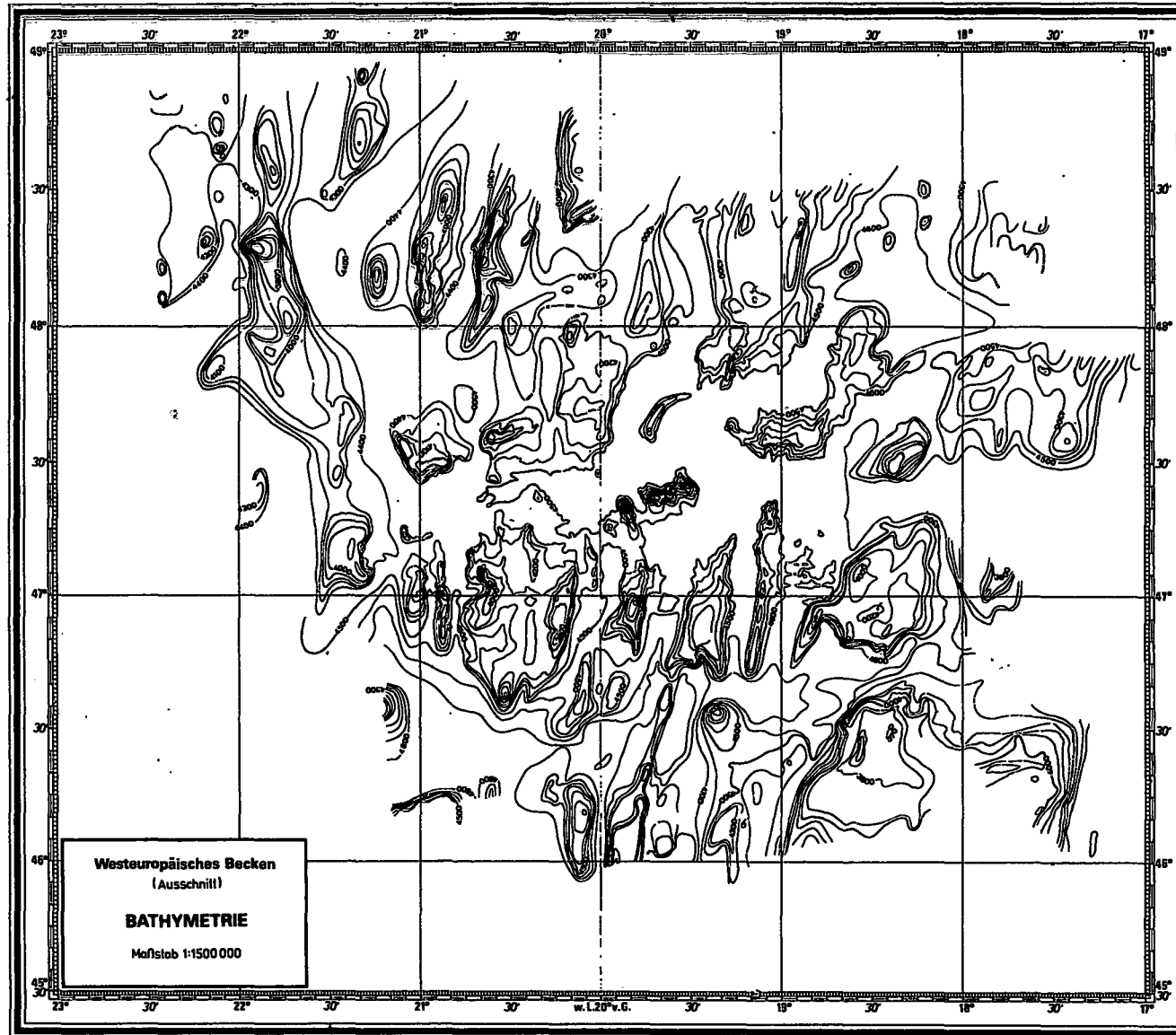
variance of east velocity comp.= 4.22 cm²/s²
variance of north velocity comp.= 5.91 cm²/s²
covariance= 1.66 cm²/s²

EKE= 5.07 cm²/s²
MKE= 0.19 cm²/s²

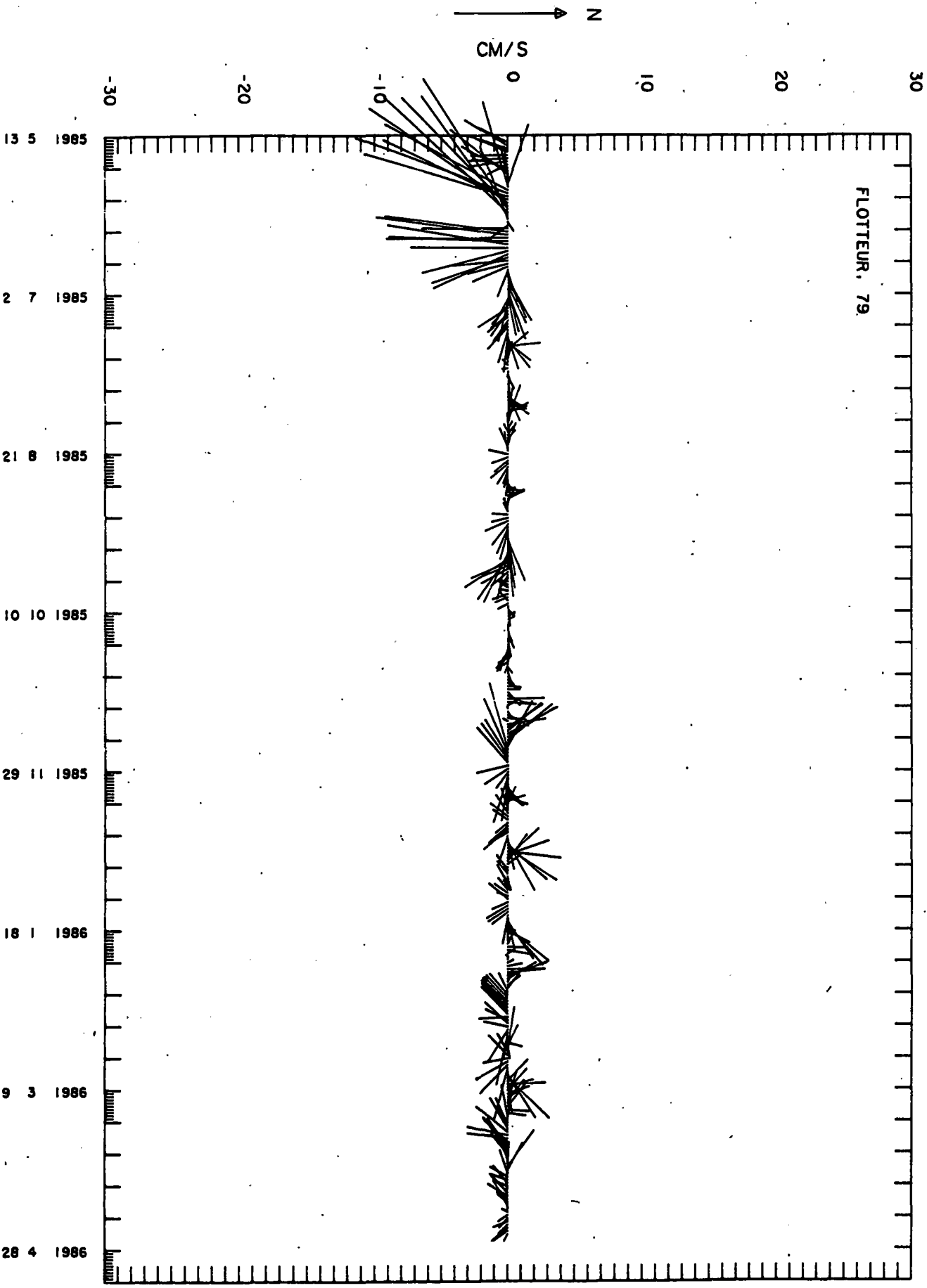
covar(u,temp)= 0.01 cm.degreeC/s
covar(v,temp)= 0.03 cm.degreeC/s



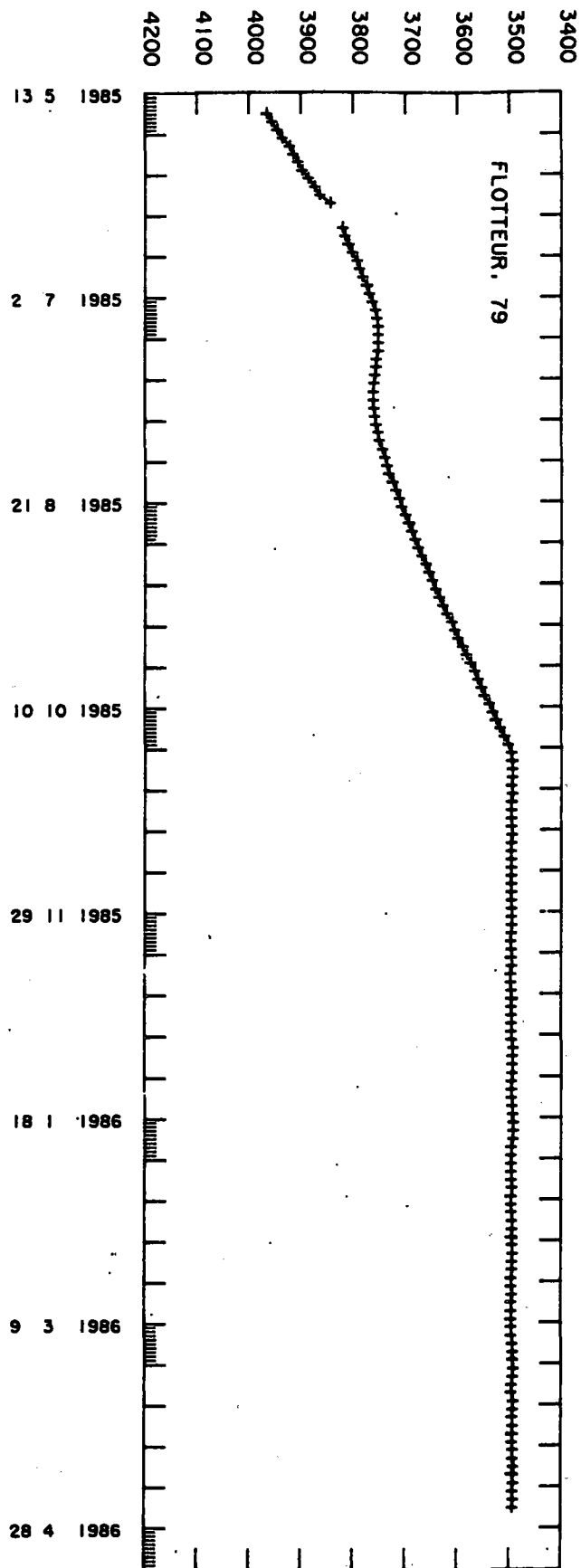
H. Heinrich: **Bathymetrie und Geomorphologie des NOAMP-Gebietes, Westeuropäisches Becken (17° W bis 22° W, 46° N bis 49° N)**



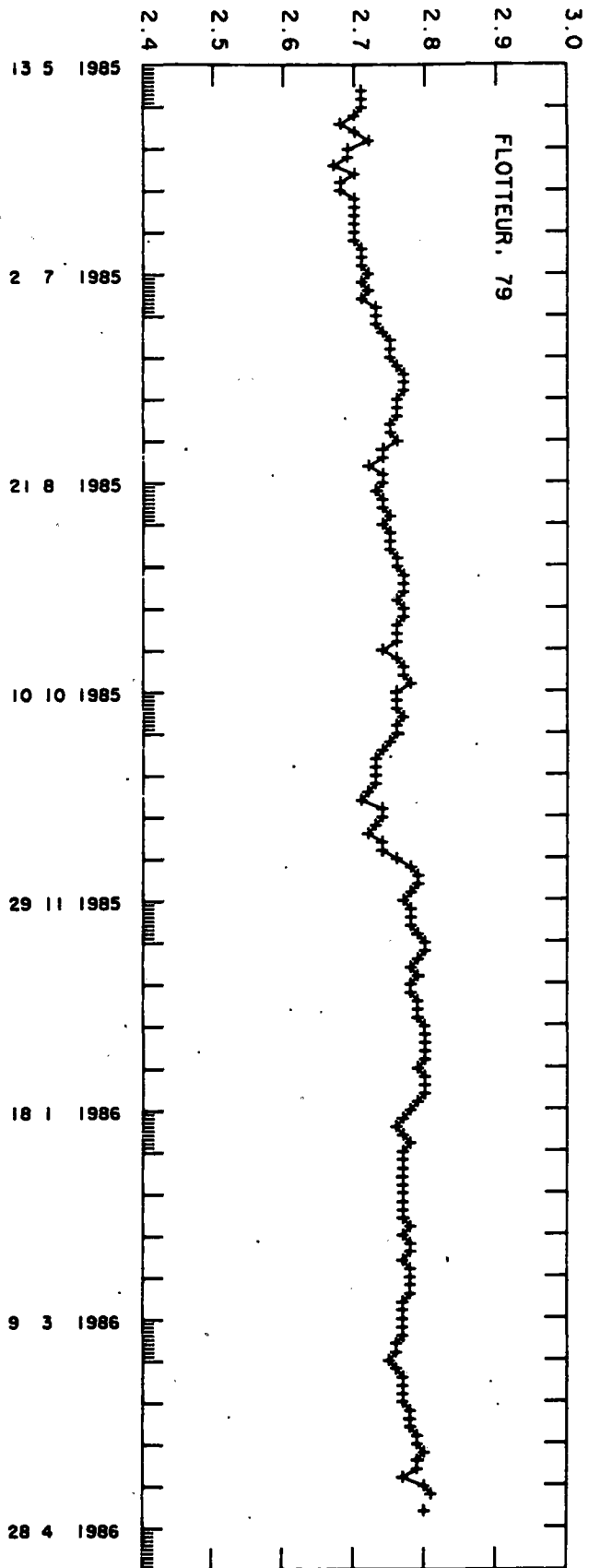
Bearbeiter: H. Heinrich, R. Pätz (Deutsches Hydrographisches Institut)



PRESSURE DBARS



TEMPERATURE DEGREES C



NOAMP experiment

float no: 80

launch date	launch lat	launch long			
1985 5 15 5h UT	47.35 N	-19.65 W			
date of first pos	first lat	first long	init. pres.	init. temp.	
1985 5 15 6h UT	47.35 N	-19.65 W	4070.	2.73	
date of last pos	last lat	last long	last pres.	last temp.	life (days)
1986 1 8 2h UT	46.49 N	-19.94 W	3550.	2.80	237.8

total displacement 237.9 days after launching

eastward displacement= -22.6 km mean eastward velocity= -0.10 cm/s
northward displacement= -110.5 km mean northward velocity= -0.46 cm/s

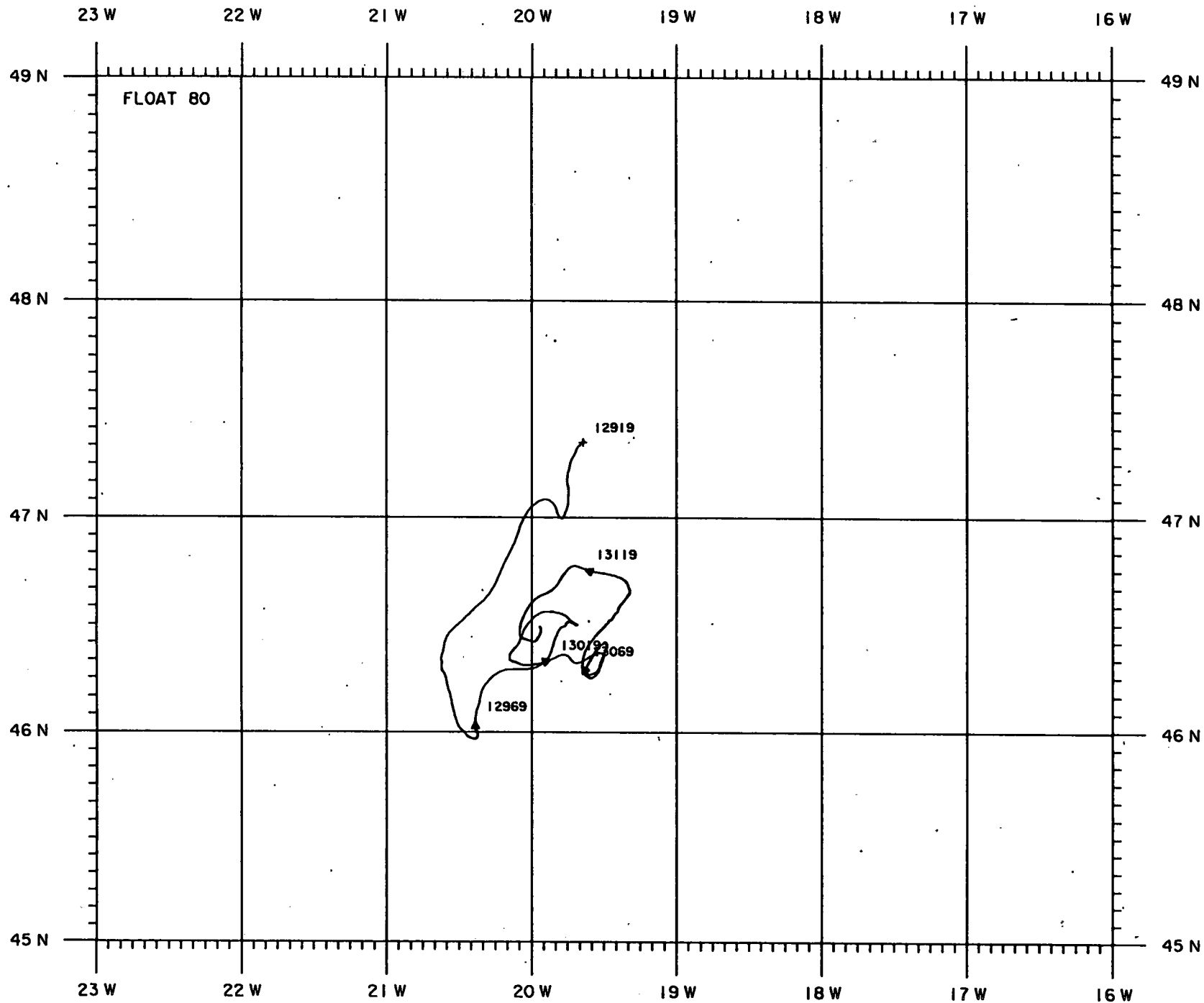
velocity time series statistics:

number of samples= 1428
average east velocity comp.= -0.10 cm/s
average north velocity comp.= -0.47 cm/s

variance of east velocity comp.= 6.06 cm²/s²
variance of north velocity comp.= 9.06 cm²/s²
covariance= 3.56 cm²/s²

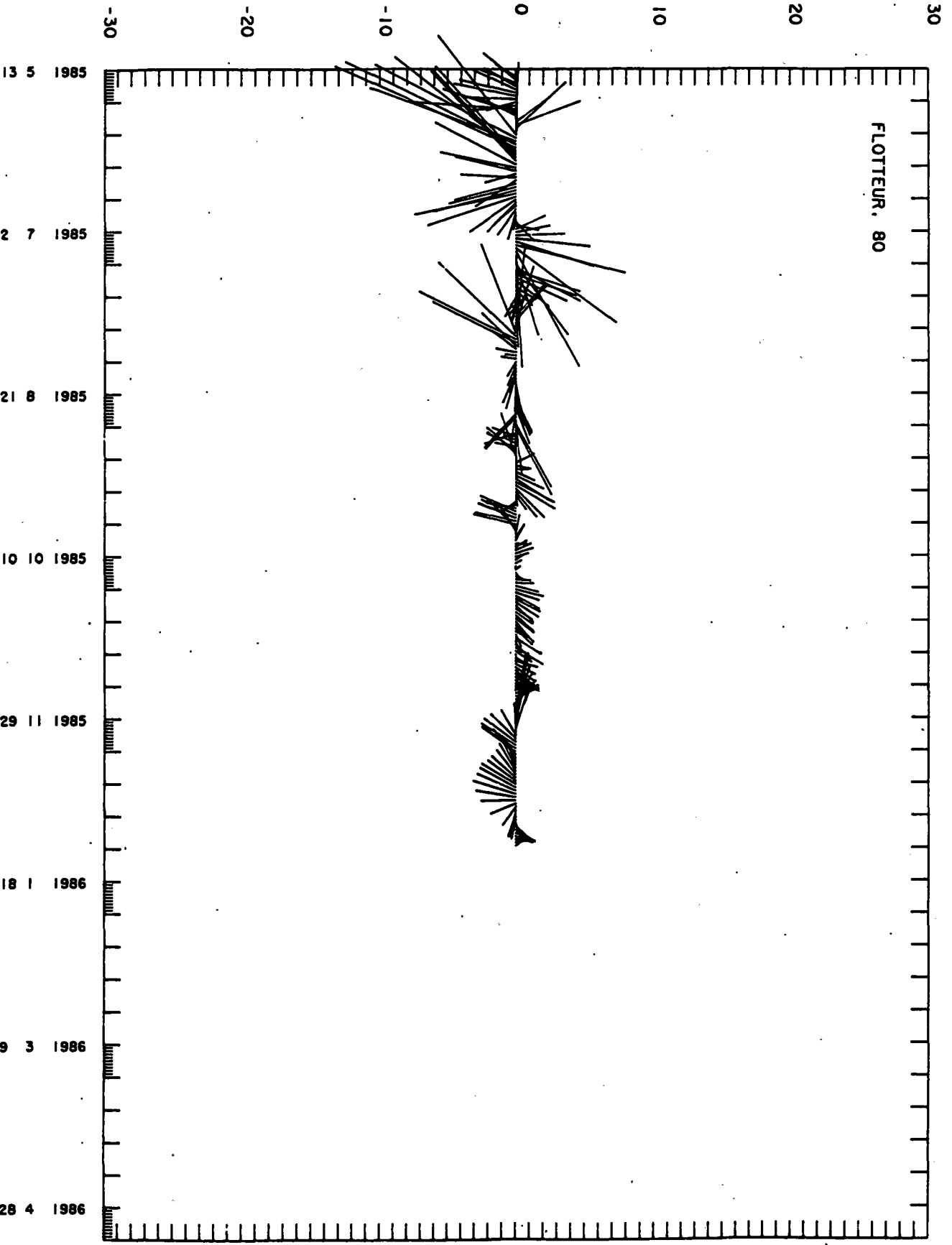
EKE= 7.56 cm²/s²
MKE= 0.11 cm²/s²

covar(u,temp)= 0.00 cm.degreeC/s
covar(v,temp)= 0.01 cm.degreeC/s

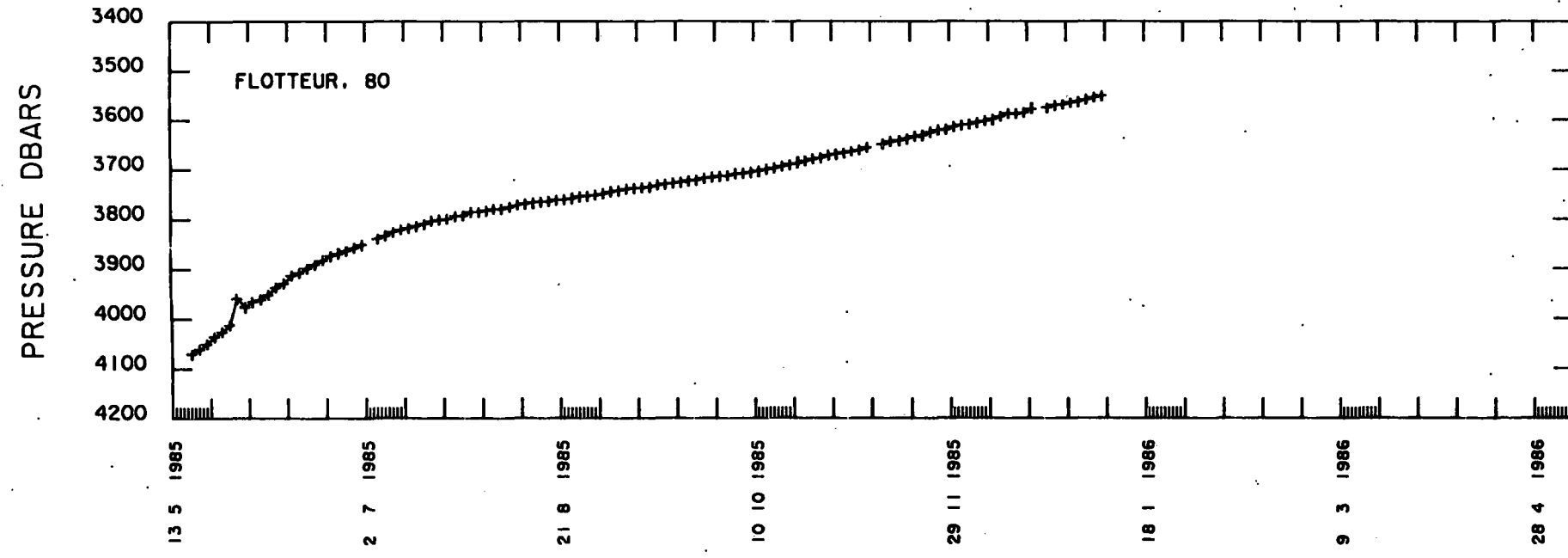
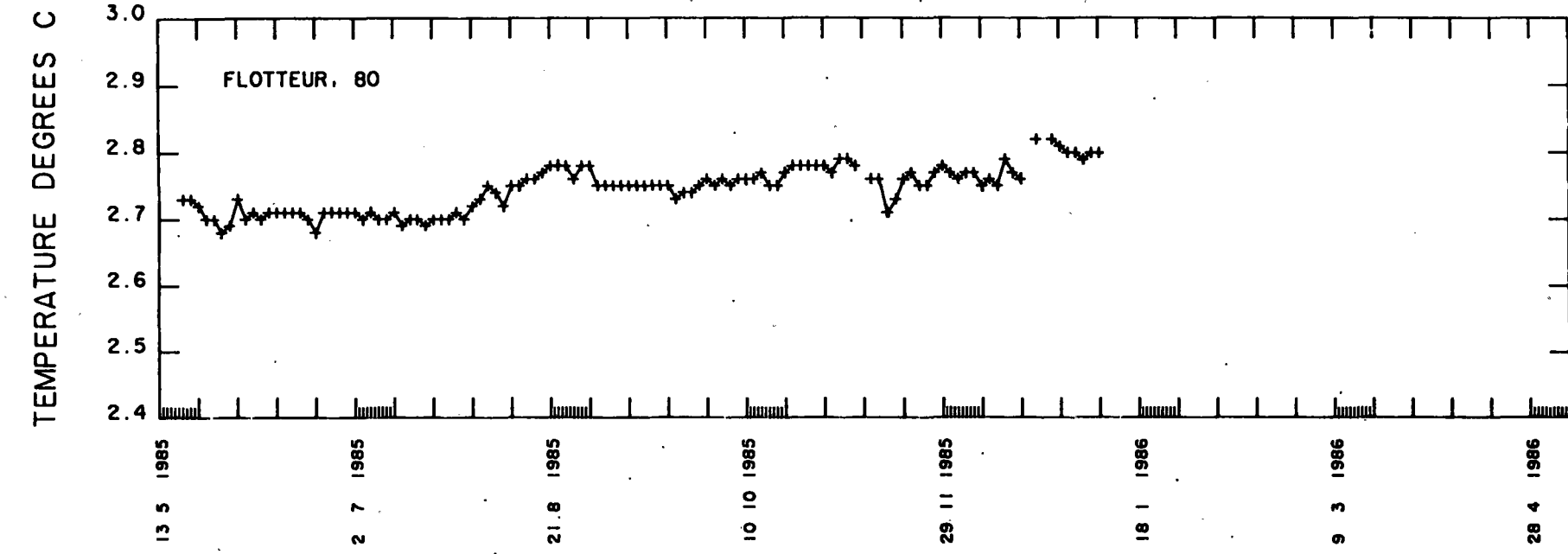


N

CM/S



FLOTTEUR, 80



NOAMP experiment

float no: 81

launch date	launch lat	launch long			
1985 5 15 5h UT	47.35 N	-19.65 W			
date of first pos	first lat	first long	init. pres.	init. temp.	
1985 5 15 11h UT	47.35 N	-19.64 W	3752.	2.72	
date of last pos	last lat	last long	last pres.	last temp.	life (days)
1986 4 24 15h UT	45.32 N	-19.85 W	3493.	2.70	344.2

total displacement 344.4 days after launching

eastward displacement= -15.5 km mean eastward velocity= -0.05 cm/s
northward displacement= -260.7 km mean northward velocity= -0.76 cm/s

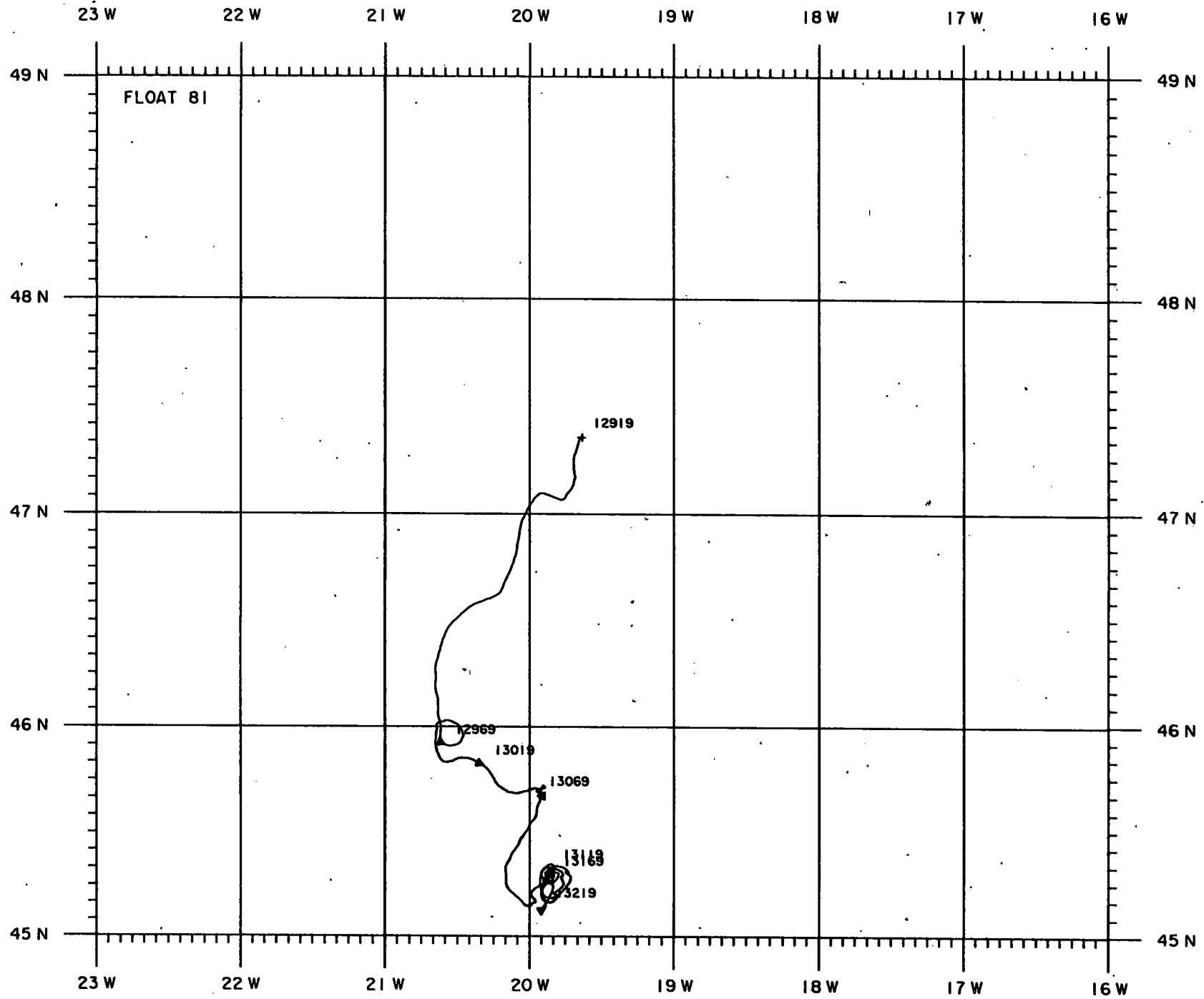
velocity time series statistics:

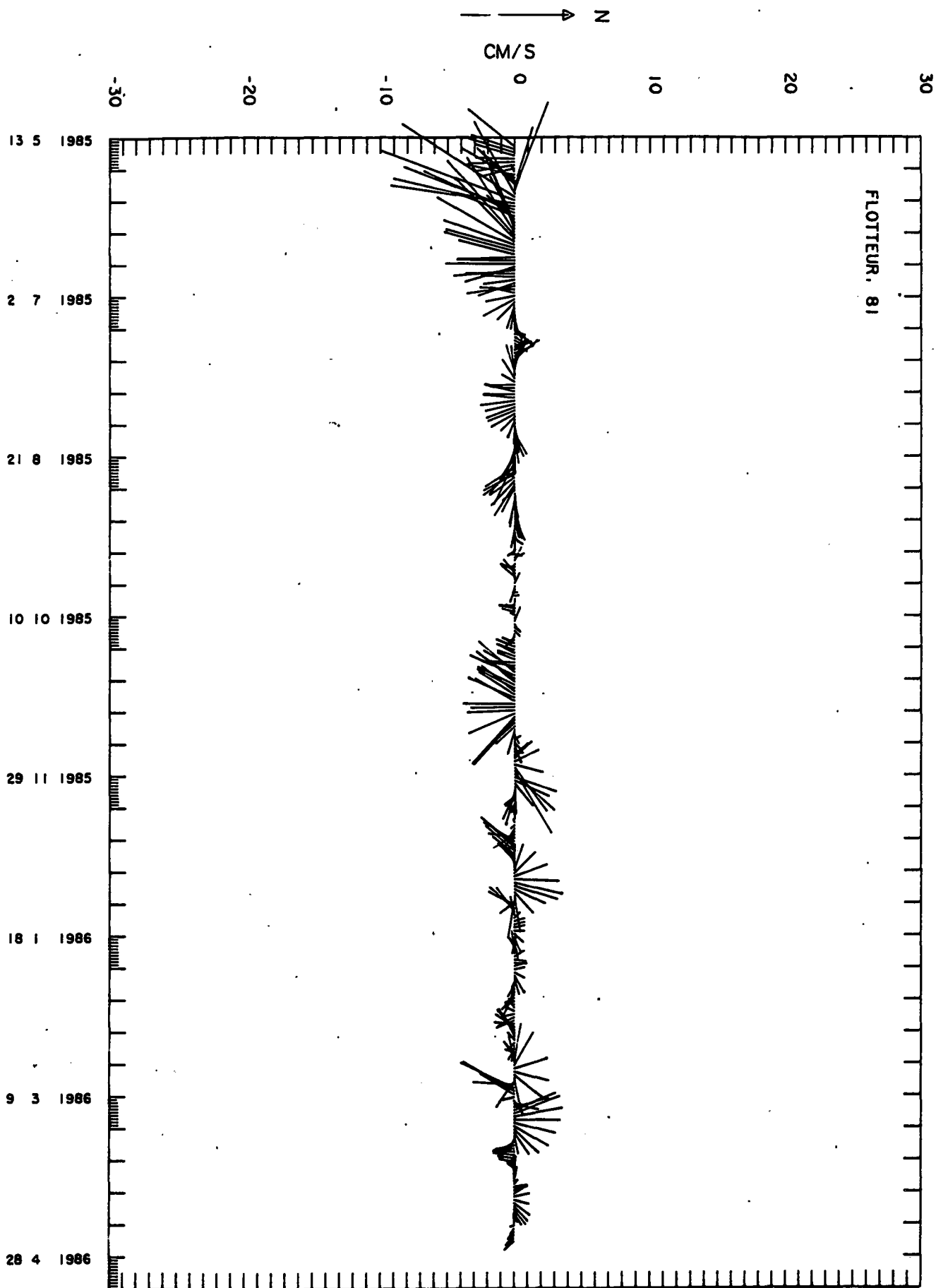
number of samples= 2066
average east velocity comp.= -0.05 cm/s
average north velocity comp.= -0.76 cm/s

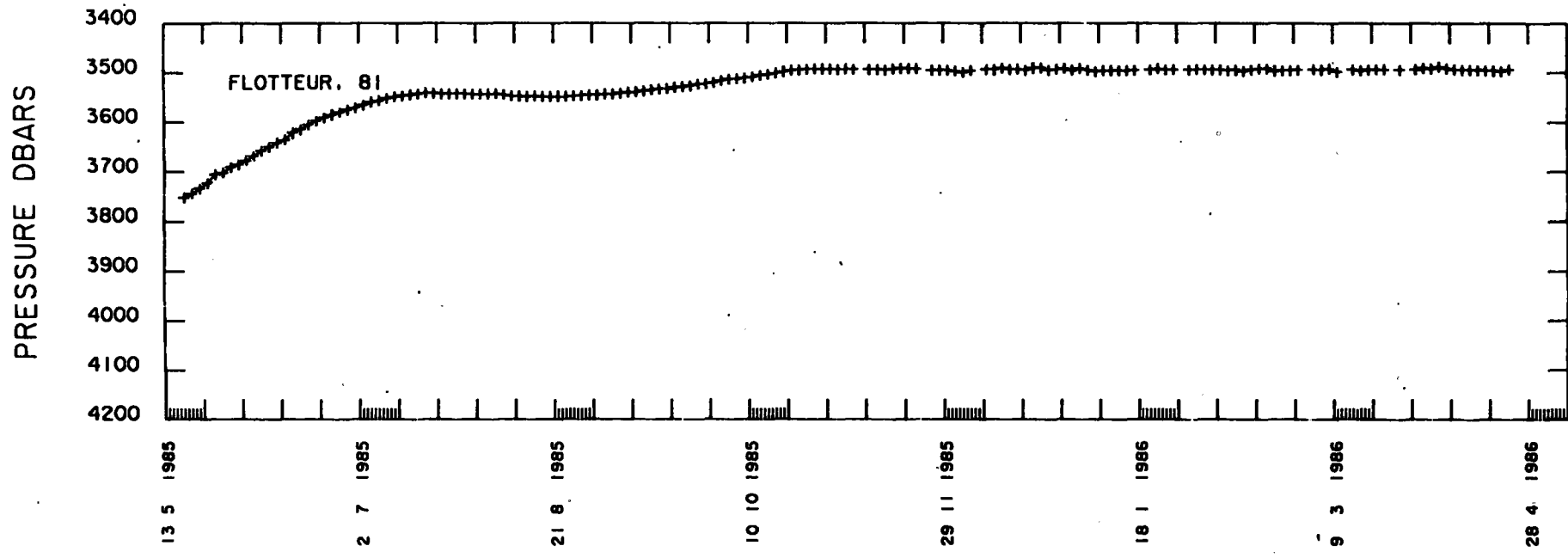
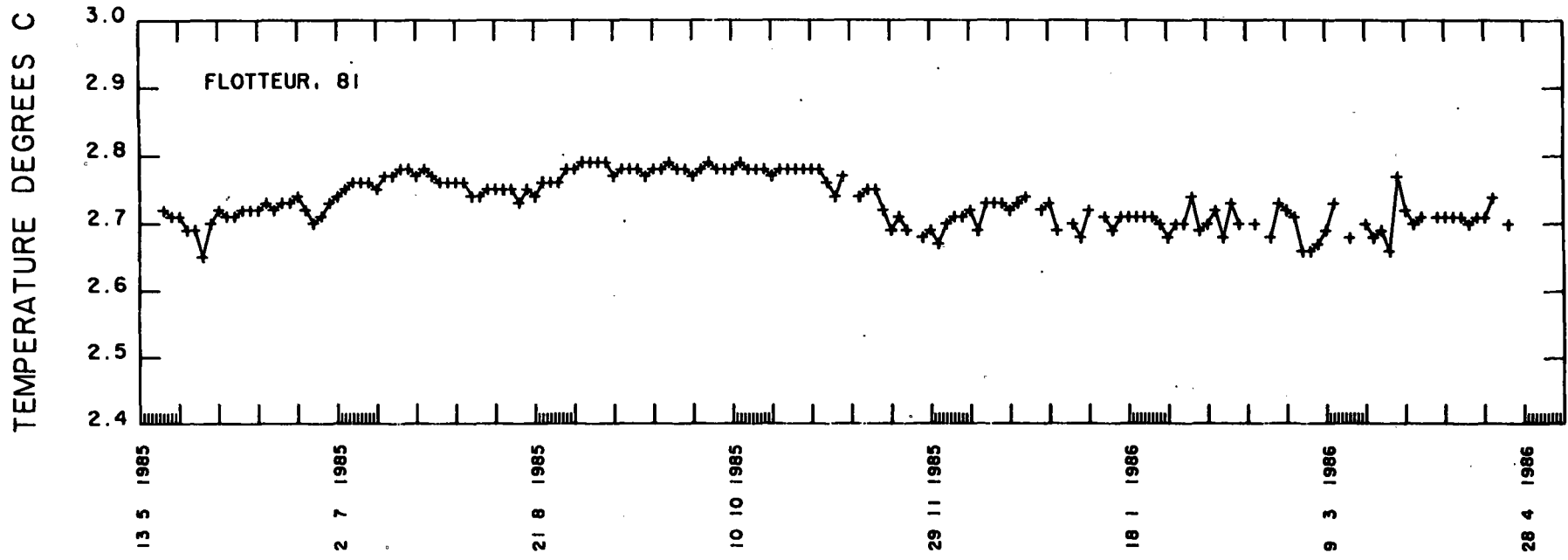
variance of east velocity comp.= 2.57 cm²/s²
variance of north velocity comp.= 4.27 cm²/s²
covariance= 1.13 cm²/s²

EKE= 3.42 cm²/s²
MKE= 0.29 cm²/s²

covar(u,temp)= 0.01 cm.degreeC/s
covar(v,temp)= 0.00 cm.degreeC/s







NOAMP experiment

float no: 82

launch date	launch lat	launch long			
1985 8 21 21h UT	47.35 N	-19.64 W			
date of first pos	first lat	first long	init. pres.	init. temp.	
1985 8 21 23h UT	47.37 N	-19.62 W	3765.	2.73	
date of last pos	last lat	last long	last pres.	last temp.	life (days)
1986 2 2 23h UT	47.23 N	-18.58 W	3054.	3.10	165.0

total displacement 165.1 days after launching

eastward displacement= 80.1 km mean eastward velocity= 0.48 cm/s
northward displacement= -15.9 km mean northward velocity= -0.10 cm/s

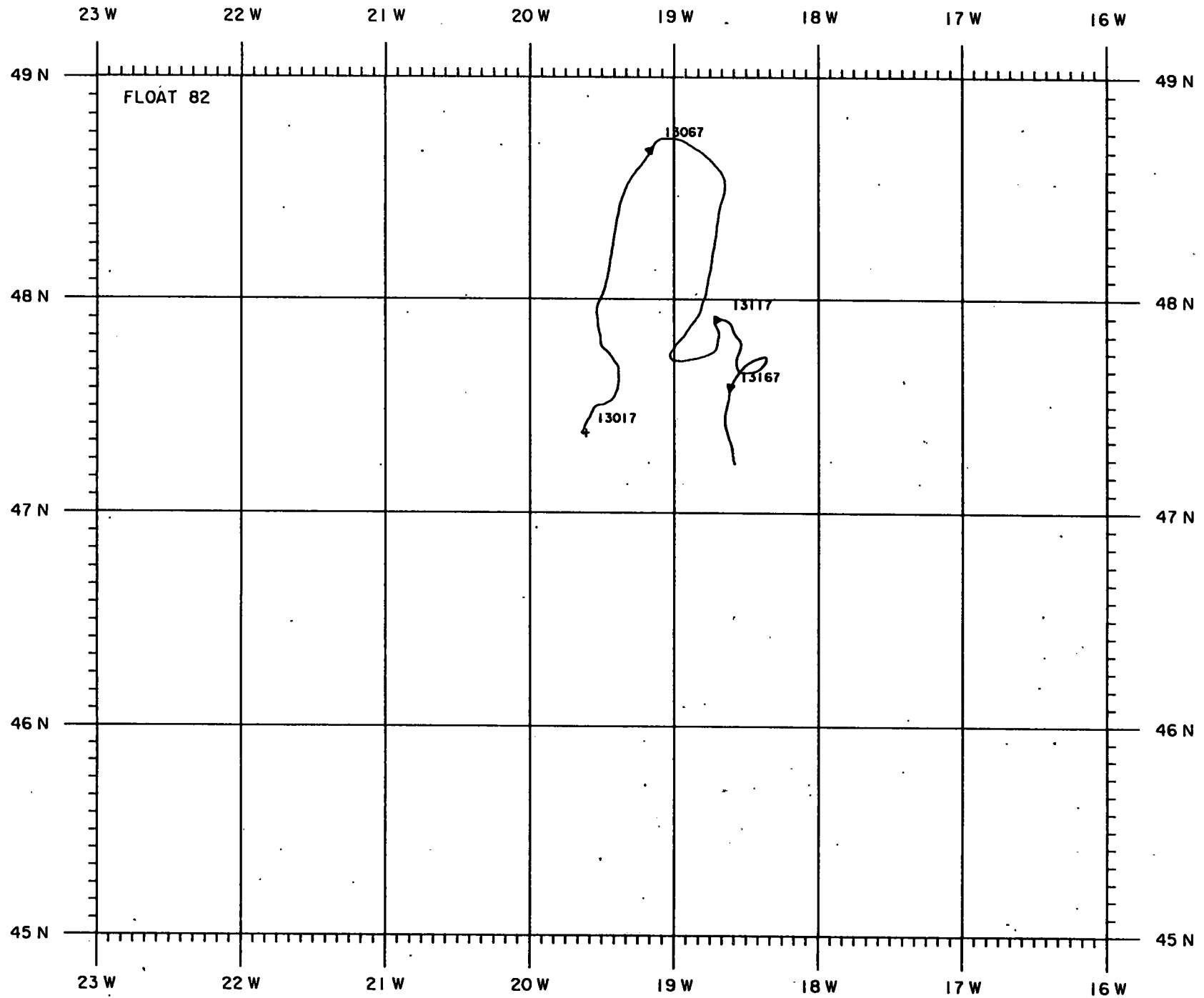
velocity time series statistics:

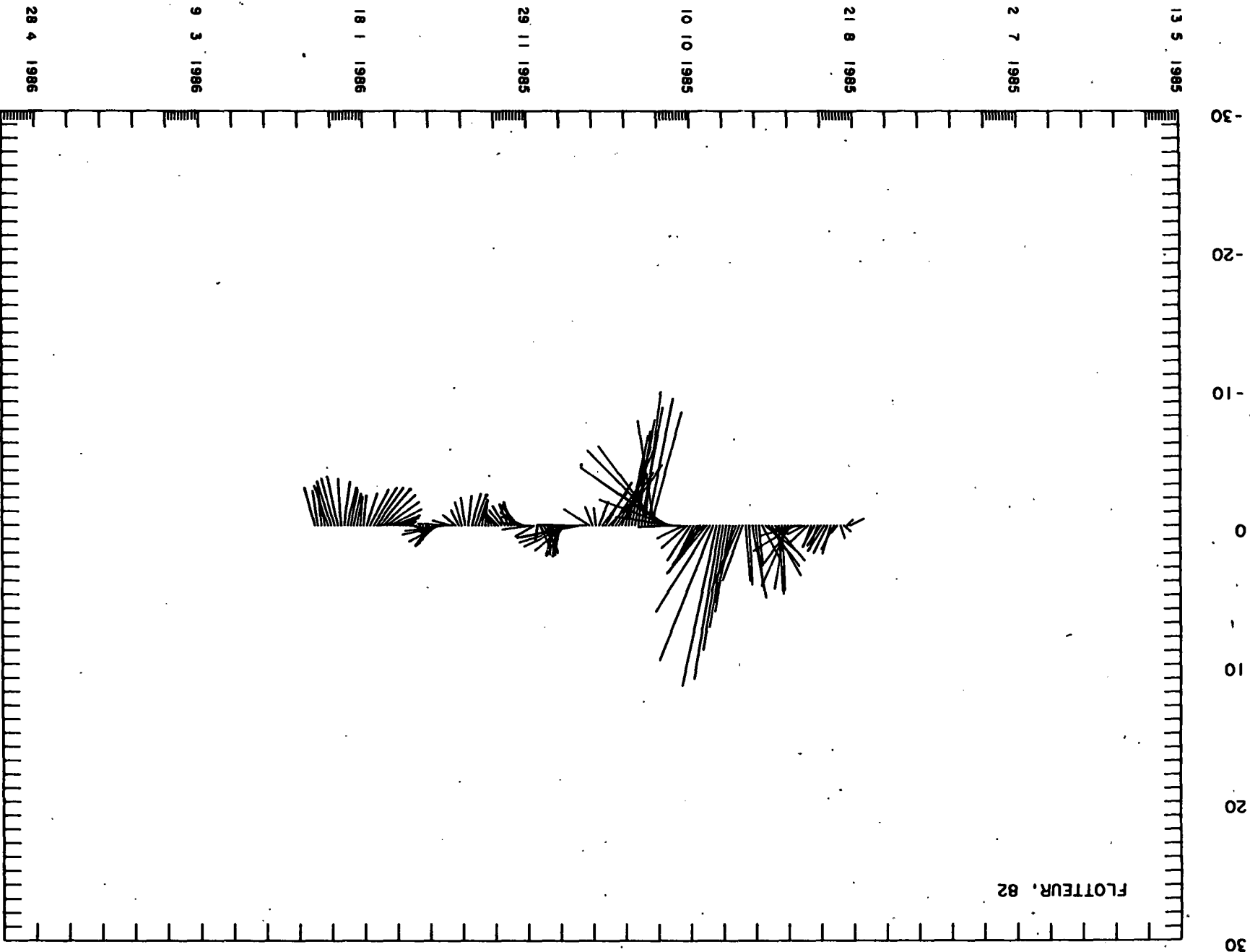
number of samples= 991
average east velocity comp.= 0.54 cm/s
average north velocity comp.= -0.11 cm/s

variance of east velocity comp.= 3.47 cm²/s²
variance of north velocity comp.= 12.52 cm²/s²
covariance= 2.01 cm²/s²

EKE= 8.00 cm²/s²
MKE= 0.15 cm²/s²

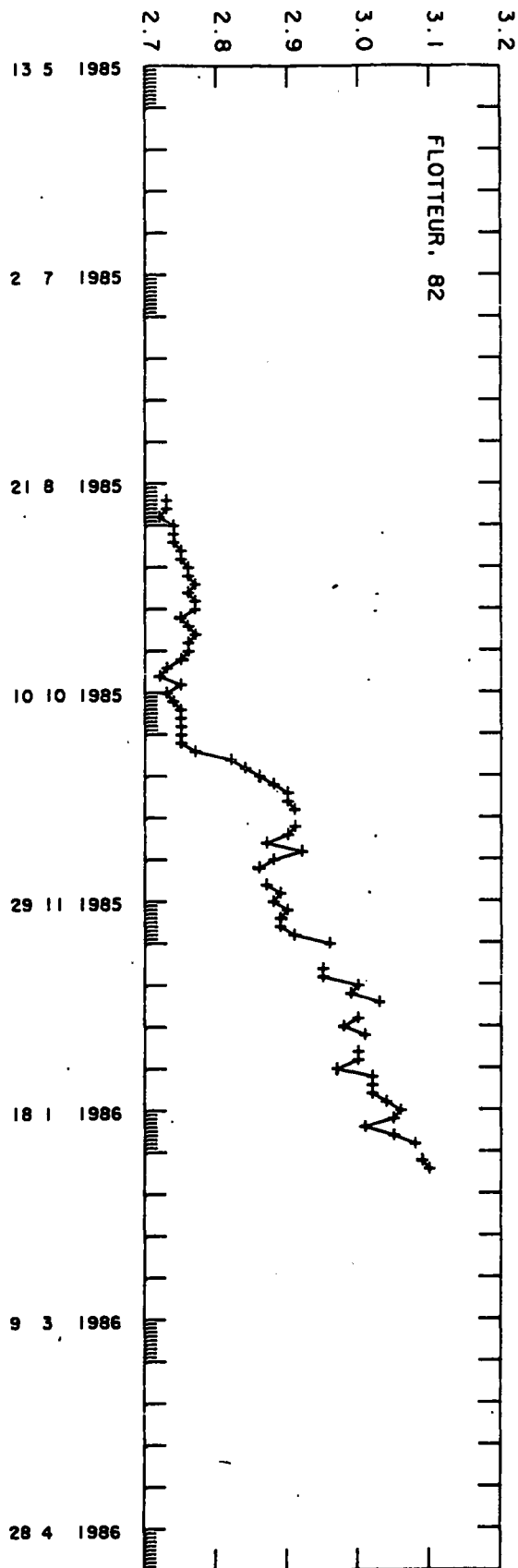
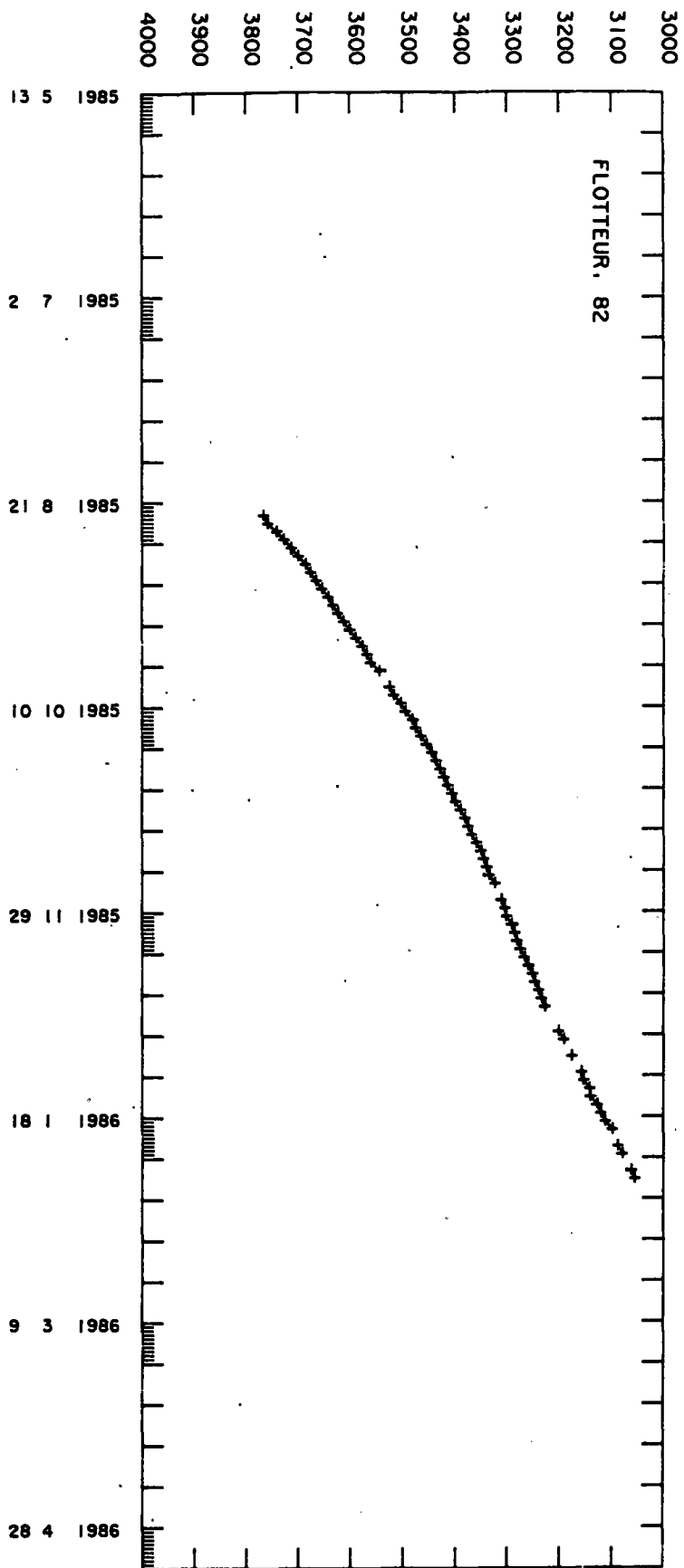
covar(u,temp)= -0.07 cm.degreeC/s
covar(v,temp)= -0.17 cm.degreeC/s





PRESSURE DBARS

TEMPERATURE DEGREES C



6 APPENDICES

6.1 Appendix A : Float and Listening Station Technical Characteristics

Deep floats consisted of 43 cm diameter glass spheres manufactured by Benthos with a quarter wave length aluminum tubing attached for acoustic emission (see Figure 3). The thermocline float was a "classical" aluminum SOFAR float (Rossby, Woorhis and Webb, 1975). Each float emitted a linear FM chirp 40 seconds long, every four hours. Within a multiplicative constant the signal sent can be written as :

$$S(t) = \sin 2\pi \left(f_0 + \frac{f_1 t}{2\Delta} \right) t \quad \text{for the interval } [0, \Delta]$$

with

$$\begin{aligned} f_0 &= 780 \text{ Hz} \\ f_1 &= 5 \text{ Hz} \\ \Delta &= 40 \text{ s} \end{aligned}$$

The "instantaneous" frequency is given by $\frac{1}{2\pi} \frac{d}{dt} (\text{phase}) = f_0 + \frac{f_1 t}{\Delta}$.

The frequency excursion is equal to $f_1 = 5 \text{ Hz}$.

Electric power consumption for the floats is 2.5 mW when sleeping, and 100 W when emitting, while acoustic power emitted omnidirectionally is roughly 7 W.

Listening was done by a linear vertical array of hydrophones. The electric signal generated was passed through filters to produce a series of 800 bits (20 bits per second) which was compared to the reference bit string stored in the station memory.

More precisely, the experimental bit string is first correlated with the reference bit string obtaining a correlation height comprised between 0 and 200 ; and then with the same reference bit string phase shifted by 90° , obtaining a second correlation height.

The final correlation height is the root squared sum of the two previous ones. Figure 24 shows the reference bit string and the correlation function for a perfect signal (no noise, no delay, no deformation,...).

Electric power consumption of listening stations was roughly 100 mW.

For further details concerning correlation the reader is referred to Ollitrault (1987) and Spain, O'Gara and Rossby (1980).

```

0000111100001111000011110000011110000111
1100001111100001111100000111110000011110
0000011111000001111100000011111000000111
11000000111110000001111110000001111110
00000011111100000001111111000000001111
11110000000011111111000000000111111110
00000000001111111111000000000000111111
1111100000000000000001111111111111110
00000000000000000000000011111111111111
11111111111111111111111111111111111110
11111111111111111111111111111111111111
111111111111111000000000000000000000000
111111111111111100000000000000000111111
11111000000000000111111111100000000000
11111111000000000111111111000000011111
11100000000111111100000001111110000000
1111100000011111100000011111000000111
1100000011110000001111000001111000000
1111000001111000001111000011110000111
110000111100000111100001111000011110000

```

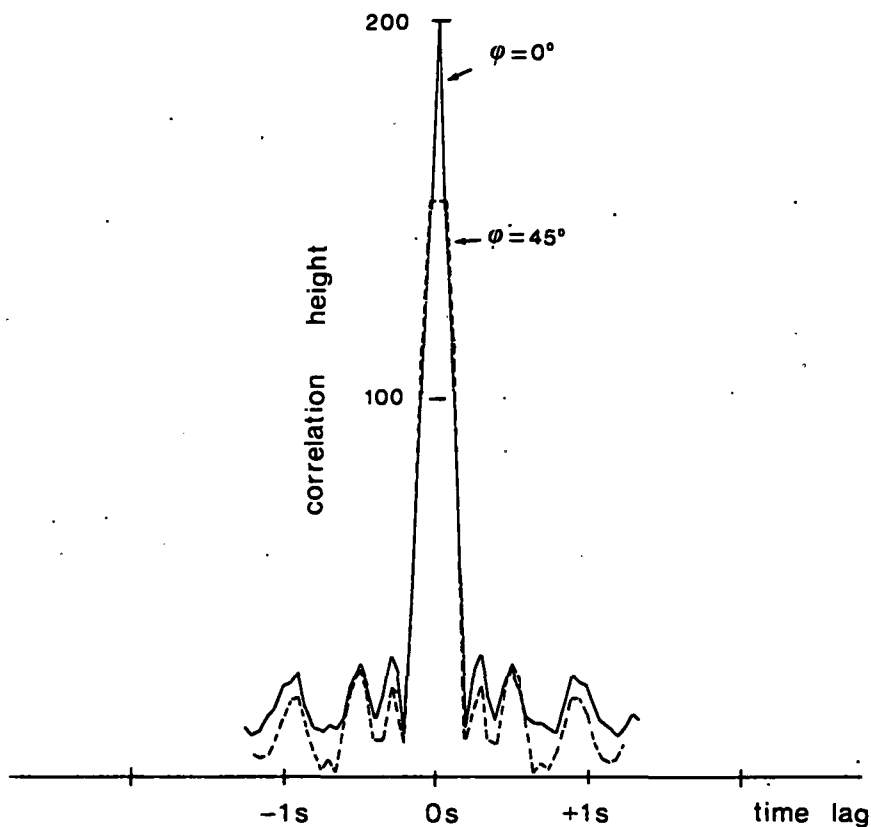


Figure 24 : Reference bit string and correlation function for a perfect signal. The curve for $\phi = 0^\circ$ corresponds to a signal which is in phase with the reference bit string, while that for $\phi = 45^\circ$ corresponds to a signal whose phase falls between the reference bit string and the reference string shifted by 90° .

6.2 Appendix B : Calendars

In the listening stations, days are Modified Julian Days (MJD) truncated to the lowest 3 digits (for example, January 1st of 1985 is MJD number 46066, which will be 066 on the SEADATA tape).

MJD number 0 begins at 0hUT on November 17th of 1858.

In the processing of the data, we have used what we have called Julian Days referred to 1950 : day number 1 begins at 0hUT on January 1st of 1950.

In the final float file we have used ordinary Julian Days, but slightly modified. We recall that Julian Day number 0 begins at 12hUT on January 1st of 4713 B.C. (in the Julian calendar). For example, Julian Day 2446067 begins at 12hUT on January 1st of 1985.

In fact, in the final float file, Julian Days are referred to 0hUT, instead of 12hUT (i.e. our Julian Day 2446067 begins at 0hUT on January 1st of 1985).

Table below gives some examples of correspondence between truncated MJD, Julian Day referred to 1950, and Julian Day referred to 0hUT, for the time period of the NOAMP experiment.

Date (Gregorian calendar)	Truncated MJD	1950 JD	JD referred to 0h
1985 May 1	186	12905	2446187
1986 January 1	431	13150	2446432
1986 June 1	582	13301	2446583

Readers interested in calendars can refer to *Ephémérides astronomiques* (Gauthier-Villars, 1984).

6.3 Appendix C : List of tables and figures

Table 1 : Characteristics of NOAMP listening stations	7
Table 2 : Life histories of all the floats	13
Table 3 : Elementary "Lagrangian" statistics for all the floats	31
Table 4 : "Eulerian" statistics for the deep floats in $1^\circ \times 1^\circ$ boxes	38
Figure 1 : Mooring configuration for the autonomous listening stations	8
Figure 2 : Sound speed at 1500 m depth and situation of the deep float experiment	9
Figure 2bis : Location of listening stations and launch positions of the floats	10
Figure 3 : A trio of floats in their housing before launching	11
Figure 4 : Bar graph showing the time that each float was tracked	14
Figure 5 : Sound rays typical of the NOAMP floats and listening stations	15
Figure 6 : Pressure history for the 14 deep floats	16
Figure 7 : Plot of the times of arrival received at a listening station	18
Figure 8 : Constant distance arcs in the vicinity of the float position	20
Figure 9 : Residual drift of N17 listening station as obtained by least squares fit	23
Figure 10 : N17 listening station non-linear drift assumed in the processing	25
Figure 11 : Sound speed profiles typical of the NOAMP zone	26
Figure 12 : Times of propagation for a few days after launching	27
Figure 13 : Error ellipses on position due to geometry of float and station positions	28
Figure 14 : Raw and final fitted longitudes	29
Figure 15 : All the float trajectories	34
Figure 16 : Composite first and last point plot for the deep floats	35
Figure 17 : Elementary "Eulerian" statistics for the deep floats in $1^\circ \times 1^\circ$ boxes	36
Figure 18 : Mean velocity and r.m.s. ellipses for the deep floats in $1^\circ \times 1^\circ$ boxes	37
Figure 19 : Deep float trajectories for the first 84 days (n° 12197 to 13000)	39
Figure 19bis : Deep float trajectories for the next 100 days (n° 13000 to 13100)	41
Figure 19ter : Deep float trajectories for the next 100 days (n° 13100 to 13200)	43
Figure 20 : Depth history for deep floats 68, 69, 70, 71, 72, 73, 74 and 75	45
Figure 20bis : Depth history for deep floats 76, 78, 79, 80, 81 and 82	47
Figure 21 : Temperature as seen by floats 68, 69, 70, 71, 72, 73, 74 and 75.	49
Figure 21bis : Temperature as seen by floats 76, 78, 79, 80, 81 and 82	51
Figure 22 : Normal modes for the Levitus profile in the centre of the NOAMP zone	53
Figure 23 : Bathymetric map of the NOAMP region obtained by H. Heinrich (1986)	54
Figure 24 : Reference bit string and correlation function for a signal without noise	118

7 REFERENCES

- Batchelor G.K., 1952. Diffusion in a field of homogeneous turbulence. II - The relative motion of particles. Proc. Camb. Phil. Soc., 48, 345-362.
- Burden R.L. and J.D. Faires, 1985. Numerical analysis 3rd edition, Prindle Weber and Schmidt editors.
- Colin de Verdière A., Mercier H. and M. Arhan, 1988. Mesoscale variability transition from the Western to the Eastern North Atlantic along 48°N, submitted to Journal of Physical Oceanography.
- Freeland H., Rhines P. and T. Rossby, 1975. Statistical observations of the trajectories of neutrally buoyant floats in the North Atlantic. Journal of Marine Research, 34, 69-92.
- Heinrich H., 1986. Bathymetrie und geomorphologie des NOAMP-Gebietes, Westeuropaishes Becken (17°W bis 22°W, 46°N bis 49°N). Deutsche Hydrographische Zeitschrift, 39, 183-196.
- Levitus S., 1982. Climatological atlas of the World Ocean, NOAA Professional Paper n° 13.
- Mittelstaedt E., Bock M., Bork I., Klein H., Nies H. and U. Schauer, 1986. NOAMP, Deutsches Hydrographisches Institut, internal report, 202 p.
- Mittelstaedt E., 1987. Cyclonic cold-core eddy in the Eastern North Atlantic. Marine Ecology - Progress Series, 39, 145-152.
- Ollitrault M., 1987. Traitement des données de flotteurs lagrangiens SOFAR. Rapports Scientifiques et Techniques IFREMER n° 7, 200 p.
- Rossby T., Voorhis A. and D. Webb, 1975. A quasi-lagrangian study of mid-ocean variability using long range SOFAR floats. Journal of Marine Research, 33, 355-382.
- Spain D., O'Gara R. and T. Rossby, 1980. SOFAR float data report of the Polymode local dynamics experiment. University of Rhode Island Technical Report n° 80-1, 200 p.

8 ACKNOWLEDGMENTS

Thanks are due to E. Mittelstaedt (DHI) and A. Vangriesheim (IFREMER) for the initiation and the planning of this experiment. U. Schauer kindly provided the CTD data to calculate sound speed profiles and R. Perchoc and G. Auffret (IFREMER) were indispensable during the preparation of the moorings and for the launching. John Garrett (Institute of Ocean Sciences, British Columbia) carefully read the manuscript and made helpful comments.

This work was supported by the Bundesministerium für Forschung und Technologie (FRG) grant MF 40519-9, the Commissariat à l'Énergie Atomique (France) grant MC 14.850, and IFREMER (France).

Imprimé en France
IFREMER - SDP
BP 70 - 29263 PLOUZANE

Dépôt légal 4ème trimestre 1988

Des mesures lagrangiennes des échelles moyennes dans les couches profondes de l'Atlantique nord-est ont été réalisées à l'aide de flotteurs SOFAR. Quatorze flotteurs ballastés pour 3500 dbars ont été lâchés vers 47°N, 20°W et suivis pendant près d'un an grâce à quatre stations d'écoute autonomes mouillées à environ 100 km autour de la zone de lâcher. Après un an, les flotteurs se sont dispersés dans une zone d'environ 300 km x 300 km, et révèlent une circulation générale très faible mais une forte influence de la topographie sous-marine.

Lagrangian measurements of mesoscale motions near the bottom of the North East Atlantic were made by tracking SOFAR floats. 14 deep floats ballasted for 3500 dbars were launched near 47°N, 20°W and followed during one year by 4 autonomous listening stations moored around the launching zone at a hundred kilometres distance. After one year the floats have dispersed in a zone of 300 km x 300 km indicating a very weak overall mean current but strong topographic influences.

Service de la Documentation
et des Publications (S.D.P.)
IFREMER - Centre de Brest
BP 70 - 29263 PLOUZANÉ
Tél. 98 22 40 13 - Télex 940 627F

ISSN - 0761-3970
Institut français de recherche pour l'exploitation de la mer, 1988